Strong and Tough Double Network Hydrogels based on Poly(2-oxazoline) and Polyacrylates

Zur Erlangung des akademischen Grades eines

Dr. rer. nat.

von der Fakultät Bio- und Chemieingenieurwesen
der Technischen Universität Dortmund
genehmigte Dissertation

vorgelegt von

M.Sc. Paola Andrea Benitez-Duif

geb. Benitez Rengifo

aus

Cali, Kolumbien

Tag der mündlichen Prüfung: 14.01.2025

1. Gutachter: Prof. Dr. Jörg C. Tiller

2. Gutachter: Prof. Dr. Dieter Vogt

Dortmund 2025

Acknowledgements

This Ph.D. thesis would not have been possible without the support, dedication, and encouragement of several people, to whom I am truly grateful.

First and foremost, I would like to express my sincere gratitude to my supervisor, Prof. Dr. Jörg C. Tiller, for his continuous support, insightful discussions, and for giving me the opportunity to develop an exciting research topic during my Ph.D. research. I deeply appreciate the invaluable scientific exchange and guidance throughout this journey—it has been an honor to work under his supervision.

Additionally, I extend my heartfelt gratitude to Prof. Dr. Dieter Vogt and Prof. Dr. Norbert Kockmann for reviewing and examining my doctoral thesis. Their valuable time, insightful feedback, and critical evaluation have significantly shaped this dissertation. Their expertise and constructive comments were instrumental in refining my work.

I am immensely grateful to the students who contributed to this research through their dedication, experimental efforts, and commitment. Their hard work played a crucial role in making this project a success. In particular, Sebastian Weckes, Daniel Kurka, Karlina M. Edel, Mathusiha Santhirasegaran, and Semra Gökcay did an outstanding job during their final theses.

I also appreciate the collaboration and support of our research partners. Dr. Marina Breisch from the BG University Hospital Bergmannsheil Bochum, Surgical Research, Ruhr University Bochum, for her advice and the execution of the cell tests. Prof. Dr. Wolfgang Tillmann and Dr. Dominic Stangier from the Institute of Materials Engineering, TU Dortmund, for their guidance and for giving me the opportunity to conduct the tribological investigations.

A special thanks goes to my colleagues in the research group and the past and present members of *Lehrstuhl BMP*, whose collaboration, discussions, and support have enriched both my scientific work and my personal experience as a researcher. The stimulating exchange of ideas and the strong team spirit within our group made this journey both productive and enjoyable. I am especially grateful for the professional and personal support from Dr. Frank Katzenberg, Dr. Montasser Hijazi, Dr. Marko Milovanovic, Dr. Alina Romanovska, Sascha Wilhelm, Lena Benski, Michail Maricanov, Robert Jerusalem, Jonas Tophoven, Alexandra Riedel, and Thorsten Moll. To the newer members of the group—although our paths only crossed briefly,

your support during the final stages of my Ph.D. did not go unnoticed. Sebastian Weckes, Suan Yang, Tim Stuck, Cemran Toydemir, and Jonas Lichtenstein, I sincerely appreciate your encouragement and wish you all the best in your own academic journeys.

Beyond the academic and technical aspects, I am deeply grateful for the unwavering support of my family: Enelia Rengifo, Ingelman Benitez, Eliana Benitez Rengifo, and David Benitez Rengifo. I also want to thank my family in Germany: Birgit and Christian Duif, along with Anna, Mia and Damion; and the Vahlhaus-Aretz family, for their kindness and support. A special mention goes to Julia Galindez, Inge and Karl Vahlhaus, who are no longer with us but remain in my heart.

Most importantly, I would like to express my deepest gratitude to my husband, Carsten Duif. Thank you for standing by my side all these years, from the moment I arrived in Germany until now. Words are not enough to express how much your love and support have meant to me throughout this journey.

Finally, I want to thank all my friends, and those who have become like family, for their unconditional support, care, and friendship over the years, especially Dr. Michael Cortazar, Lali Lopez Conesa, Zamanyi Vargas, Liliana Gonzalez Gomez, and Kristina and Jasper Klahm.

To all those who have contributed—scientifically, through their hard work, or through their steadfast support—I extend my heartfelt gratitude.

Thank you all.

The present work was conducted from May 2019 to April 2023 under the supervision of Prof. Dr. Jörg C. Tiller, Chair of Biomaterials and Polymer Sciences in the Faculty of Bio- and Chemical Engineering at the TU Dortmund University.

Publications

P. A. Benitez-Duif, M. Breisch, D. Kurka, K. Edel, S. Gökcay, D. Stangier, W. Tillmann, M. Hijazi, J. C. Tiller, Ultrastrong Poly(2-Oxazoline)/Poly(Acrylic Acid) Double-Network Hydrogels with Cartilage-Like Mechanical Properties. *Adv. Funct. Mater.* **2022**, 32, 2204837. https://doi.org/10.1002/adfm.202204837

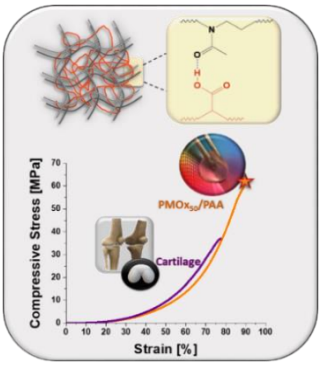

P. A. Benitez-Duif, S. Weckes, R. M. Pinto Ferreira, D. Kurka, J. C. Tiller, Insights on the influence of functional side groups on the mechanical performance of Poly(2-oxazoline)/Poly(acrylate) double network hydrogels. *Polymer*, **2025**, 319, 128014. https://doi.org/10.1016/j.polymer.2024.128014

Poster Presentation

P. Benitez-Duif, Double-Network Hydrogels based on Poly(2-methyl-2-oxazoline) and Poly(Acrylic Acid) as Artificial Cartilage, Freiburg Macromolecular Colloquium 2023, Freiburg, Germany, **February 2023**.

Declaration regarding the reproductions of previously published content

Parts of this work were previously published by the author of this thesis ([A] and [B]) and parts of this work are based on data, which were obtained during the preparation of Bachelor´s and Master´s theses performed at the Chair of Biomaterials and Polymer Science ([C]-[G]) under the supervision of the author.

This is a comprehensive list of the individual contributions to this work's chapters:

Chapter 3: contains parts based on data from [A], [C], [D], [E]

Chapter 4: contains parts based on data from [A], [B], [D], [G]

Chapter 5: contains parts based on data from [A], [B], [F]

[A] **P. A. Benitez-Duif**, M. Breisch, D. Kurka, K. Edel, S. Gökcay, D. Stangier, W. Tillmann, M. Hijazi, J. C. Tiller, Ultrastrong Poly(2-Oxazoline)/Poly(Acrylic Acid) Double-Network Hydrogels with Cartilage-Like Mechanical Properties. *Adv. Funct. Mater.* **2022**, 32, 2204837.

[B] **P. A. Benitez-Duif**, S. Weckes, R. M. Pinto Ferreira, D. Kurka, J. C. Tiller, Insights on the influence of functional side groups on the mechanical performance of Poly(2-oxazoline)/Poly(acrylate) double network hydrogels. Polymer, **2025**, 319, 128014.

[C] Edel, Karlina M. Untersuchung der mechanischen Eigenschaften von Doppelnetzwerken auf Basis von Poly(2-methyl-2-oxazolin)/Poly(acrylsäure) in Abhängigkeit des Quellmittels.TU Dortmund University, **2020**. [Bachelor´s Thesis]

[D] Kurka, Daniel. Untersuchung der mechanischen Eigenschaften von Doppelnetzwerk-Hydrogelen auf Basis von Poly(2-oxazolinen) in Abhängigkeit des zweiten Netzwerkes. TU Dortmund University, **2021**. [Master´s Thesis]

[E] Gökcay, Semra. Synthese und Charakterisierung von Doppelnetzwerk-Hydrogelen auf Basis von Poly(2-Methyl-2-oxazolin)/Poly(Acrylsäure). TU Dortmund University, **2021**. [Master´s Thesis]

[F] Santhirasegaran, Mathusiha. Doppelnetzwerk-Hydrogele auf Basis von Poly(2-methyl-2-oxazolin) und Acrylat-Copolymeren. TU Dortmund University, **2022**. [Master´s Thesis]

[G] Weckes, Sebastian. Synthese und Charakterisierung von Co-Doppelnetzwerken auf der Basis von Poly(2-Methyl-2-Oxazolin). TU Dortmund University, **2023**. [Master´s Thesis]

Table of Contents

Abstract

Double network hydrogels (DNHs) are known for their exceptional stiffness, toughness, and tunable characteristics, making them valuable for applications in membrane technology, energy storage, and, of significant importance, in biomedicine. These materials show great potential for replicating complex biomaterials such as cartilage. This work presents, for the first time, the development of DNHs based on poly(2-oxazoline) as the primary network and various polyacrylates as the secondary network, resulting in materials with remarkable toughness. The thesis is structured into three main parts, each addressing different features and challenges involved in developing these DNHs.

The first section focuses on the synthesis and optimization of DNHs using poly(2-oxazoline)s (POx) and poly(acrylic acid) (PAA), yielding materials with biomechanical properties comparable to cartilage, including high compressive strength and durability under physiological conditions. The second section further explores the potential of POx-based DNHs by incorporating various polyacrylates as secondary networks. This part emphasizes the investigation of interactions, functional groups, and the structural influence of the networks involved on the mechanical performance of the resulting hydrogels, achieving superior mechanical properties compared to conventional DNHs composed solely of polyacrylate networks.

Additionally, the thesis addresses the critical challenge of maintaining hydrogel functionality across a wide pH range, essential for implantable materials exposed to varying tissue environments and inflammatory responses. A novel DNH formulation, comprising poly(2-methyl-2-oxazoline) and poly(acrylic acid-*co*-acrylamide) P(AA-*co*-AAm), is developed, demonstrating remarkable stability and mechanical integrity across pH levels from 3.4 to 10.5. Through extensive mechanical testing, this research highlights the robustness and versatility of these advanced DNHs, positioning them as strong candidates for use in tissue regeneration, implants, and other biomedical applications where durability and adaptability are crucial. This work contributes significantly to the understanding and application of DNHs in complex physiological environments.

Zusammenfassung

Doppelnetzwerk-Hydrogele (DNHs) sind bekannt für ihre außergewöhnliche Steifigkeit, Zähigkeit und anpassbaren Eigenschaften, was sie wertvoll für Anwendungen in der Membrantechnologie, Energiespeicherung und, von besonderer Bedeutung, in der Biomedizin macht. Diese Materialien zeigen großes Potenzial, um komplexe Biomaterialien wie Gelenkknorpel nachzubilden. Diese Arbeit stellt erstmals die Entwicklung von DNHs auf Basis von Poly(2-oxazolinen) als primärem Netzwerk und verschiedenen Polyacrylaten als sekundärem Netzwerk vor, was zu Materialien mit bemerkenswerter Zähigkeit führt. Diese Dissertation ist in drei Hauptteile gegliedert, die sich jeweils mit unterschiedlichen Merkmalen und Herausforderungen bei der Entwicklung dieser DNHs befassen.

Der erste Abschnitt konzentriert sich auf die Synthese und Optimierung von DNHs unter Verwendung von Poly(2-oxazolinen) (POx) und Poly(acrylsäure) (PAA), wobei Materialien entstehen, die biomechanische Eigenschaften aufweisen, die mit Gelenkknorpel vergleichbar sind, darunter eine hohe Druckfestigkeit und Haltbarkeit unter physiologischen Bedingungen. Der zweite Abschnitt untersucht das Potenzial von POx-basierten DNHs weiter, indem verschiedene Polyacrylate als sekundäre Netzwerke integriert werden. Dieser Teil hebt die Untersuchung von Wechselwirkungen, funktionellen Gruppen und den strukturellen Einfluss der beteiligten Netzwerke auf die mechanische Leistungsfähigkeit der resultierenden Hydrogele hervor, wobei überlegene mechanische Eigenschaften im Vergleich zu herkömmlichen DNHs, die ausschließlich aus Polyacrylat-Netzwerken bestehen, erreicht werden.

Darüber hinaus behandelt die Arbeit die zentrale Herausforderung, die Funktionalität der Hydrogele über einen weiten pH-Bereich aufrechtzuerhalten, was für implantierbare Materialien, die unterschiedlichen Gewebeumgebungen und entzündlichen Reaktionen ausgesetzt sind, unerlässlich ist. Eine neuartige DNH-Formulierung, bestehend aus Poly(2-methyl-2-oxazolin) und Poly(acrylsäure-*co*-acrylamid) P(AA-*co*-AAm), wird entwickelt und zeigt bemerkenswerte Stabilität und mechanische Integrität über pH-Werte von 3,4 bis 10,5. Durch umfangreiche mechanische Tests unterstreicht diese Forschung die Robustheit und Vielseitigkeit dieser fortschrittlichen DNHs und positioniert sie als starke Kandidaten für den Einsatz in der Geweberegeneration, Implantaten und anderen biomedizinischen Anwendungen, bei denen Haltbarkeit und Anpassungsfähigkeit entscheidend sind. Diese Arbeit leistet einen wichtigen Beitrag zum Verständnis und zur Anwendung von DNHs in komplexen physiologischen Umgebungen.

1. Introduction

1.1 Addressing Articular Cartilage Degeneration in The Aging Population: The Potential of Tough Hydrogels

As global demographics shift toward an aging population, healthcare systems face increasingly complex challenges.[1] One significant consequence of this demographic change is the rising prevalence of age-related health issues, such as osteoarthritis (OA), which affects millions of people worldwide, around 7.6 % of the global population. Osteoarthritis, a degenerative joint disease, leads to pain, reduced mobility, and diminished quality of life, particularly in older adults.[2] The World Health Organization in its global ageing and health report in 2015 already highlighted OA as a leading cause of disability in adults aged 60 years and older.[3] OA leads not only to a burden on health, but also imposes high costs; up to $ 15,600 a year per patient[1]; on the healthcare system due to ongoing, often minimally effective treatments.

Issues regarding articular cartilage degeneration have led to a growing demand for effective and long-lasting treatments. Traditional strategies for cartilage repair, such as non-/pharmacological methods and surgical interventions (e.g., microfracturing, Autologous Chondrocyte Implantation (ACI), Osteochondral Autograft/Allograft transplantation, total joint replacement),[4-5] often fall short due to the limited natural healing capacity of the cartilage tissue, especially considering the complex mechanical and biological requirements of cartilage.[6-7] However, hydrogel-based treatments,[8-9] such as hydrogels as scaffolds, cell-embedded hydrogels, bioprinted hydrogels[10] and double network hydrogels, hold great promise for improving cartilage repair outcomes.[11-12]

From a material perspective, articular cartilage is a multifunctional interpenetrating hydrogel composed of proteoglycans and collagen type II fibers,[13] exhibiting compressive strength values up to 59 MPa[14-15] and fracture energy of 1000 J m^{-2},[16-17] despite having a high water content of 60 to 85 wt%.[18-20] Additionally, cartilage has an exceptionally low coefficient of friction (0.001-0.5),[21] which makes this tissue particularly challenging to mimic.[17] In this context, research on tough hydrogels, such as double network hydrogels (DNHs), is particularly interesting because these materials have the potential to closely mimic the mechanical performance of natural cartilage, making them especially promising for long-term cartilage repair in high-stress areas.[22]

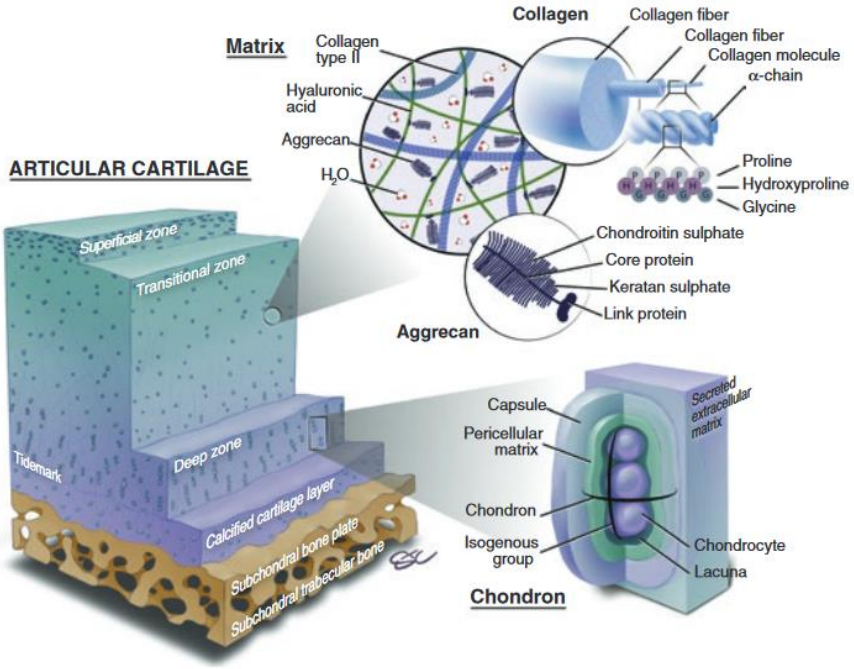

Figure 1: *Structure of articular cartilage.*[23]

1.2 ENGINEERING TOUGH HYDROGELS: DOUBLE NETWORK HYDROGELS

Hydrogels are three-dimensional cross-linked polymer networks capable of containing large amounts of water within their structure. Polymer hydrogels have been extensively investigated and applied, particularly in biomedical fields, due their tunable functional properties, such as capacity to bind water, swelling/deswelling behavior, stimuli-responsiveness and good biocompatibility.[24-26] However, conventional polymer hydrogels often suffer from weak mechanical performance, with low elastic modulus around 10 kPa and fracture energy values between 1 to 10 J m^{-2}, which limits their extensive application in drug delivery, soft robotics and tissue engineering,[27] where a certain resistance to extreme mechanical impact and load-bearing needs to be ensure.[28] The limitations of traditional hydrogels have driven research efforts in recent years towards developing tougher hydrogels that mimic high-performance natural tissues, such as tendons or cartilage, characterized for their toughness and high stiffness in MPa and even in the GPa range.

Unlike traditional hydrogels, which are often brittle and prone to failure under stress, tough hydrogels are engineered to withstand significant deformation and stress without breaking. In the design of these innovative hydrogels materials, the physicochemical properties at the

molecular level must be precisely adjusted to engineer a material whose macroscopic mechanical properties meet the specific requirements of the intended application, by following the so-called structure-property relationship.[29] To develop successfully stiff and tough materials, their molecular structure must be optimized to enable an efficient energy dissipation throughout the network during mechanical stress.

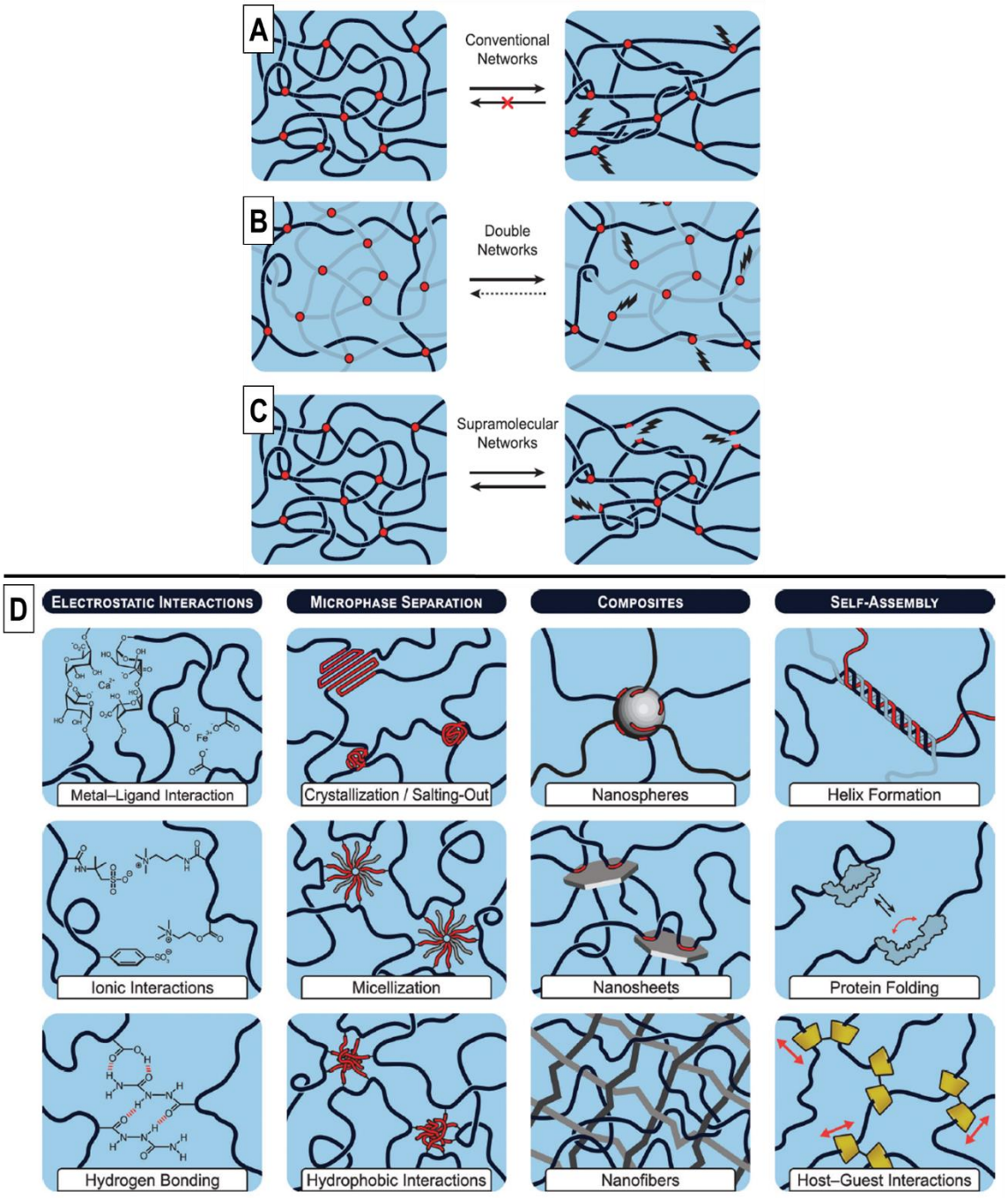

Figure 2: *Energy dissipation during mechanical stress in A) conventional hydrogels, B) double networks, and c) non-covalently cross-linked networks. D) Overview of different energy dissipation modes via specific molecular interactions/architectures. Figure adapted from* PETELINŠEK *et al.*[29]

In conventional hydrogels, when deformation occurs, tensile stress is concentrated on the nearest neighboring cross-links, which eventually leads to their rupture and subsequent material failure due to the lack of an effective energy dissipation mechanism. The incorporation of sacrificial bonds in tough hydrogels is a widely employed strategy for energy dissipation, making these bonds crucial for the reversible recovery of the network during and after mechanical stress. As described by PETELINŠEK and MOMMER,[29] sacrificial bonds can be introduced by polymerizing a second, more brittle network within an initially loosely cross-linked network, forming a double network. When the material is subjected to mechanical stress, bonds within the second, more brittle network break, leading to energy dissipation. Alternatively, sacrificial bonds can be formed through supramolecular transient interactions, which are capable of reversible breaking and reformation.[30] In this case, the sacrificial bonds are of non-covalent nature, allowing then to reversibly break and re-form. Non-covalent interactions that contribute to this mechanism include, but are not limited to, metal-ligand coordination, ionic interactions, hydrogen bonding, microphase separation, hydrophobic interactions, polymer-nanomaterial adsorption, host-guest complexation, or supramolecular self-assembly.[29] This diverse array of interactions can be effectively harnessed in hydrogel structures such as double network hydrogels, which are designed to exploit these interactions for enhanced mechanical properties and energy dissipation.

Double network hydrogels (DNHs) are polymeric materials consisting of two interpenetrating or semi-penetrating polymer networks, superior to either individual network in terms of mechanical strength or toughness. J. P.GONG et al.[31] advanced the concept of double network hydrogels and, in 2003, demonstrated for the first time how hydrogels with exceptionally high mechanical strength can be achieved using a double-network architecture.[29,32] The first network was composed of 2-acrylamido-2-methylpropane sulfonic acid (AMPS), which was highly cross-linked, rigid, and brittle. Subsequently, a second network of elastic, lightly cross-linked polyacrylamide (PAAm) was introduced. The resulting double network, despite containing approximately 90% water, exhibited remarkable mechanical strength, withstanding compression stress up to 17 MPa. In contrast, pure PAMPS alone fractures at just 0.4 MPa with a water content of also 90%. This significant enhancement in mechanical performance is attributed to the brittle chains of the first network, which function as sacrificial bonds that dissipate energy, while the elastic second network maintains the integrity of the hydrogel under higher strains. Although each of the two individual networks are mechanically weak, the high strength of the resulting DN is not attributed to a linear combination of the two components,

but to the synergistic effect of this binary structure. Thus, the resulting DN hydrogels are stiff but not brittle, ductile but not soft.[31]

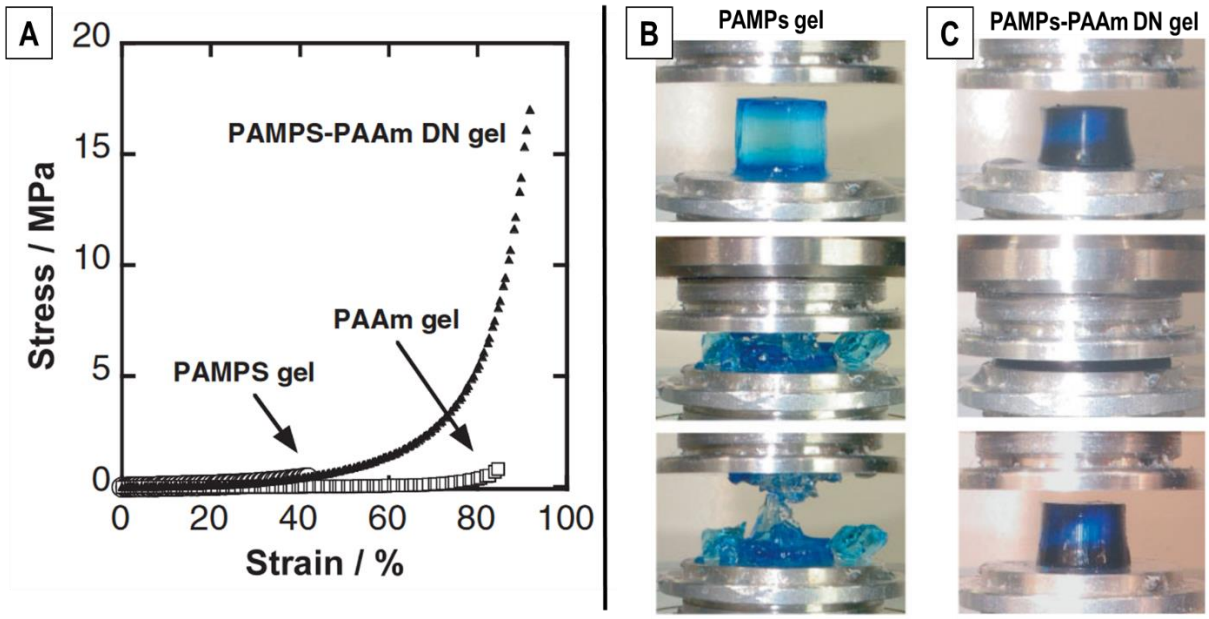

Figure 3: *A) Compression stress-strain curve for the single networks PAMPS and PAAm and the combined PAMPS-PAAm DN gel. Graphic demonstration how B) PAMPS gel and C) PAMPS-PAAm DN gel sustain the compression stress. Figure adapted from* GONG *et al.*[31]

Through Gong's pioneering work, three primary methods have been introduced for synthesizing DN hydrogels (refer to Figure 4), each with distinct advantages and applications. The first of these methods, the ***two-step approach*** originally proposed by GONG, involves the sequential formation of two distinct polymer networks.[27-28] The first network is a rigid, highly cross-linked polyelectrolyte, which is synthesized via UV-induced photo-polymerization to provide structural integrity. Following the formation of this first-network, it was immersed in a solution containing monomer, initiator and crosslinker for the second network, which is neutral and more flexible. Polymerization of the second network then occurs within the swollen first network, resulting in a DN hydrogel where both networks are chemically cross-linked. Although this method is limited by its reliance on the swelling ability of the first network and the diffusion of the second network´s monomer within it, the separate formation of the networks allows better control over the structure and features of each polymer network, resulting in hydrogels with exceptional mechanical performance and tunable properties.[33-34]

In the two-step method, polyelectrolytes, which exhibit significant swelling behavior, are typically used to form the first network. However, this poses a challenge when using neutral networks, which have poor swelling capabilities. To address these limitations, NAKIJAMA[35] developed an alternative method known as the ***molecular stent approach***. This technique generally involves the incorporation of linear polyelectrolyte chains or ionic micelles into an initially neutral network, which serves to elevate the osmotic pressure within the composite neutral network.[28,36-37] This process leads to the formation of highly swollen, yet mechanically weak and brittle gels. Subsequently, stent-DN (st-DN) hydrogels are synthetized through the polymerization of a secondary precursor solution within the swollen first network. This is followed by the removal of the polyelectrolyte chains or ionic micelles by prolonged washing or electrophoresis.[35] This approach circumvents the limitations of the classical DN hydrogels synthesis method by not relying on the swelling of the initial network, thereby providing enhanced control over the mechanical properties of the final network hydrogel.

The two-step and molecular stent methods are often time-consuming and resource intensive. To simplify the synthesis process, ***one-step method*** was developed, which involves the simultaneous incorporation of monomers, initiators and cross-linkers required for both the first and second network into a single mixture (as illustrated in Figure 4-B). This mixture is subjected to, initiated by either temperature or UV light to form the DN hydrogels.[27-28,36] Most of the studies that report the use of this method focus on the synthesis of DNHs based on polysaccharides with thermoreversible sol-gel transitions, such as agar, κ-carrageenan, and sodium alginate.[38-41] These materials require specific gelation conditions, making it difficult to control the polymerization of the second network, as well as cross-linking reactions and the overall hydrogel structure, among other challenges. The DNHs synthesized using these methods achieve tensile strengths of up to 1.0 MPa, compressive strengths of up to 39 MPa,[40] fracture strain values of up to 3500%, and an elastic modulus of ca. 0.2 MPa,[40-41] which indicates that they are not stiff enough and hence show high deformation values. It is also known that hydrogels based on these polysaccharides have a swelling capacity exceeding 1000%,[42] and many studies do not report the swelling conditions of these materials under mechanical testing.[43]

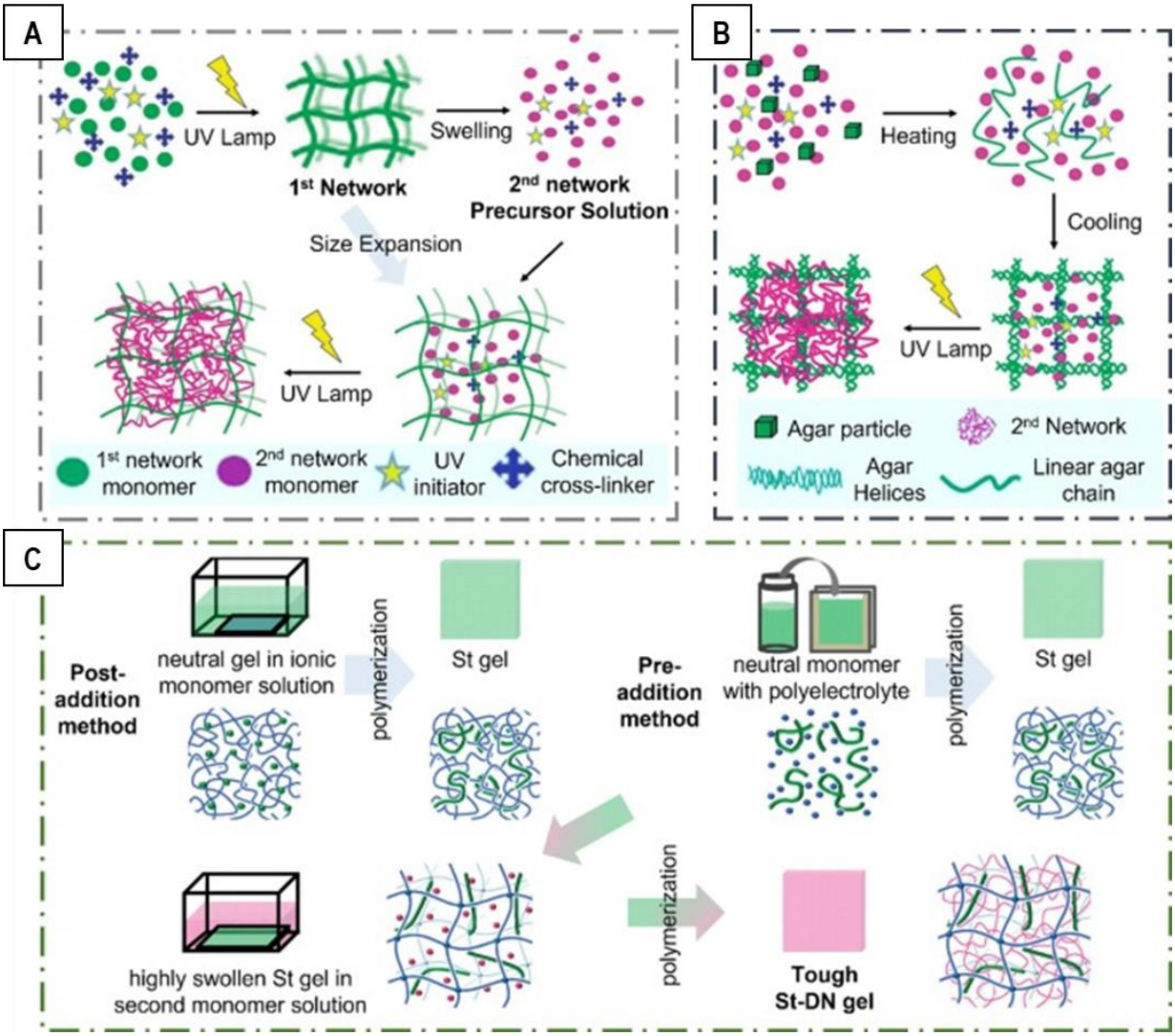

Figure 4: *Different preparation methods for DN hydrogels. (A) Two-step polymerization method. (B) One-step mixing method. (C) Molecular stent method.*[28,34-35]

1.3 Covalent and Non-covalent Double Network Hydrogels and their Applications

The different synthesis methods for double network (DN) hydrogels enable the fabrication of materials with a diverse range of properties, achieved by combining two interpenetrating polymer networks with contrasting mechanical and chemical characteristics. The unique properties and potential applications of these hydrogels arise from the specific interactions between the two networks and the cross-linking mechanisms employed during their synthesis. Accordingly, DN hydrogels can be categorized based on the type of interactions that stabilize the networks: covalent (involving strong, irreversible chemical bonds) and non-covalent (involving weaker, reversible interactions such as hydrogen bonding, ionic interactions, or

hydrophobic forces). These differing interaction types contribute significantly to the mechanical properties, swelling behavior, and responsiveness of the DN hydrogels, thereby influencing their suitability for various biomedical, industrial, and environmental applications.[28,44]

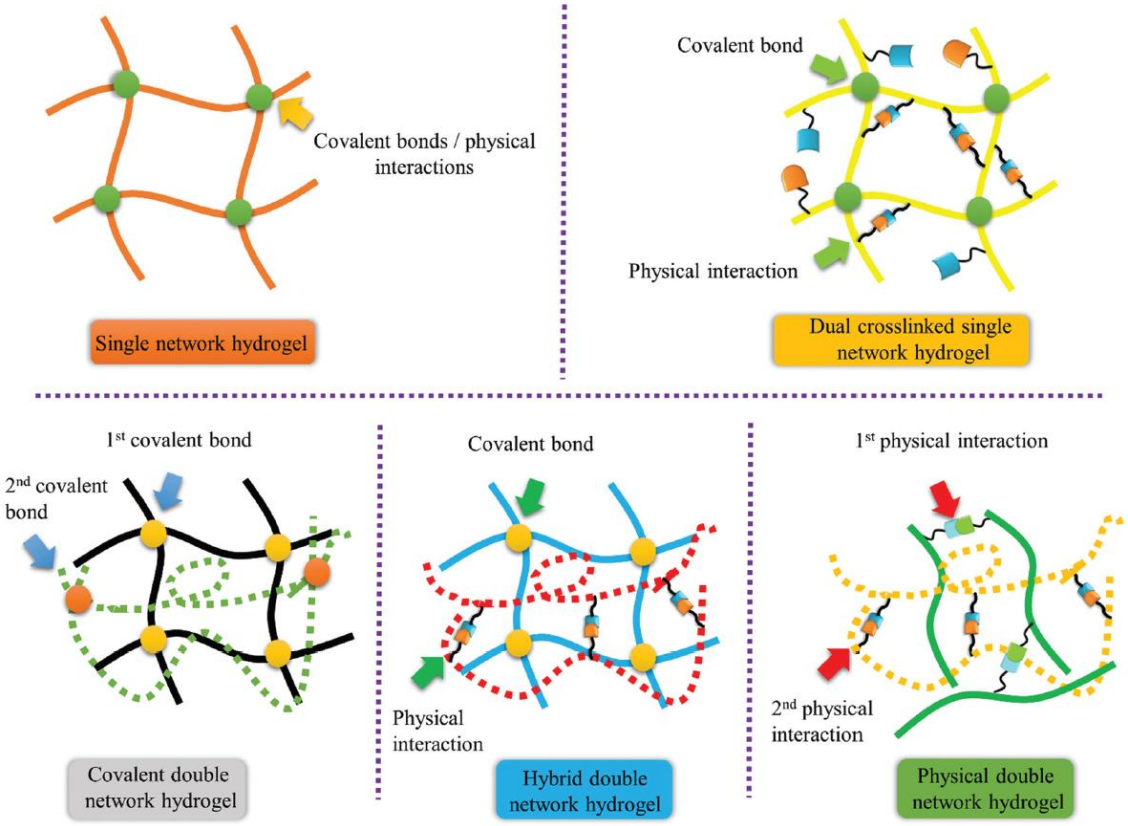

Figure 5: *Classification of double network hydrogels.*[36]

Covalent DN hydrogels consist of two networks that are chemically cross-linked through covalent bonds.[27-28] The first network is typically rigid and brittle, while the second is more flexible, allowing the material to absorb stress and dissipate energy efficiently. Covalent DN hydrogels are known for their high mechanical strength and durability. However, their synthesis often involves complex, multi-step processes, and once damaged, they cannot easily self-repair.[36] An example of a covalent DN hydrogel is the combination of poly(2-acrylamido-2-methylpropanesulfonic acid) (PAMPS) and polyacrylamide (PAAm), which has been used as a building block for various double network hydrogels sytems,[31,36,45] including reinforcement mechanisms using silica nanoparticles.[46]

Building on their first work, GONG et al.[47] developed DN hydrogels composed of a brittle network of poly (2-acrylamido-2-methylpropanesulfonic acid) sodium salt (PNaAMPS) and a stretchable network of poly(acrylamide) (PAAm). These hydrogels exhibit an ability to increase their strength under mechanical stress that closely resembles the behavior of natural muscle tissue. In order to mimic this feature of muscle tissue, the synthesized chemically cross-linked PNaAMPS- PAAm DN hydrogel has to be capable of withstanding repeated mechanical stress, which leads to a form of "growth" within the networks. This phenomenon occurs because the mechanical force applied to the network causes the breaking of covalent cross-links, resulting in the formation of mechanoradicals. These mechanoradicals are able to initiate a reconstructive polymerization process, allowing the network to rebuild and strengthen itself over time.[36,47-48] This strategy is illustrated in the Figure 6.

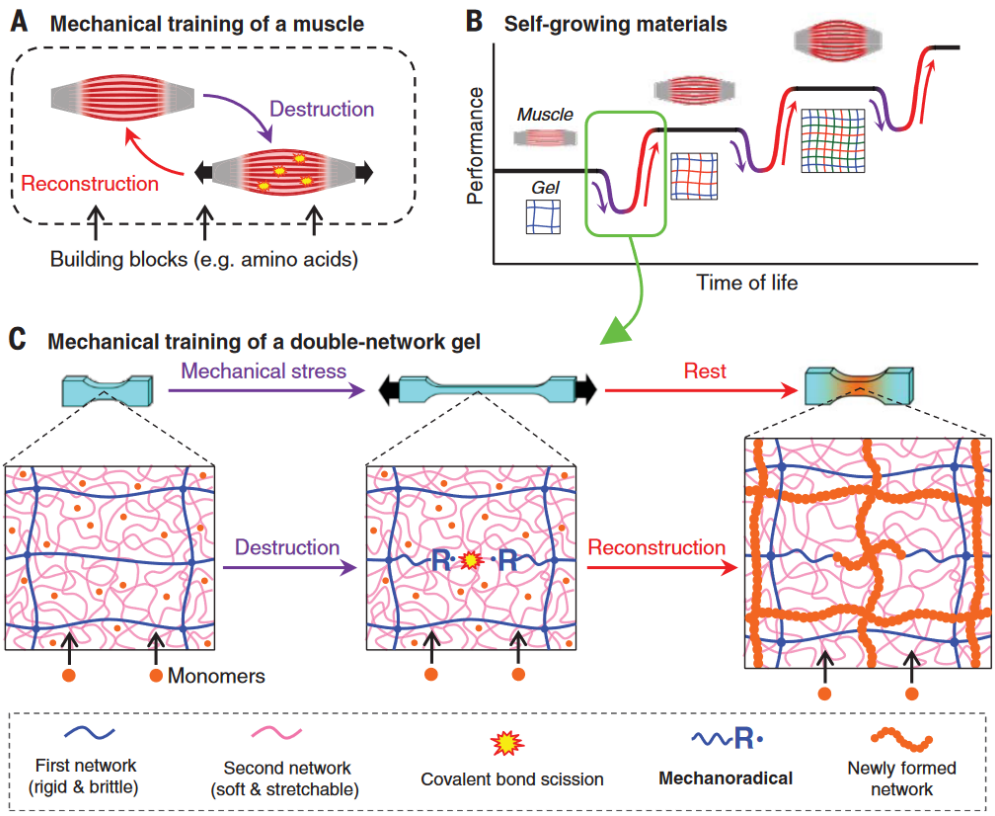

Figure 6: *Conceptual scheme of self-growth PNaAMPS- PAAm DN hydrogel by mimicking the mechanical training of the muscle tissue.*[47,49]

Non-covalent DN hydrogels, in contrast to their covalent counterparts, rely on physical interactions such as hydrogen bonds, hydrophobic and ionic interactions, metal-ligand coordination, and host-guest interactions to form their network structures. These physical

crosslinks are dynamic and reversible, allowing the resulting hydrogels to exhibit self-healing properties. The nature and dynamics of these physical crosslinks play a crucial role not only in regulating the network's mechanical properties but also in imparting stimuli-responsive and self-recovery features to the hydrogel.[22,50] However, while non-covalent DN hydrogels generally exhibit lower mechanical strength compared to the covalent DNHs, the diversity of non-covalent interactions can significantly enhance their resistance to fracture. This makes them suitable for a wide range of applications where flexibility, self-healing, and responsiveness are desired.[51-53] Additionally, the incorporation of different types of interactions in DN hydrogels allows for the formation of various configurations. For example, **hybrid double network hydrogels**[27-28] can be created by combining covalent crosslinks with non-covalent interactions as reinforcement, which can be tailored for more complex material structures and applications. These hybrid DN hydrogels are of particular interest due to their enhanced mechanical properties and multifunctional capabilities, which can be advantageous for applications in tissue engineering, drug delivery, and soft robotics.[37,54]

He and Yuan[55] developed a multifunctional organohydrogel with exceptional antifreezing and antidrying properties, achieving over 85% optical transparency, high stretchability (up to 1200%), and strong adhesion to various substrates. This organohydrogel consists of a poly(acrylic acid) (PAA)/gelatin (GE) double network, tannic acid (TA), and aluminum ions (Al^{3+}) in a water/glycerin solvent. PAA and gelatin form a double network, where gelatin moieties are partially cross-linked by tannic acid. The physically cross-linked gelatin acts as "sacrificial bonds" for dynamic energy dissipation, improving the hydrogel's recovery during deformation, while the chemically cross-linked PAA strengthens the material. Additionally, Al^{3+} ions not only serve as conductive ions, imparting electrical conductivity to the organohydrogel, but also form metal ionic coordination interactions with the free carboxyl groups on the PAA chains and the phenolic hydroxyl groups on the TA in the cross-linked network, further enhancing the mechanical strength. Inspired by mussel adhesion, the introduction of TA provides repeatable adhesive performance across various surfaces, such as glass, metal, plastic, and pigskin. The organohydrogel is synthesized using a one-pot method with rapid UV irradiation, offering a simple and efficient preparation. This antifreezing, antidrying organohydrogel holds promise for applications in flexible electronics, human–machine interfaces, and healthcare monitoring in varied environments.[55]

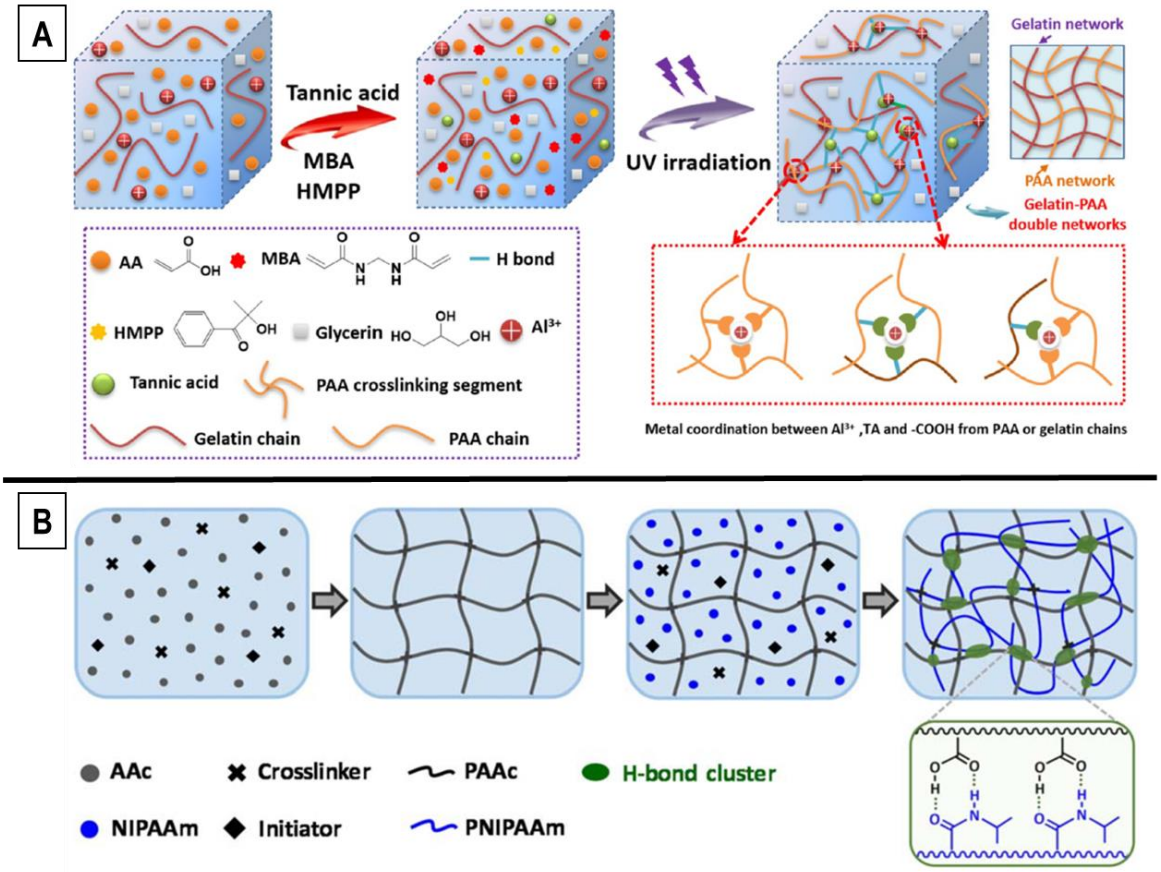

Figure 7: *A) Physically cross-linked Multifunctional organohydrogel based on poly(acrylic acid) (PAA)/gelatin (GE) double network by HE and YUAN.[55] B) poly(acrylic acid) (PAAc) and poly(N-isopropylacrylamide) (PNIPAm) double network hydrogels with cooperative hydrogen bonds by ZHENG et al.[56]*

The dynamic nature of hydrogen bonding interaction in DNHs enables the development of materials that exhibit both toughness and elasticity, which are increasingly sought after for biomedical applications, particularly in engineering load-bearing artificial tissues and devices. ZHENG et al.[56] reported the development of tough poly(acrylic acid) (PAAc) and poly(N-isopropylacrylamide) (PNIPAm) double network hydrogels (see Figure 7-B). These hydrogels, containing between 44 % and 72 % water in their structure, demonstrated outstanding mechanical properties, with tensile strength ranging from up to 4.6 MPa, elongation at break between 98% and 275%, and an elastic modulus from 11 to 226 MPa. These high values of elastic modulus were achieved due to dense cooperative hydrogen bonds between the two polymer networks. Additionally, these hydrogels show a pH-sensitive and temperature-responsive shape memory effect. Materials with this kind of mechanical performance bridges the gap between synthetic tough hydrogels and natural soft tissues, making this kind of material ideal for advanced biomedical applications.

Another approach to synthetizing materials that can mimic complex natural tissues, such as articular cartilage, involves incorporating copolymers and leverage hydrophobic interactions in DNHs. GRUNLAN et al.[45] successfully developed thermoresponsive DNHs composed of an anionic poly(2-acrylamido-2-methylpropane sulfonic acid) (PAMPS) first network and a tunable, thermoresponsive second co-network of poly(N-isopropylacrylamide-*co*-acrylamide) [P(NIPAAm-*co*-AAm)]. These DNHs exhibit compressive strength of 25 MPa with 80% water content, and an elastic modulus of ca. 1 MPa and low coefficient of friction similar to the natural cartilage tissue. In these DNHs, ionic interactions within the first network and reversible hydrophobic interactions within the second network contribute to their remarkable properties.

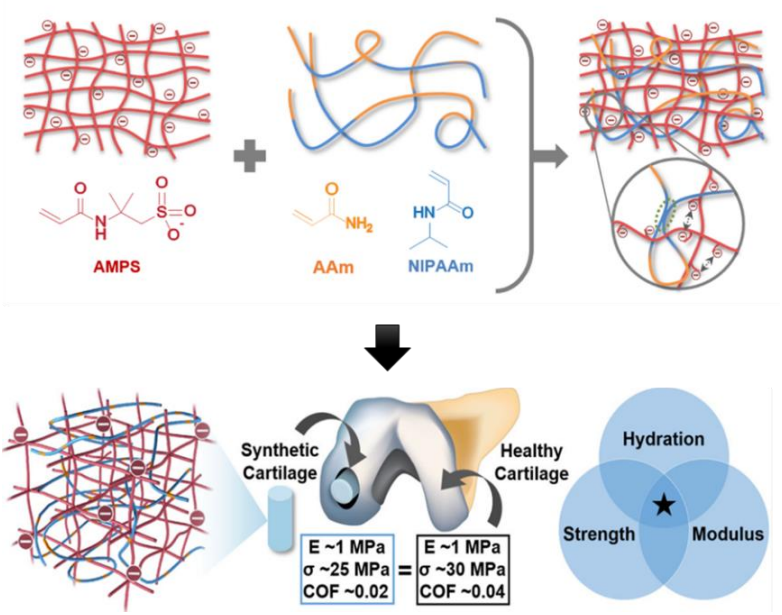

Figure 8: *DNHs composed of poly(2-acrylamido-2-methylpropane sulfonic acid) (PAMPS) and poly(N-isopropylacrylamide-co-acrylamide) [P(NIPAAm-co-AAm)] with cartilage-like mechanical performance. This figure was adapted from GRUNLAN et al.*[45]

These examples of DN hydrogels (DNHs) represent only a small fraction of the extensive research dedicated to their preparation over the last two decades. The development and understanding of double network hydrogels represent a frontier in material science with immense potential. By mastering the intricate mechanisms of energy dissipation and material reinforcement,[46] researchers can craft hydrogels with tailored properties that mimic the complexity of natural tissues. This ability to customize DN hydrogels opens up exciting opportunities for innovative applications in energy storage, environmental sustainability, and

biomedical engineering, promising solutions to some of the most pressing challenges in these fields.[57-61] As research continues to evolve, DN hydrogels are poised to transform the landscape of material science, offering new insights and breakthroughs for future technologies.

Double network hydrogel systems with remarkable mechanical performance are primarily synthesized using two-step methods, and most of them are based on poly(2-acrylamido-2-methylpropanesulfonic acid) (PAMPS) and polyacrylamide (PAAm).[54,62-63] However, the inclusion of polyelectrolytes like PAMPS in these systems poses significant challenges in controlling the water uptake, which directly affects mechanical performance under varying pH and salt concentrations. This lack of control makes it difficult to achieve consistent properties in diverse environments. A common strategy to mitigate this issue involves adding thermoresponsive polymers like poly(N-isopropylacrylamide) (PNIPAAm),[45] which can suppress swelling above its lower critical solution temperature (LCST) of 32 °C.[64] However, this approach is still limited, particularly when designing hydrogels for biological applications, where control over swelling and mechanical behavior in a broad range of conditions is crucial.

Giving the growing importance of developing tough materials with versatile features and the limitless possibilities in designing double network systems, this study introduces novel double network (DN) hydrogels based on Poly(2-oxazoline) (POx) as the first network and polyacrylates as the second. Poly(2-oxazolines) are particularly attractive due to their application in biomedical fields,[65-66] as they exhibit biocompatibility similar to Polyethylene glycol (PEG).[67] Their versatile cationic ring-opening polymerization mechanism enables precise control over polymerization degree, introduction of comonomers and functionalization, inter alia, by end-groups. Additionally, formation of segmented copolymers provides responsive behavior in solvents or in response to temperature changes.[68-70] The two-step synthesis method employed to create these DN hydrogels enables independent control over each network, allowing the fine-tuning of properties. This makes POx an ideal polymer class for developing DN hydrogels with customizable mechanical and functional features. Research on POx-based polymer systems opens new possibilities in the DNHs field, with the potential to develop advanced materials with enhanced mechanical strength and versatile functionality

2. Goals

The unique structure of double network hydrogels (DNHs) endows them with enhanced toughness and durability, making them suitable for various demanding biomedical applications such as biomaterials for scaffolds in tissue engineering and artificial implants for challenging load-bearing tissues like articular cartilage. The primary aim of this research work is to develop and design DNHs with remarkable mechanical performance, specifically to mimic the mechanical features of the articular cartilage. To address this, the study explored the use of poly(2-oxazoline) derivatives, such as poly(2-methyl-2-oxazoline) (PMOx) and poly(2-ethyl-2-oxazoline) (PEtOx), as the first network, combined with different polyacrylates like pol(acrylic acid) (PAA) as a second network. This combination aimed to form hydrogel systems with enhanced mechanical properties and stability in physiologically relevant environments.

To achieve the overarching aim, the research involved developing and optimizing DNHs composed of a primary network of POx and a secondary network of polyacrylate derivates such as PAA and polyacryamide (PAAm). By exploring different polyacrylates, this research sought to analyze and determine the contributions of functional groups in the interactions between the networks involved, particularly focusing on hydrogen bonding, which plays a crucial role in the mechanical stability of the formed DNHs. With a deep understanding of DNHs design and the importance of strong dynamic hydrogen bonding interactions for mechanical performance, this study aimed to create DNHs with improved compression strength that remain stable in basic environments, addressing the challenge of pH sensitivity in hydrogels containing ionic components. This approach aimed to advance the development of pH-resistant hydrogels for biomedical applications where environmental conditions can vary significantly. The findings from this study are expected to guide the design of next-generation hydrogels with tailored properties for specific medical and engineering applications.

3. Ultrastrong Poly(2-oxazoline)/Poly(acrylic acid) Double network Hydrogels with Cartilage-like Mechanical Properties

This chapter is based on a paper publication by P. BENITEZ-DUIF[17] as the first author. Also some results were obtained with the collaboration of D. KURKA,[71] S. GÖKCAY[72] and K. EDEL[73] as part of their final thesis work.

3.1 ABSTRACT

The exceptional stiffness and toughness of double-network hydrogels (DNHs) make them ideal candidates for mimicking complex biomaterials such as cartilage, which has limited regenerative capacity and often requires artificial replacement. These DNHs, made from cross-linked poly(2-oxazoline)s (POx) and poly(acrylic acid) (PAA), were synthesized using a two-step process via UV-initiated polymerization. Stabilized by hydrogen bonding even at physiological pH 7.4 (PBS buffer), this stability is attributed to the pKa-shifting effect of POx on PAA.[17] DNHs based on poly(2-methyl-2-oxazoline), which contain around 66 wt% water and are non-cytotoxic, exhibit biomechanical properties that closely resemble cartilage. These include similar water content, stiffness, toughness, friction coefficient, compression under physiological stress, and viscoelastic behavior. The material also demonstrates impressive strength in PBS at pH 7.4 and in egg white as a synovial fluid substitute, with compression strength reaching up to 60 MPa, highlighting its superior performance.[17]

3.2 INTRODUCTION

Osteoarthritis (OA) is one of the most prevalent diseases affecting, inter alia, the articular cartilage (AC) in load bearing joints like hip, shoulder, and knee. OA is currently a leading cause of disability for 500 million people worldwide, around 7 % of the global population, and it is expected that the number of people affected by this condition will considerably increase in the coming years.[17,74-75]

Currently, there are several treatment strategies to mitigate the effects of cartilage damage, such as non-pharmacological methods (i.e., weight loss), pharmacological methods [e.g., Non-Steroidal Anti-Inflammatory Drugs (NSAIDs)[74] and surgery intervention such as macrofracturing and Autologous Chondrocyte Implantation (ACI).[20,59] However, most of the

treatment strategies mentioned above are still not a long-term solution to this condition. Due to the articular cartilage´s complex structure the implementation of a suitable medical treatment remains a challenge. On one hand, the articular cartilage structure is highly compacted and has no vascularity. This makes delivery of drug molecules to the tissue unfeasible. On the other hand, the cartilage lacks a fully self-healing capability and is a non-neural tissue, which means that symptoms appear when the cartilage damage is already severe.[18] In some cases, the only treatment left is a hip or a knee joint replacement upon detection. Nevertheless, approximately 90 to 95% of all joint replacements have an endurance time limited to 10 years.[20] Typically, mechanical failure of the implant material is the main reason for a new surgical intervention, which increases not only the burden of disease, but also the cost of treatment. Complications related to implant failure could still be prevented through the implementation of materials with long-term stable mechanical properties that could increase the functionality and the period of use.[17]

The development of materials with cartilage-like features has steadily gained significance in the recent years. Since articular cartilage has a load bearing function with compressive strength values from 14 MPa up to 59 MPa,[14-15] an Equilibrium Water Content (EWC) between 60 and 85 wt%,[18-20] as well as a very low Coefficient of Friction (COF) (0.001-0.5)[21]; developing of materials that mimic these biological features is highly challenging. Novel hydrogels systems,[76] such as double network (DN) hydrogels,[20,28,76-78] fibre-reinforced DNs,[14] nanocomposite hydrogels,[16,79-80] and Extracellular Matrix (ECM)-based materials[81] have been developed in the recent years in order to obtain materials with highly tough mechanical properties and tissue-like water content.[76,82] Among all these materials, double network hydrogels with at least one polyelectrolyte component such as salts of poly(2-acrylamido-2-methylpropansulfonic acid) (PAMPS)[14,76,83-86] and poly(acrylic acid) (PAA)[59,87-90] have been particularly highlighted as potential cartilage-like materials. Thus, the incorporation of ionic components into the network leads not only to a better hydration of the hydrogel, but also to the improvement of the mechanical properties by hydrogen bonding and/or ionic interactions between the polymers involved.[28,44,76,82,91] Several double-network systems as promising artificial cartilage have been reported. Many of them have been based on the work done by GONG,[31] in which PAMPS/PAAm DN gels with a water content of 90 wt% could bear up to 17 MPa of compressive stress. MEANS et al.[76] showed a DN hydrogel based on PAMPS/(PNIPAAm-*co*-AAm) with cartilage-like performance, with compressive strength of 25 MPa and water content values between 80-85 wt%. DING et al.[59] reported a hydrogel composite of $P(AA_{0.35}$-*co*-$AM_{2.0})/XG_{1.0}$-$GG_{1.0}/Fe^{3+}$/B,

which exhibited a compression strength above 15.3 MPa and a water uptake up to 72 wt%. The mechanical behaviour of both mentioned systems were determined in distilled water; however, only B. J. WILEY et al.[14] have recently presented a system based on bacterial cellulose, poly(vinyl alcohol) (PVA), and PAMPS, which has cartilage-like performance in a physiologically relevant medium, 0.15 M PBS buffer. This material takes up around 55 wt% of water and shows a compression strength of 17.3 MPa similar to the natural idol and an exceptional wear resistance.[17]

Although these materials are very promising, the water uptake and therefore the mechanical properties of polymer networks with ionic components strongly vary with environmental conditions, such as pH and ion/salt concentration.[90,92-93] Thus, environmental changes during the *in vivo* implementation could cause problems, because the ionic network materials can change their dimensions and mechanical behaviour in presence of fluids such as blood.
Presumably, most suitable material for cartilage replacement would be one that does not undergo great variation in either water-uptake or mechanical performance upon environmental changes. Such a material would be more easily handled and would not substantially change dimensions or functionality upon implementation. In this work, we report on novel double network hydrogels based on poly(2-oxazoline)s (POx) and non-ionized poly (acrylic acid) with excellent mechanical cartilage-like behaviour as potential new materials for artificial cartilage in varying physiologically relevant media.

3.3 RESULTS AND DISCUSSION

The goal of this work was to create a DN hydrogel with cartilage-like mechanical properties in physiological environments that are not strongly affected by the concentration of salts and other compounds. Thus, the double network should facilitate strong reversible bonds, such as hydrogen bridges, but no ionic functions.[17] A strong hydrogen bond former is poly(acrylic acid), which has already been used as component to create stiff and strong physically cross-linked DN hydrogels with potential biomedical applications.[92,94-96] However, PAA based networks tend to lose their excellent mechanical behaviour in non-acidic environments, because the carboxylic acid groups of PAA are mostly deprotonated in aqueous medium with a pH-value above 4.7. In consequence, the formation of H-bonds between the networks involved are impaired. For example, previously reported DNHs based on PAA and PEG showed excellent mechanical strength at pH values up to pH 4, but above this a dramatical reduction of the strength was

observed.[90,97] Interestingly, it has been reported that the pK_a value of poly(acrylic acid) can be shifted to higher values in the presence of polymer networks with hydrophobic components, or a high degree of hydrogen bonding between the networks.[98-99] Several studies have emphasized the capability of POx to form stable hydrogen bonds with PAA or tannic acid (TA), particularly in Layer-by-layer (LbL) systems.[98,100-102] Thus, these systems are more stable at higher pH values. We have explored, if this is valid for DN hydrogels based on these two polymers (see Figure 1). To this end, telechelic poly(2-methyl-2-oxazoline) (PMOx) and poly(2-ethyl-2-oxazoline) (PEtOx) with acrylate end groups and different degree of polymerizations (25, 50, 100) were prepared by cationic ring-opening polymerization followed by end-group modification with N,N-dimethylaminopropylmethacrylamide (DMAP-MAA). Such end group functionalized POx have already been successfully used to form POx based homo-networks or amphiphilic conetworks.[69,103-105] All polymers could be obtained with narrow molecular weight distributions and nearly complete end group functionalization (see Table 3 in experimental section).

The telechelic POx were cross-linked as films from their aqueous solutions via photo-polymerization. These primary networks were thoroughly rinsed in water for around 24 h, which is important to obtain a homogenous material as end product. Then, the single POx networks were soaked in a neat monomer solution of acrylic acid, containing photoinitiator and crosslinking agent (tetraethylene glycol dimethacrylate, TEGDMA), after which the swollen hydrogels underwent photopolymerization. The final DNHs were washed with water for at least 48 h and then given to a high access of the aqueous test medium and conditioned for at least another 48 h. The obtained DN hydrogels are transparent, bendable materials (see Figure 9).

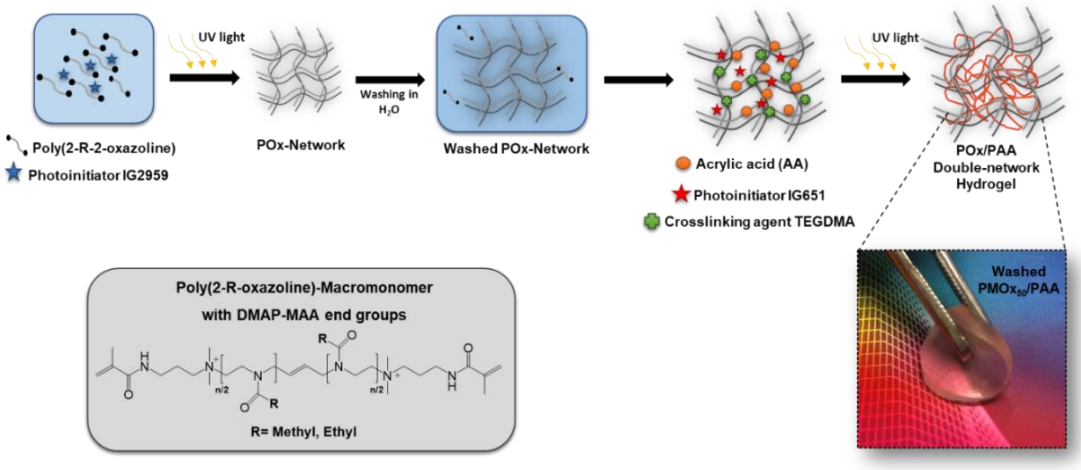

Figure 9: *Steps of the synthesis of POx/PAA double-networks hydrogels.*[17]

The water content (WC) of articular cartilage is estimated to be 60 to 85 wt%. Water enables the exchange of nutrients, salts and, other metabolites through the cartilage matrix[106] and its content is used as indicator for cartilage damage.[107] It was observed that the water uptake of the POx/PAA hydrogels is mainly controlled by the degree of polymerisation of the macromonomer, i.e. by theoretical mesh size of the primary POx-single network. DNHs based on POx macromonomers with a degree of polymerisation of 25 exhibited water contents with values of 48 ± 4 wt% for $PMOx_{25}$ and 50 ± 2 wt% for $PEtOx_{25}$ in PBS (pH 7.4) solution, which are too low and consequently not suitable to be used as cartilage replacement. DNHs based on PMOx with 50 and 100 repeat units showed WC values between 66 ± 3 and 88 ± 1 wt% in PBS, which corresponds to the WC-range of articular cartilage[17]. The respective PBS-swollen $PEtOx_{50}$/PAA DNH contains 59 ± 6 wt% of water and 74 ± 1 wt% for $PEtOx_{100}$/PAA, which is most likely due to the less hydrophilic character of PEtOx. All highly, PBS swellable DNHs were subjected to mechanical testing (see Figure 10).

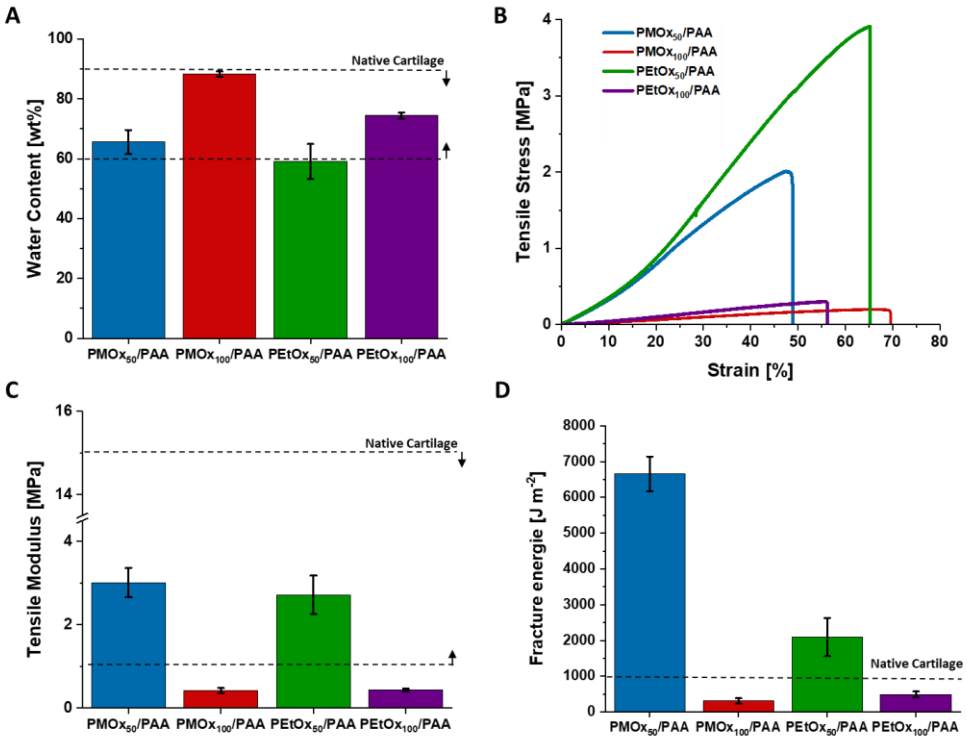

Figure 10: *A) Water Content (WC), B) initial tensile Stress-Strain curve, C) tensile modulus, D) fracture energy of DNHs $PMOx_{50}$/PAA, $PMOx_{100}$/PAA, $PEtOx_{50}$/PAA and $PEtOx_{100}$/PAA in PBS (pH 7.4) media. The corresponding literature values for water content[18-20], initial tensile modulus[108-109] and fracture energy[16] of native articular cartilage are indicated by black lines. Values in Figures A, C and D are expressed as mean ± SD (n = 4-5). The tensile stress-strain curves are recorded with a strain rate of ≈ 0.001 s^{-1}. The reference values for cartilage from the literature are recorded at similar strain rates.[17]*

As seen in Figure 10, only DNHs composed of POx with a degree of polymerization of 50 show a stiffness in PBS of around 3 MPa, which might be suitable for artificial cartilage, while the DNHs based on the respective polymers with 100 repeating units are not stiff enough for this purpose. Interestingly, the significantly less swollen $PEtOx_{50}$-based DNH does not exhibit a higher stiffness compared to the respective $PMOx_{50}$-based system. This might be due to the less strong hydrogen bridges formed between PAA and PEtOx. A different scenario is found, when determining the tensile fracture energy. This experiment includes the propagation of a crack in the stress-stain-experiment. As seen in Figure 10-D, the tensile fracture energy of the $PMOx_{50}$ system is with 6.9 ± 0.7 kJ m^{-2} exceptionally high. In contrast, the $PEtOx_{50}$/PAA DNH exhibits a tensile fracture energy of 2.1 ± 0.5 kJ m^{-2}, which is much lower than that of the $PMOx_{50}$ system, but still higher than that of natural cartilage (1 kJ m^{-2}).[16] This can be explained by the fact that the PEtOx system is not as homogeneous as the respective PMOx-based DNH. This can cause an easier crack propagation. In comparison, DNH $PMOx_{100}$/PAA and $PEtOx_{100}$/PAA showed a poor mechanical behavior when stretched.[17]

Based on these results, it can be assumed that the interactions by hydrogen bonds between the segments of PAA and PMOx inside the network serve as sacrificial bonds in order to dissipate the mechanical stress effectively, leading to DHNs with remarkable toughness. The cross-linking density of the primary POx network can control the mechanical properties and water-uptake of the DNH. Particularly, the $PMOx_{50}$/PAA DNH shows a water content, stiffness and fracture energy in physiological PBS that makes it a promising candidate for artificial cartilage. Only this material was subjected to further experiments.[17]

Cartilage is a load-bearing tissue with compressive strength values between 15 and 57 MPa.[14] Mimicking of close to real physiological conditions is often performed in PBS buffer at pH 7.4, because it has the salt concentration and the pH of blood. However, the cartilage is surrounded by synovial fluid, which not only transports nutrients inside of the cartilage, but also supports the lubricity and has a cushioning-effect.[110] It is well known that egg white has similarities to the synovial fluid regarding consistence[111] and also containing glycosaminoglycans (GAGs), such as chondroitin sulfate, hyaluronic acid and keratan sulfate, which are also part of the cartilage structure/composition and play a fundamental role in the mechanical behaviour of cartilage.[18,20,112] Many studies have shown interest on hen egg white as source of exogenous GAGs such as keratin sulfate, in order to supress the cartilage damage.[113-115] Thus, we

performed the compressive test not only in PBS, but also in egg white, in order to observe the effect of GAGs in the mechanical behaviour of the DNHs.

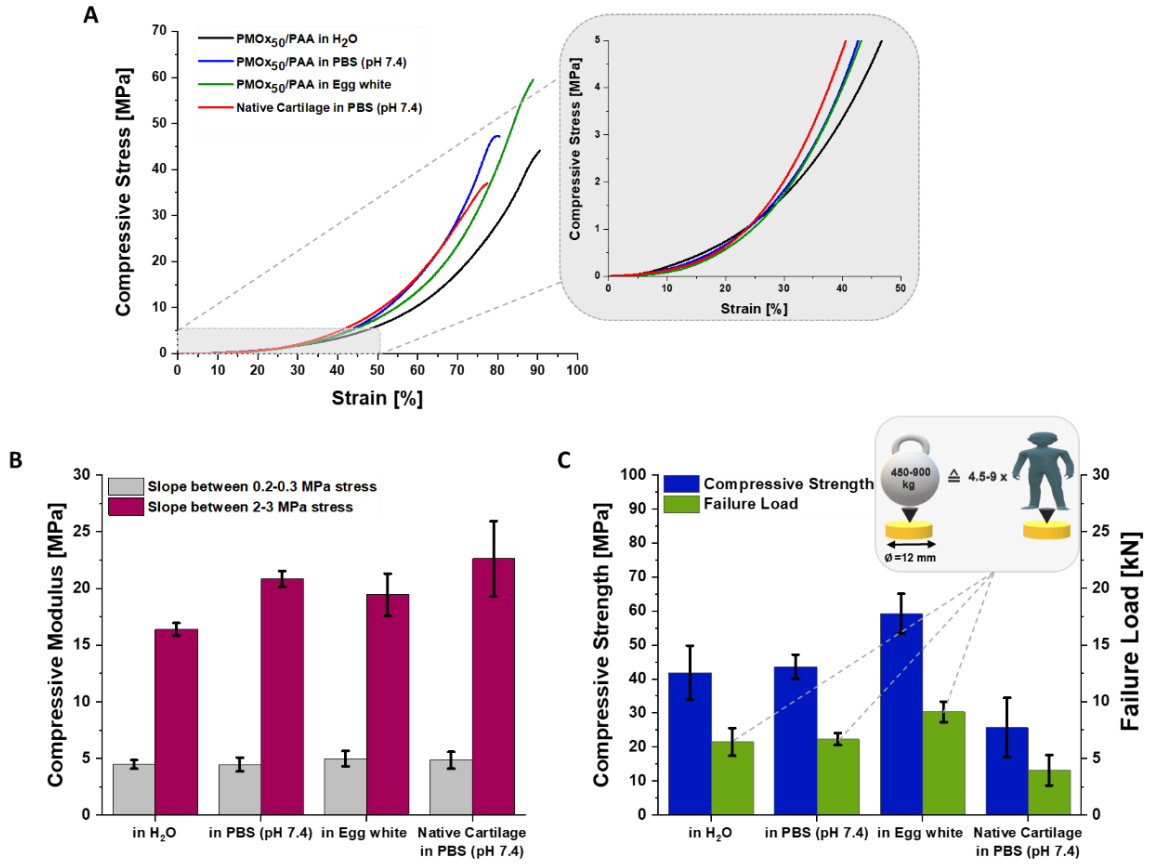

Figure 11: *A) Compressive stress-strain curve, B) compressive strength and compressive modulus, C) failure load of native cartilage in PBS (pH 7.4) and PMOx$_{50}$/PAA in PBS (pH 7.4) and in egg white media. The samples have a diameter of 12 mm and an average thickness of 2.0 ± 0.2 mm. The compressive stress-strain curves are recorded with a strain rate of 0.0043 s^{-1}. Values in (B, C) are expressed as mean ± SD (n=5).*[17]

As seen in Figure 11-A, PMOx$_{50}$/PAA in both media - PBS and egg white - exhibits a compression profile similar to articular cartilage. The compression moduli were determined from the slopes of the compression profiles in two different stress ranges between 0.2-0.3 MPa and 2-3 MPa. Both ranges are relevant; thus, it has been documented that the contact stress of articular cartilage can reach values between 0.02-5 MPa.[19,76,116] As seen in Figure 3-B, the compression moduli at a stress of 2-3 MPa of PMOx$_{50}$/PAA are 20.8 ± 0.7 MPa in PBS and 19.4 ± 1.8 MPa in egg white, which are both not significantly lower than that of articular cartilage with 22.6 ± 3.3 MPa. Noticeably, the GAGs in egg white do not influence the compression modulus of the material compared to those in PBS. The DNH also shows a similar

compression modulus in water. The compression modulus values of both materials also do not exhibit significant differences at lower stress ranges. The same effect was observed after the treatment of the DNH with the hydrolase-enzyme Lipase, which can be found in human blood (for details see supporting information). Thus, this ubiquitous hydrolase cannot easily degrade the hydrogel.

The compressive strength values of $PMOx_{50}$/PAA are 45 MPa in PBS and 60 MPa in egg white and thus both exceed that of the measured native articular cartilage in PBS (29.6 ± 8.7 MPa). Considering, that the DNH has a water content of 67 wt% in egg white, its compression strength in egg white is remarkably high. We thus assume that the GAGs in egg white have not only a shock absorber functionality, but also play a role as a third network, which protects the hydrogel from the compressive stress. Cartilage is known to have the capability to resist loads of several times the body weight.[117] The $PMOx_{50}$/PAA DNH can bear even higher loads between 450 and 900 kg, which implies the withstanding of 4.5 up to 9 times of a body weight of 100 kg in a surface area of 113 mm^2 (see Figure 11-C), it makes this DNH a promising material with an extraordinary compressive mechanical performance.[17]

Cartilage is a material that needs to withstand always varying mechanical stress. Therefore, the mechanical properties of $PMOx_{50}$/PAA hydrogels were further explored by applying a sequential dynamic movement profile. The parameter of interest in such an experiment is to determine if the material shows plastic deformation (creep) and how fast it recovers to its original state. Moreover, the mechanical properties of the material after the dynamic stress experiment are of interest. The experiment was started with a creep test applying a total constant force of 8.7 N (approx. 0.3 MPa, typical load of the human knee) to simulate the standing position for 30 min. In order to simulate the gait movement, a static force of 8.7 N and a dynamic force of 8.5 N (total stress approx. 0.6 MPa) with a frequency of 1 Hz was applied for another 30 min. A frequency of 1Hz has been reported as characteristic gait frequency.[118] Afterwards, the material was kept at 0.3 MPa for 3 min (standing) and then the load was removed (see Figure 12-A). The thickness or rather the strain of the material was measured after 1 s unloading and again after 1800 s of recovery (Figure 12-B, C).[17]

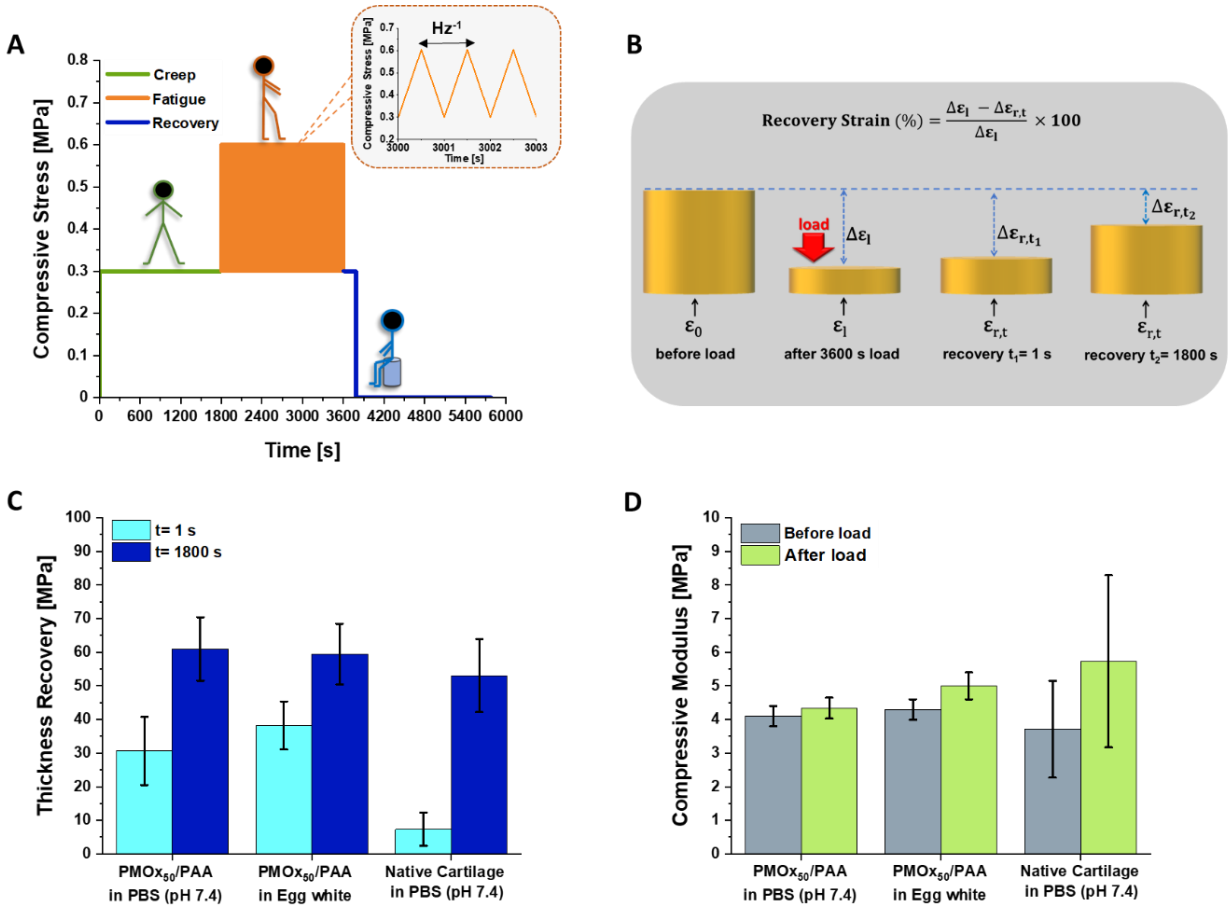

Figure 12: *A) Viscoelasticity test (creep, fatigue and recovery), B) illustrated determination of the recovery strain, C) recovery strain and D) compressive modulus of native cartilage in PBS (pH 7.4) and PMOx$_{50}$/PAA in PBS (pH 7.4) and in egg white media. The samples have a diameter of 6 mm and an average thickness of 1.8 ± 0.2 mm. Values in (C, D) are expressed as mean value ± SD (n = 5).*[17]

As seen in Figure 12-C the DNH exhibits in both media - PBS and egg white - a higher instantaneous recovery of its initial thickness than native cartilage. However, after 30 minutes both materials showed a no significant difference of their thickness recovery with values of 53 ± 11%, 59 ± 9% and 61 ± 9% for the native cartilage, DNH in egg white and in PBS, respectively. One reason for the faster recovery of the PMOx$_{50}$/PAA hydrogels could be linked to the differences of the compressive modulus before and after the load exposure (see Figure 12-D). The PMOx$_{50}$/PAA exhibited a slight increase of their compressive modulus compared to cartilage. Thus, the DNH in the different media was not as strongly deformed by the load as cartilage, and so can recover more quickly. The slow deformation recovery of cartilage compared to DNHs has been also observed in a work of GRUNLAN et al.[76], in which PAMPS/P(NIPAAm-*co*-AAm) double network hydrogels and cartilage were subject to a creep test with a compressive stress of 0.35 MPa for 1 h. While the DN showed recovery strains above

70% immediately after removal of the load, a recovery strain of 6-8% was observed for cartilage. After 30 minutes of recovery, cartilage and the PAMPS/P(NIPAAm-*co*-AAm) exhibited recovered strain values between 80-90%.[17]

Having established that the $PMOx_{50}$/PAA shows mechanical properties similar to native cartilage, it was next investigated whether the material also possesses a low coefficient of friction (COF), which is a crucial characteristic of the natural biomaterial. To this end, the DN hydrogels was swollen in PBS (pH 7.4) and egg white, respectively, and subjected to a tribological test applying a load of 5 N (maximum Hertzian contact stress 1.2 MPa) with a sliding velocity of 5 mm s^{-1} at room temperature for 1 h (375 laps with a stroke length of 8 mm).[71]

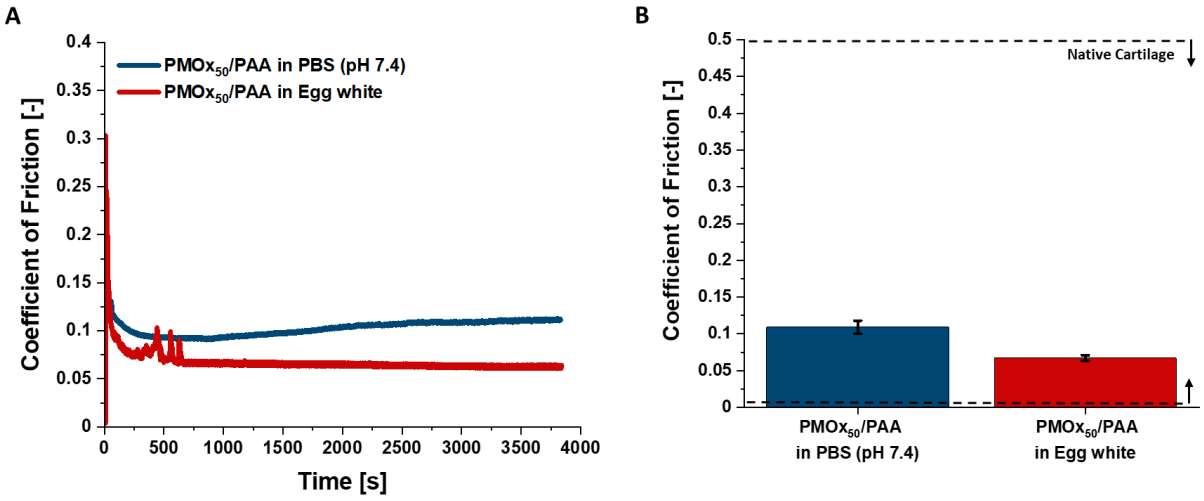

Figure 13: *A) Coefficient of friction vs time and B) coefficient of friction of $PMOx_{50}$/PAA in PBS (pH 7.4) and egg white as swelling media and lubricant. The black lines indicate the corresponding native articular cartilage values [21]. Values in (B) are expressed as mean value ± SD (n = 4).[17]*

As seen in Figure 13-A the DNH has a COF in PBS of 0.11 and in egg white of 0.07. Both values are well in the range of COFs given for natural cartilage in the literature. The kinetics of the friction experiment shown in Figure 13-B indicates that the COF quickly drops at the beginning in both media. In the case of PBS (pH 7.4) as medium, the friction coefficient slightly increases with time, while the COF in egg white remains constant after the initial drop. The lower friction of the DN hydrogels in egg white confirms the suitability of the latter as synovial fluid substitute, which is responsible for the low friction of cartilage in the body. The

tribological test also confirms the remarkable mechanical performance of the PMOx$_{50}$/PAA DNHs in relevant physiological media.[17]

As already mentioned, a particularity of networks with polyelectrolyte components is the response of the swelling and mechanical behaviour to changes in the salt content and in the pH value of the swelling media. In order to avoid this, we choose the system POx and PAA, because the strong hydrogen bonds between these two would increase the pK$_a$ value of PAA. Thus, the DNH might not undergo deprotonation even in physiological environments and would thus retain its excellent mechanical properties. In order to confirm this and to explore the limitations of the material, the PMOx$_{50}$/PAA hydrogels was conditioned in media with varying the pH value of PBS solution for one week and the degree of swelling and the compressive strength was determined (see Figure 14).[17]

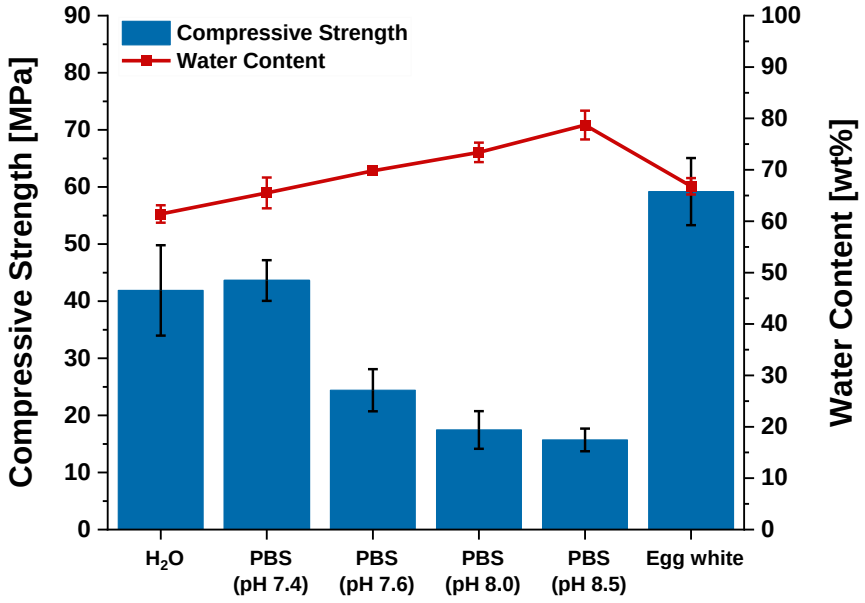

Figure 14: *Effect of the pH-value on the mechanical performance of PMOx$_{50}$/PAA. All materials were swollen in a high excess of the respective medium at room temperature for at least 48 h before determining the mechanical performance in the corresponding medium. The samples have a diameter of 12 mm and an average thickness of 2.0 ± 0.2 mm. Values are expressed as mean value ± SD (n = 5).*[17]

As seen in Figure 14, the water uptake of the DNH in water, PBS (pH 7.4), and egg white, respectively, is nearly identical in a range of 61-67 wt%. The compressive strength is similar in water and PBS, clearly showing that salt concentration and a pH of up to 7.4 do not affect the

material. Increasing the pH value in PBS to 7.6 results in increased water uptake of 70 wt% and a drop in strength to almost half (24.4 MPa) the value at pH 7.4. Further increasing the pH to 8.0 and 8.5 results in an increased water uptake and a somewhat less dramatic drop in strength. In order to find, what causes the pH-induced changes in swelling and strength, FTIR spectra of $PMOx_{50}$/PAA in media with different pH values were recorded (see Figure 15).

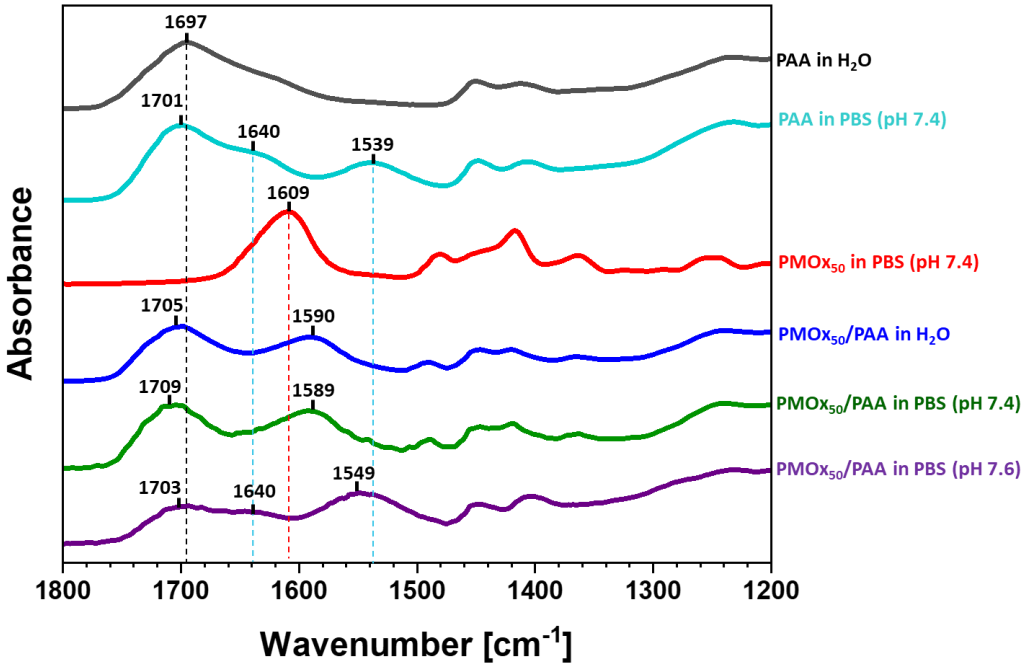

Figure 15: *FTIR-spectra of the single networks, PAA and $PMOx_{50}$, and $PMOx_{50}$/PAA double network hydrogels in H_2O and in PBS at pH-values between 7.4 and 8.5.*[17]

As seen in the top of Figure 15, the FTIR spectrum of a PAA single network exhibits the characteristic peak of the stretching vibration of the C=O function of the protonated carboxylic acid at 1697 cm^{-1}. When treating this PAA network with PBS buffer, pH 7.4 overnight, the FTIR spectrum of the dried material is significantly changed as seen by the appearance of two new peaks at 1640 cm^{-1} and 1539 cm^{-1}, which are typical for the deformation vibrations of C-OH and the symmetrical stretching of COO^- of the salt form of PAA.[119-120] The still existing peak at 1701 cm^{-1} of the protonated carboxylic group indicates that the deprotonation of PAA in not complete in PBS, pH 7.4. The third spectrum from the top of Figure 15 is of the PMOx single network with the typical C=O stretching vibration at 1607 cm^{-1}. The FTIR spectrum of the $PMOx_{50}$/PAA washed with water is characterized by two dominant peaks at 1705 and 1589 cm^{-1}. The first signal can be attributed to the carboxylic acid function of PAA, while the second

peak is the red-shifted peak of the C=O stretching vibration of PMOx. This red shift is a strong indicator of the formation of hydrogen bridges between PMOx and PAA including all C=O functions of the first. This DNH was soaked in PBS, pH 7.4, overnight and dried. The FTIR spectrum of this network looks exactly the same as that of the DNH just treated with water, indicating that no deprotonation of the acid functions occurs in contrast to the free PAA network. Next, the DNH was soaked in PBS, pH 7.6, overnight and dried. The FTIR spectrum of this material shows a new signal at 1540 cm^{-1}, which is attributed to the salt form of PAA and an almost complete disappearance of the signal at 1590 cm^{-1}, which is the marker for the hydrogen bonds. These results show that the combination of PAA and PMOx in a DNH results in a dramatic apparent increase in the pK_a value of PAA due to strong hydrogen bond formation. The DNH does not deprotonate in PBS pH 7.4 and thus retains its excellent mechanical strength in this environment. However, increasing the pH to only 7.6 leads to strong deprotonation and a drastic drop in strength due to the destruction of the hydrogen bonds.[17]

In addition to the mechanical behaviour, another important aspect for the implementation of an artificial material is its cytocompatibility. PAA is a well-known biocompatible material. POx is also discussed to be biocompatible. However, there are studies that show that POx with certain end groups can be enzyme inhibitors.[121-122] On the other hand, modification of proteins with POx does not deactivate the enzymes.[123-124] Therefore, it is necessary to explore the cytotoxicity of the POx-based material. To this end, the $PMOx_{50}$/PAA samples were placed in a petri dish only covering a part of the bottom. Then human mesenchymal stem cells (hMSC) were placed on top and incubated for 24 h. Afterwards, the samples were photographed, and the viability of the cells was determined with a fluorescence assay (see Figure 16).

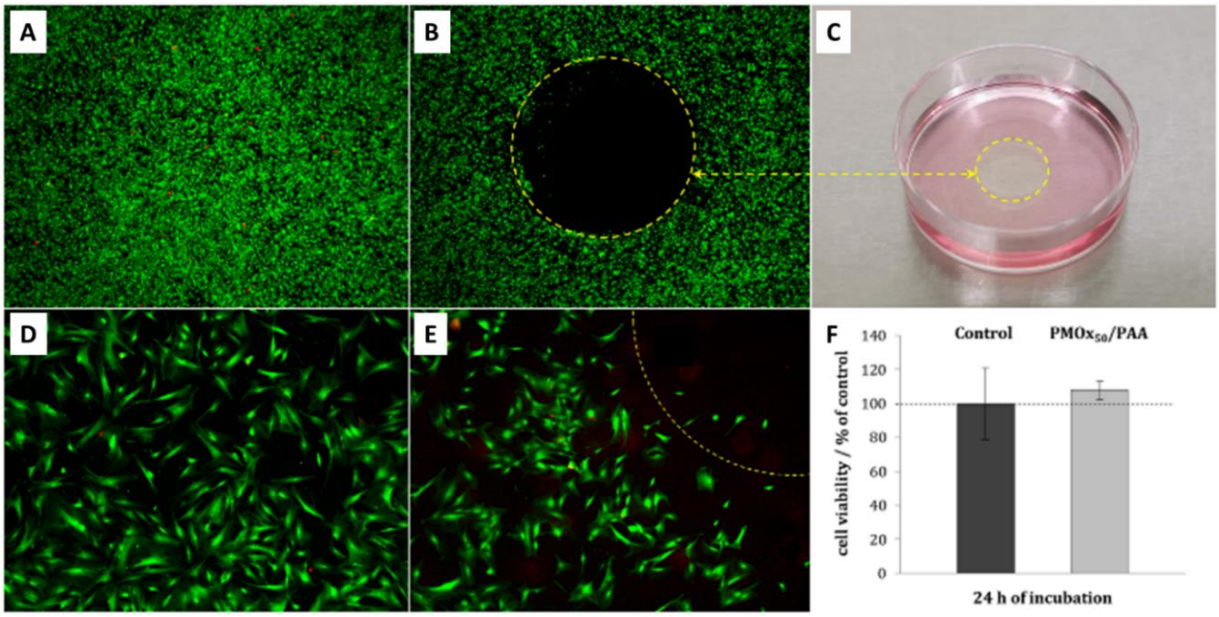

Figure 16: *Cell morphology and viability of hMSC in the presence of $PMOx_{50}$/PAA DNH after 24 h of incubation. Cells were stained with calcein-AM (green fluorescence) and PI (red fluorescence) to visualize the morphology of live and dead cells, respectively. (A, D) Representative fluorescence images of hMSC control (cultivated on a cell culture petri dish without hydrogel). (B, E) Representative fluorescence images of hMSC cultivated in the presence of $PMOx_{50}$/PAA DNH. (C) Representative light microscopic image of $PMOx_{50}$/PAA DNH placed in the middle of a cell culture petri dish in RPMI/FCS. (F) Quantification of cell viability of hMSC performed by phase analysis of the calcein-AM staining using a region of interest. Data are expressed as mean value ± SD of n≥3 independent experiments and given as the percentage of hMSC control.*[17]

As seen in Figure 16-B, C, the stem cells did not grow on top of the hydrogel, which is a typical and desirable feature of cartilage-like materials due to their hydrogel character. However, the cells did attach and grow to the very proximity of the DNH indicating that the material does not leach toxic components. This is also shown by the spreading of the cells, which looks very much like that of the control (see Figure 16-D, E). The viability of the cells was also not affected as seen in Figure 16-F. Altogether, it can be stated the $PMOx_{50}$/PAA is not cytotoxic and does not allow attachment and growth of human stem cells on its surface.

3.4 Conclusion

In summary, the novel PMOx/PAA networks were developed to use the pK_a shifting effect of the combination of PAA and POx to obtain a non-ionic high-performance double network hydrogel. The resulting material is shifting the pK_a of PAA by almost three orders of magnitude, which makes the material a cartilage-like hydrogel, which does not react on environmental salt

concentration changes or pH changes up to 7.4. The hydrogel takes up to 66 wt% of water and has a two to three-fold higher compression strength than other cartilage-like materials (see Table 1). The strong drop of mechanical integrity also makes it a smart material with a potentially very narrow pH switching range.

Table 1: *The mechanical properties of $PMOx_{50}$/PAA DNH are compared with native cartilage and previously reported hydrogels with cartilage-like mechanical performance. This table was taken from the supporting information content from BENITEZ-DUIF et al. [17]*

Material	WC [%]	Thickness [mm]	Compressive Modulus [MPa]	Compressive Strength [MPa]	Coefficient of Friction [-]	Swelling Medium
Native Articular Cartilage	60 - 85[18]	1-3[125-126]	0.24-0.85[127] 1.3-20[128]	14-59[15]	0.005 – 0.57[21]	-
BC-PVA-PAMPS (22.1%-40%-146kD-30%-mM)[14]	55.5	0.7	13.7 (0.4 MPa; 0.05 s^{-1})[a)]	17.3	0.06	0.15 M PBS
P($AA_{0.35}$-*co*-$AM_{2.0}$)/$XG_{1.0}$-$GG_{1.0}$/Fe^{3+}/B[59]	72	2	34 (6-12 MPa; 0.04 s^{-1}) [a)]	>15.34	-	DI water
PAMPS/P(NIPAAm-*co*-AAm)[76]	80 - 85	1-2	1 (0-0.05 MPa; 0.008 s^{-1}) [a)]	25	0.02 (in FSB)	DI water
PVA/1.5wt%GO-PEG[80]	-	8	1.12 (0.125 MPa; 0.002 s^{-1}) [a)]	> 2	0.06-0.09 (in NS, FSB)	-
$PMOx_{50}$/PAA **(This work)**	**62 - 68**	2	**5** (0.2-0.3 MPa; 0.013 s^{-1})[a)] **20** (2-3 MPa; 0.013 s^{-1}) [a)]	**42 -59**	**0.07- 0.11**	DI water PBs (pH 7.4) Egg white

a) Corresponding strain rates (in s^{-1}) and stress values (in MPa) from the compression curve used to determinate the compressive modulus.

3.5 EXPERIMENTAL SECTION/METHODS

-***Materials*:** Chloroform (Fischer Scientific) was distilled from activated aluminum oxide (Merck) under reduced pressure und under argon atmosphere stored. The monomers 2-methyl-2-oxazolin (MOx) and 2-ethyl-2-oxazoline (EtOx) were obtained from Acros Organics, these were distilled over CaH_2 (Acros Organics). *Trans*-1,4-dibromo-2-butene (DBB, Acros Organics) was recrystallized twice from n-heptane (Fischer Scientific). N,N-Dimethylaminopropylmethacrylamid (DMAP-MAA, Sigma-Aldrich) was under reduced pressure distilled. All distilled chemicals were under argon atmosphere and at -20°C stored.

Acrylic acid (AA, 98% extra pure, Acros Organics), Irgacure 2959 (IG2959, >98%, TCI-Europe), Irgacure 651 (IG651, Ciba Specialty Chemicals), Tetraethylene glycol dimethacrylate, (TEGDMA, Sigma-Aldrich), methanol (Fischer Scientific), diethyl ether (Honeywell Riedel-de-Haën™). The phosphate buffered saline, 10x Solution (10xPBS, Fischer Scientific) was diluted for the measurements with distilled water to a 1xsolution (1xPBS) with a pH value of 7.4. Egg white from fresh hen eggs. The porcine native cartilage of German Edelschwein (6-8 months old) were kindly provided from Schultenhof Dortmund, Germany.[17]

-Synthesis of poly(2-oxazoline) macromonomers with DMAP-MAA end groups: The synthesis of telechelic PMOx and PEtOx with different degree of polymerization was performed according to previously works of TILLER et al.[69] The cationic ring opening polymerization of 2-methyl-2-oxazolin (MOx) and 2-ethyl-2-oxazoline (EtOx) with DBB as initiator was carried out in dry chloroform (20 mL) under argon atmosphere in an industrial microwave reactor. Since die polymerization time and temperature depends on the degree of polymerization and monomer´s type, the polymerization time and temperature for the different polymers are liste in Table 2. The living ends of all polymers were terminated with N,N-Dimethylaminopropylmethacrylamid (DMAP-MAA) in a 10-fold molar excess (respect to the initiator) at 49 °C for 72 h. The resulting polymeric product was purified by precipitating the polymers three times in ice-cold diethyl ether and then dialyzed against mixture of methanol/H_2O (1:1) using benzoylated cellulose membranes (1000 MWCO). The methanol was first removed under reduced pressure and the remaining aqueous solution was dried by lyophilization.[17]

Table 2: *Composition and polymerization conditions for the synthesis of PMOx and PEOx with DMAP-MAA end groups.*[17,71-73]

Polymer	m_{DBB} [g]	$V_{Monomer}$ [a)] [mL]	Time [h]	Temperature [°C]	$V_{DMAP-MAA}$ [b)] [mL]
$PMOx_{25}$	0.5	5	1.5	105	4.2
$PMOx_{50}$	0.25	5	2.5	105	2.1
$PMOx_{100}$	0.125	5	4	105	1.1
$PEtOx_{25}$	0.423	5	1.5	110	3.6
$PEtOx_{50}$	0.21	5	2.5	110	1.8
$PEtOx_{100}$	0.106	5	4	110	0.9

[a)]Volume of monomer (MOx or EtOx); [b)] Volume of DMAP-MAA to functionalization of PMOx and PEtOx.

-Characterization of poly(2-oxazoline) with DMAP-MAA end groups: The degree of polymerization (DP) of the synthetized polymers and their degree of functionalization (F, in %) with DMAP-MAA were determinated by ^{1}H NMR spectroscopy, using an Agilent AV500/AV400 spectrometer at 25 °C and $CDCl_3$ as solvent (See Figure 17 and 18). The molecular weight (M_n, M_w) and the dispersity (Đ) of the polymers were obtained by size exclusion chromatography (SEC) and are reported in Table 3. The SEC was performed on a Viscotek GPCMax with a refractive index detector at 55°C, and as eluent a saline N,N-dimethylformamide (DMF + LiBr, 20 mmol). The calibration standards were poly(styrene) (Viscotek). This part was taken from the supporting information content from BENITEZ-DUIF et al.[17]

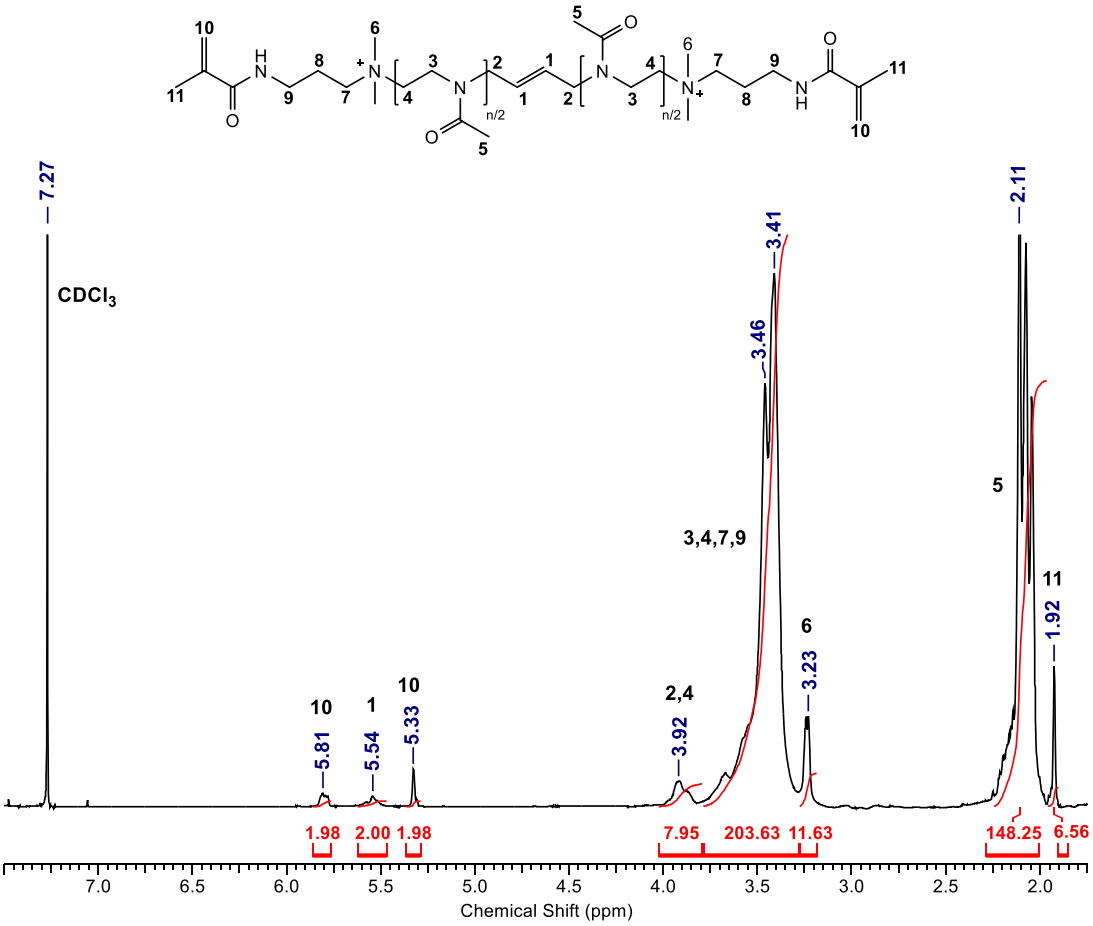

Figure 17: *^{1}H-NMR spectrum of $PMOx_{50}$ with DMAP-MAA end groups in $CDCl_3$ at 400 MHz. This figure was taken from the supporting information content from BENITEZ-DUIF et al.[17]*

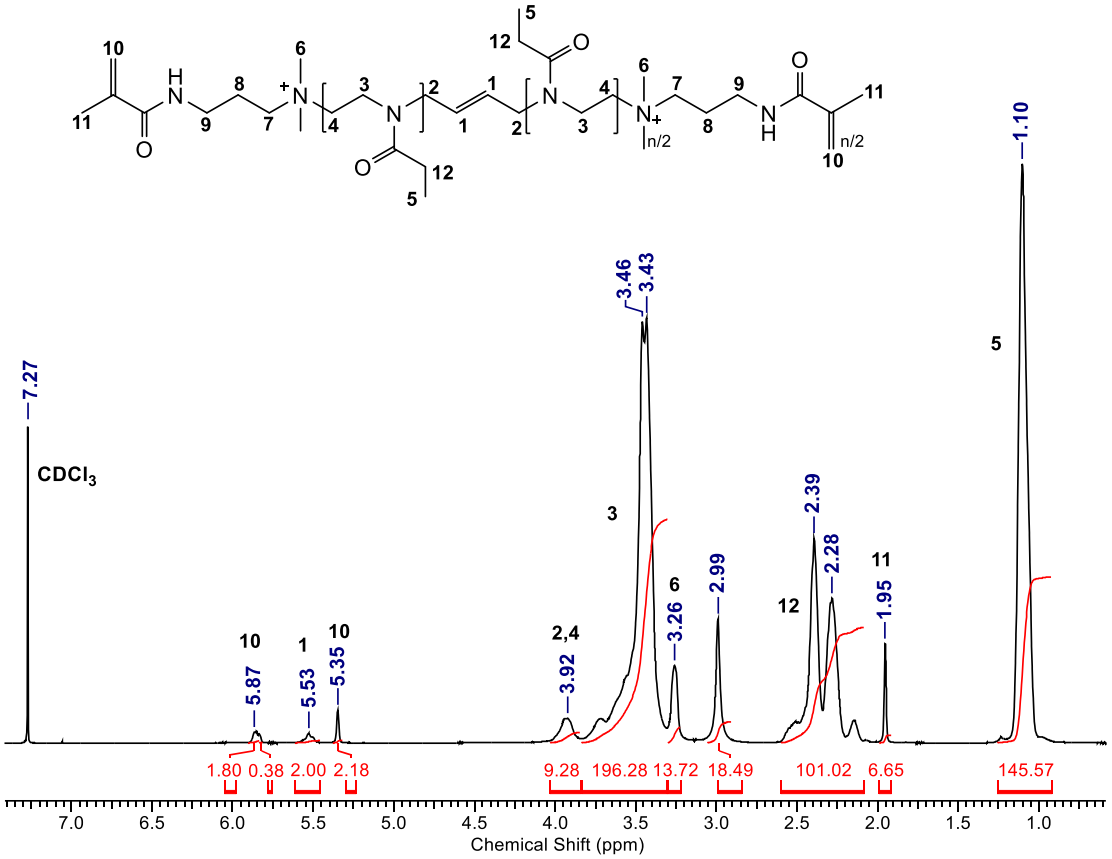

Figure 18: *^{1}H-NMR spectrum of PEtOx$_{50}$ with DMAP-MAA end groups in $CDCl_3$ at 400 MHz. This figure was taken from the supporting information content from BENITEZ-DUIF et al.[17]*

Table 3: *Analytical data of the synthetized POx with DMAP-MAA end groups. This table was taken from the supporting information content from BENITEZ-DUIF et al.[17]*

Polymer	DP,$_{NMR}$ [-]	$M_{n,NMR}$ [g mol^{-1}]	$M_{n,SEC}$ [g mol^{-1}]	$M_{w,SEC}$ [g mol^{-1}]	Đ [-]	F-$_{DMAP-MAA}$[a)] [%]
PMOx$_{25}$	25.4	2549	3124	3644	1.16	98
PMOx$_{50}$	50.2	4663	5370	6308	1.17	99
PMOx$_{100}$	100.7	8935	9700	10700	1.21	94
PEtOx$_{25}$	24.2	2787	2865	3397	1.19	98
PEtOx$_{50}$	49.4	5258	5429	6164	1.13	90
PEtOx$_{100}$	104.7	10750	8234	9931	1.21	93

[a)]Degree of funtionalization of POX with DMAP-MAA end groups.

-Fabrication of the POx/PAA double network hydrogels: The double-networks hydrogels based on POx/PAA were synthesized via the two-step polymerization method, which was first developed by GONG et al.[31] The primary hydrogel network was prepared from an aqueous solution with 34 wt% macromonomer POx with DMAP-MAA end groups and photoinitiator

IG2959 (4.6 wt% respect to the macromonomer). This precursor solution was placed between two microscope slides, which were previously coated with poly(propylene)-tape and separated by 1.05 mm thick spacers for the compression-tested samples. Spacers with 0.35 mm thickness were used for tensile-tested hydrogels, so that these could be fixed between the clamps of the tensile tester. Then, it reacted in an UV curing chamber (Emmi-Classic automatic, 36 W, λ = 340 nm) for 36 min (switching each side every 2 min). Upon the exposure to the UV light, the macromonomer underwent a free-radical induced polymerization to form a stable POx primary network (1N). Afterwards the POx network was soaked in DI water over night, in order to remove the unreacted macromonomers and impurities.[17]

To incorporate the poly(acrylic acid) (PAA) based second network, the first network was carefully removed from the water and immersed in an acrylic acid (AA) solution containing the photoinitiator IG651 (0.24 wt% with respect to AA) and tetraethylene glycol dimethacrylate (TEGDMA) as crosslinking agent (0.22 wt% with respect to AA) over night. Afterwards, the swollen hydrogel was placed between the glass plates and cured under UV source for another 20 min (switching each side every 2 min). The final POx/PAA double network (DN) hydrogel was removed from the glass plates and washed thoroughly with water for at least 48 h. All washed DN hydrogels were dried at room temperature and given in the corresponding swelling media (H_2O, PBS (pH 7.4) and egg white) at least 48 h before the measurements.[17]

-Determination of the water content: Four dry hydrogel samples with 6 mm diameter were weighted ($m_{d,1}$) and immersed in DI water, PBS (pH 7.4), and egg white, respectively, until reaching equilibrium, which corresponds to a swelling time of at least 48 h. After the samples were swelled, they were dried under vacuum at 45 °C for 48 h. In order to determinate the water content (WC) by neglecting other components such as salt or protein from the swelling media, the wet (m_g) and dry (after swelling, $m_{d,2}$) weights of the DN hydrogels were compared.[17] The WC was calculated as follows and listed in Table 4:

$$\mathrm{WC\ (wt\%)} = \frac{m_g - m_{d,2}}{m_g} \times 100 \qquad (1)$$

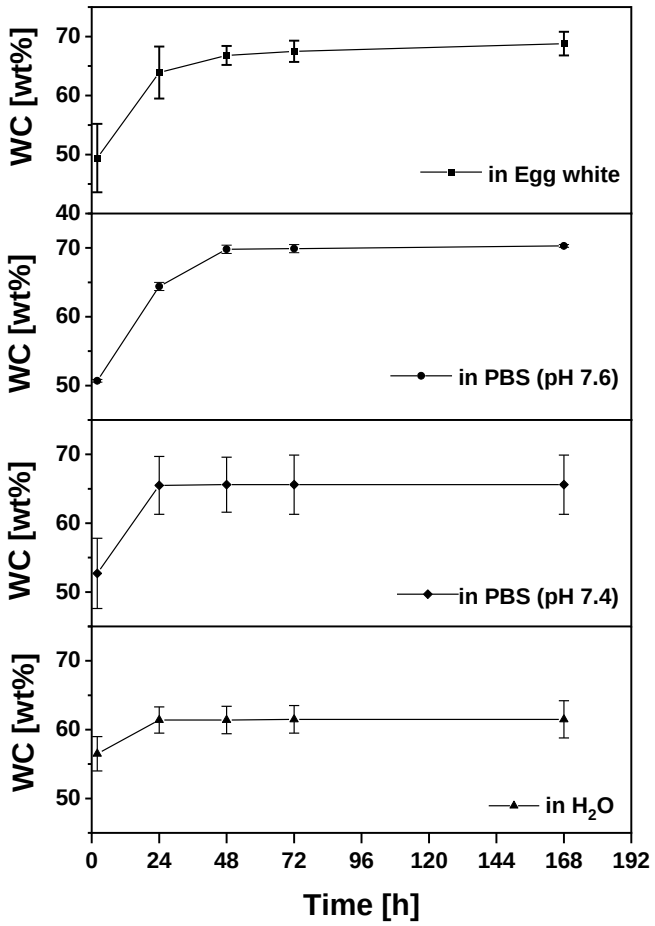

Figure 19: *Water content (WC) of PMOx$_{50}$/PAA in different swelling media for a given number of hours. This figure was taken from the supporting information content from* BENITEZ-DUIF *et al.*[17]

-Determination of the PAA content in the double-network: The PAA content in the double network was calculated from the dry weight of the POx based first network (m_{1N}) before its swelling in the acrylic acid monomer solution and the dry weight of the resulting POx/PAA hydrogel (m_{DN}) after the washing process. The PAA content in the DNHs are reported in Table 4. This part was taken from the supporting information content from BENITEZ-DUIF et al.[17]

$$\text{PAA}\ (\%) = \frac{m_{DN} - m_{1N}}{m_{DN}} \times 100 \qquad (2)$$

Table 4: *PAA content in the different POx/PAA networks and water content of POx/PAA in PBS (pH 7.4) and in DI water after 48 h of swelling. This table was taken from the supporting information content from* BENITEZ-DUIF *et al.*[17]

Network	Water Content of POx network[a)] [wt%]	PAA Content [wt%]	Water Content[b)] in PBS [wt%]	Water Content[c)] in DI Water [wt%]
$PMOx_{25}$/PAA	75.0 ± 0.2	66 ± 4	48 ± 4	43.3 ± 1.7
$PMOx_{50}$/PAA	85.2 ± 0.1	74 ± 5	66.0 ± 3	61. 4 ± 2.0
$PMOx_{100}$/PAA	97.1 ± 0.3	95 ± 7	88.3 ± 0.9	82.5 ± 1.4
$PEtOx_{25}$/PAA	72.1 ± 0.8	66.0 ± 1.4	50 ± 2	44.6 ± 1.3
$PEtOx_{50}$/PAA	76.0 ± 1.4	74 ± 4	59 ± 6	56.5 ± 2.4
$PEtOx_{100}$/PAA	87.4 ± 2.1	88.0 ± 0.1	74.4 ± 1.1	65.4 ± 0.9
PAA	-	100	93.1 ± 1	85 ± 4

a)Water Content of the single network based on POx in DI Water; Water content of POx/PAA double network Hydrogels in b) PBS (pH 7.4) and in c) DI water (n = 4).

-Tensile mechanical test: The tensile stress-strain-curves were recorded at room temperature using an Instron 3340 tensile tester with a cell with load 1 kN. At least four swelled rectangular samples of different POx/PAA networks with average dimensions of 5.2 mm x 40.0 mm x 0.76 mm (width x length x thickness) were fixed between the clamps with help of sandpaper resulting in effective lengths (l_o) between 23 and 24 mm. The experiment was performed at a crosshead speed of 5% min^{-1} until failure of the sample. During the entire course of the experiment, the samples were kept hydrated with the corresponding swelling media using a spray bottle. The tensile modulus was obtained from the initial slope of the stress-strain curve. The determination of the fracture of energy were determined based on previously works of TILLER et al.[120,129] Three additional samples, with the same dimensions as mentioned above, were notched in the center. The notch length corresponds to one third of the sample´s width. The tensile test of the notched samples was performed until failure as described above. This experiment allows to determinate the strain at which the notch turn into a running crack.[17] The corresponding fracture energy (Γ, in J m^{-2}) of the samples was calculated as follows:

$$\Gamma = l_o \times \int_0^{\varepsilon_c} \sigma(\varepsilon) d\varepsilon \qquad (3)$$

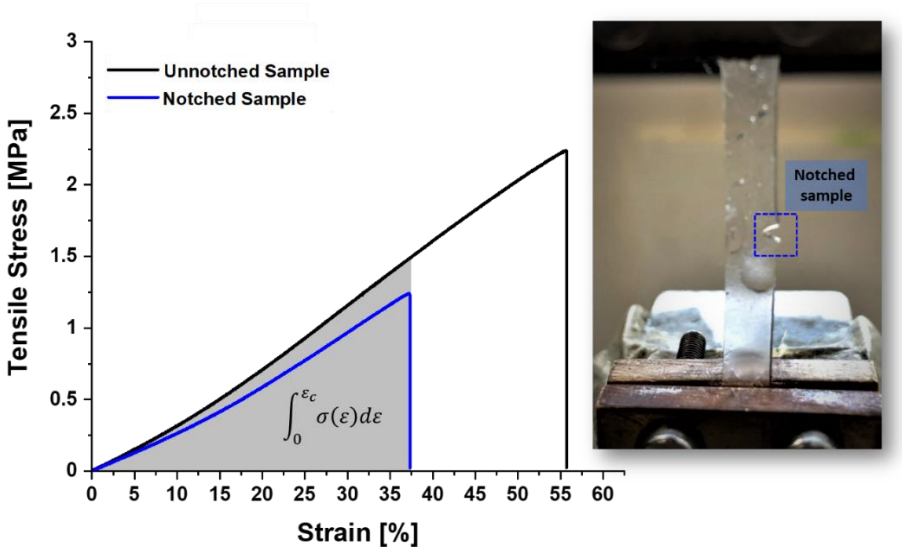

Figure 20: *Area under the curve to determination of the fracture energy for PMOx$_{50}$/PAA in PBS. This figure was taken from the supporting information content from* BENITEZ-DUIF *et al.*[17]

-Compressive mechanical test: The compressive behavior of PMOx$_{50}$/PAA and native cartilage were evaluated with an Instron 5967 tester with a cell load of 30 kN at room temperature. Five circular samples with diameter of 12 mm and thickness between 1.8 und 2.2 mm, which are thickness relevant of cartilage,[125-126] were tested. The sample was placed in the compression cell, covered with swelling media (H_2O, PBS or egg white) and compressed with an initial preload of 1N. All samples were compressed with a compressive strain rate of 0.5 mm min^{-1} until failure. Compressive stress-strain-curves were recorded. Compressive modulus values were obtained from the slope at 0.2-0.3 MPa and 2-3 MPa compressive stress, respectively.[17]

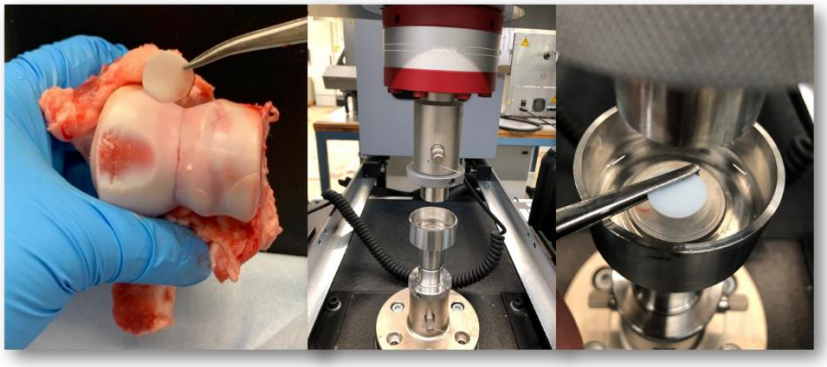

Figure 21: *Compressive test of porcine native cartilage in PBS (pH 7.4). This figure was taken from the supporting information content from* BENITEZ-DUIF *et al.*[17]

***-Viscoelasticity test*:** The viscoelastic behaviour of the $PMOx_{50}$/PAA hydrogel and native cartilage was performed by a Discovery Dynamic mechanical analysis (DMA) 850 (TA Instruments) with a compression submersion clamp. The DMA device allows a maximal total force of 18 N, in order to perform a creep sequenced fatigue test, a static force of 8.7 N and an additional dynamic force of 8.5 N were applied.[17]

The swelled samples of $PMOx_{50}$/PAA and native cartilage with 6 mm diameter and average thickness of 1.8 mm were placed in the submersion clamp and covered with the corresponding swelling media (n=5). The viscoelasticity test started with a creep test applying a total constant force of 8.7N (approx. 0.3 MPa) to simulate the standing position for 30 min. To simulate the gait movement, a static force of 8.7 N and an additional dynamic force of 8.5 N (approx. total stress 0.6 MPa) with a frequency of 1 Hz for another 30 min were applied. A frequency of 1Hz has been reported as characteristic gait frequency. Afterwards, the material was kept at 0.3 MPa for 3 min (stand) and then the load was removed. The thickness of the material was measured after 1 s and 1800 s. In addition, stress-strain curves of the samples before and after the viscoelasticity test were recorded with a strain rate of 0.5 mm min^{-1}. The compressions moduli were calculated from the slope of the curves at 0-2-0.3 MPa.[17]

Figure 22: *Viscoelasticity test by DMA of native cartilage in PBS (pH 7.4). This figure was taken from the supporting information content from* BENITEZ-DUIF *et al.*[17]

***-Tribological test*:** The coefficient of friction (COF) of the $PMOx_{50}$/PAA double network hydrogel (DNH) was determined by a ball on disc tribometer (CSM Instruments, Switzerland) with an Al_2O_3 ball (D = 6 mm) as counter body. The $PMOx_{50}$/PAA were soaked in PBS (pH 7.4) and in egg white, respectively, at least for 48 h before performing the tribological tests. Hydrogel disks with 30 mm in diameter were selected and an additional lubrication of 2 ml of the corresponding lubricant (PBS or egg white) was added. The tests were performed with a sliding speed of 5 mm s^{-1} applying a normal load of 5 N (equivalent to a Hertzian contact pressure of 1.2 MPa) which is in the range of to the joint contact stress range (0.1–5 MPa).[116] The tribological test was performed for 375 rotations using a data acquisition frequency of 10 Hz.[17]

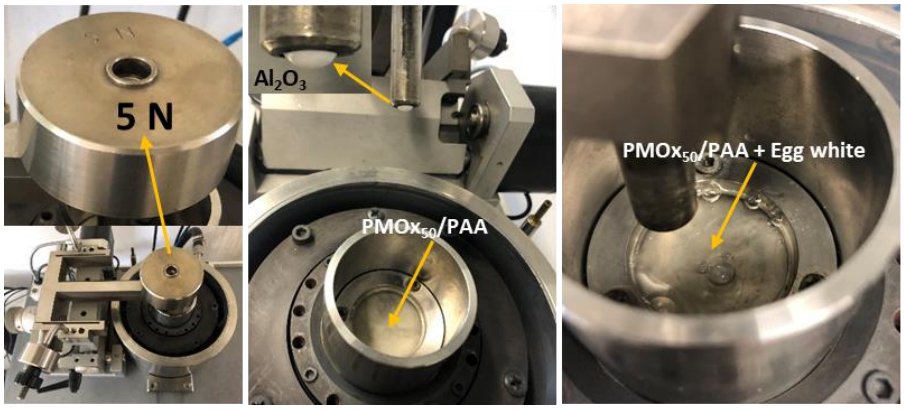

Figure 23: *Tribological test of $PMOx_{50}$/PAA network with egg white as lubricant. This figure was taken from the supporting information content from BENITEZ-DUIF et al.*[17]

-Cytocompatibility: The cytocompatibility properties of the produced $PMOx_{50}$/PAA DNH were analyzed using human mesenchymal stem cells (hMSC; Lonza, Basel, Switzerland). Cultivation of hMSC was performed in RPMI/FCS (RPMI1640 (GIBCO, Invitrogen, Karlsruhe, Germany) containing 10% fetal calf serum (FCS; GIBCO) and 0.3 g L^{-1} L-glutamine) using 75 cm^2 culture flasks (BD Falcon, Becton Dickinson GmbH, Heidelberg, Germany) in a humidified 5% CO_2 atmosphere at 37 °C (standard cell culture conditions), while sub-cultivation was performed every 7 to 14 days depending on cell proliferation. For cell culture experiments, adherent sub-confluently growing hMSC were washed with phosphate-buffered saline solution (PBS; GIBCO) and detached from cell culture flasks by 5 min of incubation with 0.2 mL cm^{-2} 0.25% trypsin/0.05% ethylenediaminetetraacetic acid (EDTA, Sigma-Aldrich, Taufkirchen, Germany) at 37 °C. Detached cells were harvested and washed twice with RPMI/FCS.[17]

Prior to biological testing, $PMOx_{50}$/PAA hydrogel disks with a diameter of 10 mm were stamped using a biopsy punch, and washed extensively in cell culture medium RPMI/FCS. Afterwards the DNHs were sterilized by 30 min of UV irradiation (UVC 500; Hoefer, Inc., Holliston, MA, USA). Sterilized hydrogel disks were placed in the middle of cell culture petri dishes (8.8 cm^2 culture area; Thermo Fisher Scientific, Waltham, USA) and hMSC were seeded at a density of 5 x 10^4 cells per mL and a total volume of 3 mL.

After 24 h of incubation, the Live-Dead assay was performed. For qualitative analysis of cell viability and morphology living cells were stained with 1 µM calcein-acetoxymethylester (calcein-AM; Calbiochem, Schwalbach, Germany; 30 min, 37 °C) and dead cells with 50 µg per mL propidium iodide (PI; Sigma-Aldrich; 10 min, RT) and the staining was analyzed by fluorescence microscopy (Olympus MVX10, Olympus, Hamburg, Germany). Quantification of cell viability was performed by phase analysis (CellSens Dimensions, Olympus). Therefore, a region of interest (ROI) was set at the location of the hydrogel within the culture dish (Figure 24-A) and the remaining calcein-fluorescent area was obtained by subtracting the area of the ROI (Figure 24-C minus 24-B and 24-F minus 24-E). The data are given as percentage of a cell control area (hMSC cultivated in cell culture petri dishes without hydrogel), which was set as 100%.[17]

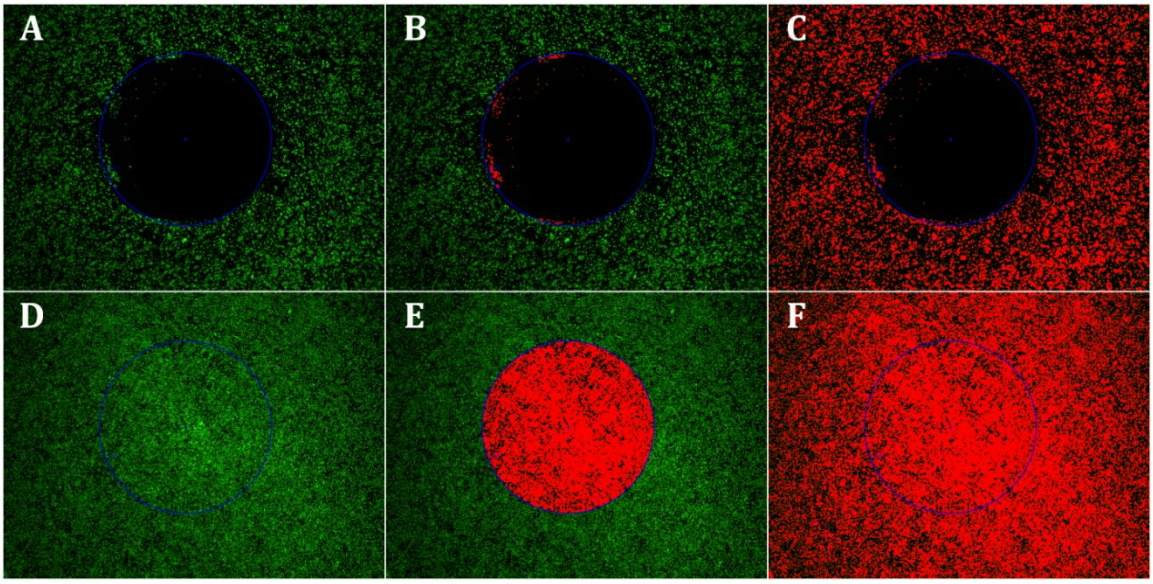

Figure 24: *Quantification of cell viability by phase analysis using a region of interest. This figure was taken from the supporting information content from* BENITEZ-DUIF *et al.*[17]

-Effect of Lipase on the compressive mechanical performance of PMOx$_{50}$/PAA: The compressive mechanical behavior of PMOx$_{50}$/PAA in presence of enzyme as lipase, which is also found in the human blood with concentrations between 40-140 U/L,[130] was carried out as follows. For this experiment, eight DNHs samples were swelled in PBS (pH 7.4) until equilibrium. Afterward, four samples were submerged in a solution of PBS (pH 7.4) with a concentration of 140 U/L of *candida rugosa* lipase (CRL, 1302 U/mg), the other four samples in PBS (pH 7.4) were used as reference. The samples remained in the corresponding media at ambient temperature for another 24h. The PMOx$_{50}$/PAA samples with diameter of 12 mm and thickness 2.0 ± 0.2 mm were tested using the same procedure and conditions as described in the experimental section "compressive mechanical test". The DNHs exhibit a compressive modulus (slope between 0.2-0.3 MPa stress) of 4.6 ± 0.7 in PBS (pH 7.4) ($p < 0.05$) and 4.9 ± 0.7 in PBS (pH 7.4) + 140 U/L CRL ($p < 0.05$). Compressive modulus values at compressive stress between 2-3 MPa of 20.4 ± 0.2 for PBS (pH 7.4) ($p < 0.05$) and 20.2 ± 3.5 for PBS (pH 7.4) + 140 U/L CRL ($p < 0.05$) were obtained. In both cases, the compressive stiffness was not significantly different between the reference medium PBS (pH 7.4) and the medium with 140 U/L CRL.[17]

-Statistical Analysis: All values were expressed as mean ± standard deviation (SD). The results were analyzed statistically using a one-way ANOVA, followed by a Tukey post-hoc test. In all cases, the significance was set at $p \leq 0.05$. Statistical analysis was carried out using OriginPro 2020b Software.[17]

4. Insights into the influence of functional groups on the mechanical performance of Poly(2-oxazoline)/Polyacrylate Double Network Hydrogels

This chapter is based on a second publication by P. BENITEZ-DUIF[131] as the first author. The findings presented in this chapter were derived from the thesis of D. KURKA[71] and, primarily, from the Master's thesis of S. WECKES.[48]

4.1 ABSTRACT

Double network hydrogels (DNHs) are strong and tough materials that surpass the performance of conventional hydrogels, making them highly attractive for various applications in biomedicine, membrane technology, and energy storage. The number of suitable systems known so far is rather limited. We have recently introduced a poly(2-oxazoline) (POx)-based DNH combined with acrylic acid that has a superior compressive strength compared to common DNHs entirely composed of two polyacrylate networks. To further explore the potential of cross-linked POx as primary networks for DNHs, a series of different poly (acrylate)s was employed as secondary network and investigated regarding its mechanical properties.[131]

4.2 INTRODUCTION

Polymer hydrogels are soft materials composed of physical and/or chemical three-dimensional cross-linked polymer networks that contain at least 50 wt% of water.[24-26] The properties of these materials can be easily tailored by modifying the chemical composition or controlling the degree of polymerization, spacing between functional groups, and pH of the surrounding environment.[28,132] One of the most relevant features of polymer hydrogels is their structural similarity to human soft tissues, making them attractive for several applications, inter alia, in medicine and biomedical engineering.[25,28,36,133-135] To enhance their functionality, such as controlling diffusion of small molecules[136-137] or proteins,[138-139] increasing their swellability in organic solvents,[103] or transforming them into carriers for biocatalysts for organic solvents,[104-105,140] polymer hydrogels can be engineered into segmented polymer networks that contain both hydrophobic and hydrophilic segments, as exemplified in amphiphilic polymer co-networks.[141-143] However, the mechanical performance of conventional hydrogels and segmented hydrogels

are rather limited, especially when it comes to the implementation of load-bearing tissues (e.g. articular cartilage), where high compressive strength and toughness are needed.[17,144-145] The low mechanical performance of conventional hydrogels can be attributed to the topology of their cross-linked network, which is not able to dissipate concentrated stress and stop crack propagation.[49]

Among all materials, nanocomposite hydrogels[16,79,120,146] and double network hydrogels (DNHs) have been highlighted as novel approaches for improving the mechanical performance of polymeric network hydrogels.[49,63,82,120] DNHs represent a specific case of interpenetrating networks (IPNs), where the primary network is swollen and thus stretched, followed by the formation of a second internal network. Consequently, DNHs are composed of a stretched and relaxed network, both being interpenetrating. This unique structure is responsible for the higher stiffness and greater ability to dissipate mechanical energy, resulting in exceptional mechanical properties,[51,61] such as high strength, toughness, and stiffness, making DNHs attractive for a range of applications in biomedical engineering,[78,147-148] soft robotics,[60,149] membrane systems,[150] and energy storage.[26,151-152] Nevertheless, DNHs under constant loading stress are susceptible to permanent damage caused by irreversible bond breakage. Therefore, stabilizing the hydrogel through dynamic and reversible physical crosslinking interactions, such as hydrogen bonds and ionic interactions is crucial for the design of these hydrogels.[30,153-156] Dynamics bonds play a significant role in stabilizing the polymer chains in the interpenetrating networks, which in turn influences fascinating properties, such as swelling behavior, self-healing, shape memory, toughness, and mechanical strength of the network.[157-158] However, the use of hydrogen bonds to develop tough hydrogels is rather challenging due their limited stability in both aqueous media and higher temperatures.[159-162] However, this can be re-adjusted by using variable hydrogen bonds with different bonding strengths and stabilities, particularly cooperative hydrogen bonding[144,163] formed in the polymeric material.[131]

Previously, we reported double network hydrogels based on poly(2-oxazoline)s (POx) and poly (acrylic acid) (PAA) with excellent mechanical performance and cartilage-like features.[17] These hydrogels are stabilized by hydrogen bonds between both involved polymers. Furthermore, the strong interactions between POx and PAA are capable to shift the pKa of the latter by nearly three orders of magnitude, which was not observed for comparable PEG/PAA DNHs.[90] Nevertheless, the general acidity of PAA might be of disadvantage in some applications,

because pH values above 7.8 weaken the DNH. In the present work we study the effect of non-acidic polyacrylates in the mechanical performance of POx-based DNH. Hydrogen bond interactions are critical for distribution and absorbing mechanical stress, and hence different structures and functionalities of both the acrylic monomers and POx side chains allow for deeper insights in the role of POx-networks and the mechanical performance of their hydrogels.

4.3 Results and Discussion

The goal of this study was to gain better understanding of the effect of functional groups that form hydrogen bonds between the proton acceptor POx network and the proton donor polyacrylate network on the mechanical performance of the resulting DNH. First, it was explored if the double network structure is the true origin of the high performance of the previously published $PMOx_{50}$/PAA DNH[17] or if the strong interactions between PMOx and PAA are sufficient to obtain good mechanical properties. To this end, a segmented polymer co-network (SPN) was synthetized by photo-polymerization of diacrylamide-terminated $PMOx_{50}$ and acrylic acid. The weight contents of $PMOx_{50}$ and PAA were adjusted to 26 and 74 wt%, respectively, which is similar to that in the previously reported respective DNH. Figure 25 and Table 5 summarize the mechanical properties of the two different networks.[131]

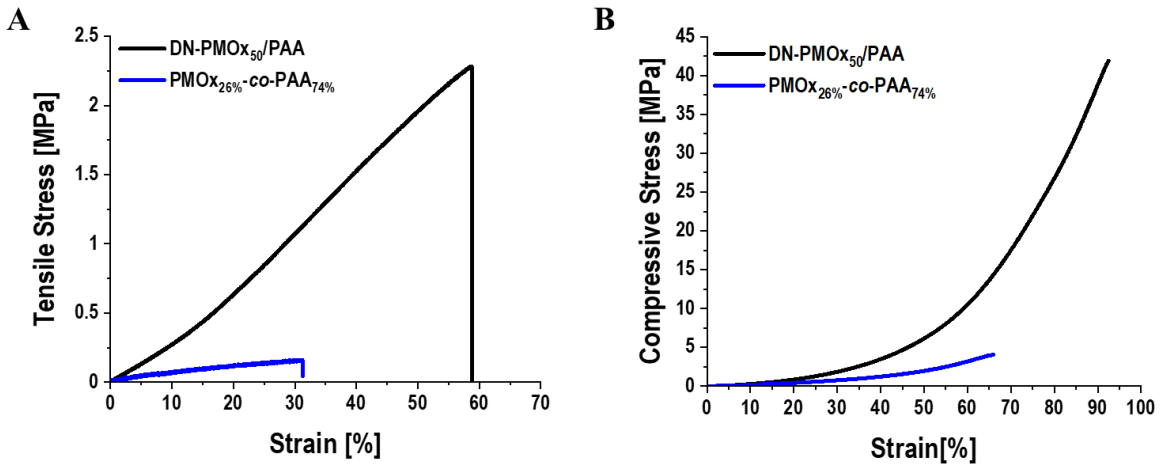

Figure 25: *A) Tensile stress-strain curve and B) compressive stress-strain curve of the co-network and double network hydrogel based on $PMOx_{50}$ and PAA in water.*[131]

Table 5: *Overview of the water content and mechanical performance of the co-network and double network hydrogels based on $PMOx_{50}$ and PAA. The values are expressed as mean ± SD (n = 3-4).*[131]

Network	Water Content [%]	Tensile Modulus [MPa]	Tensile Strength [MPa]	Fracture Energy [kJ m^{-3}]	Compressive Modulus [MPa]	Compressive Strength [MPa]
DN-$PMOx_{50}$/PAA	61.4 ± 0.4[17]	2.7 ± 0.1	2.38 ± 0.1	225.1 ± 5.2	4.5 ± 0.4	42.0 ± 8.0
$PMOx_{26\%}$-*co*-$PAA_{75\%}$	52.0 ± 4.0	0.70 ± 0.07	0.10 ± 0.01	3.7 ± 0.3	4.1 ± 2.1	3.5 ± 0.9

As seen in Figure 25 and Table 5, the SPN hydrogel exhibits a poor mechanical performance compared to the DNH. These results confirm once more the importance of the double network structure for higher stiffness and dissipating energy upon stress in DNHs. Please note that the fracture energy is given in kJ m^{-3}, which is simply the area under the stress-strain curve until break of the notched samples. The often-used value in kJ m^{-2} (area times length of the sample) is not applicable in this study, because the length of the samples in the stress-strain experiment could not be kept constant due to the greatly varying mechanical properties of the here investigated DNH samples.

Having established that the double network structure for PMOx-based hydrogels is required for their exceptional properties of $PMOx_{50}$/PAA DNH, a series of DNHs with cross-linked $PMOx_{50}$ as primary network and different poly(acrylic acid) derivatives were employed as secondary network. The investigated acrylates, depicted in Figure 26, were chosen regarding their capability to build hydrogen bonds with the carbonyl groups of PMOx. Poly(N,N-dimethylacrylamide) (PDMA) was used as negative control because no hydrogen bonding is expected in the respective DNHs. All DNHs were synthetized using the same two step polymerization starting with photo-cross-linking PMOx followed by photopolymerization of the acrylate swollen PMOx-network.[17]

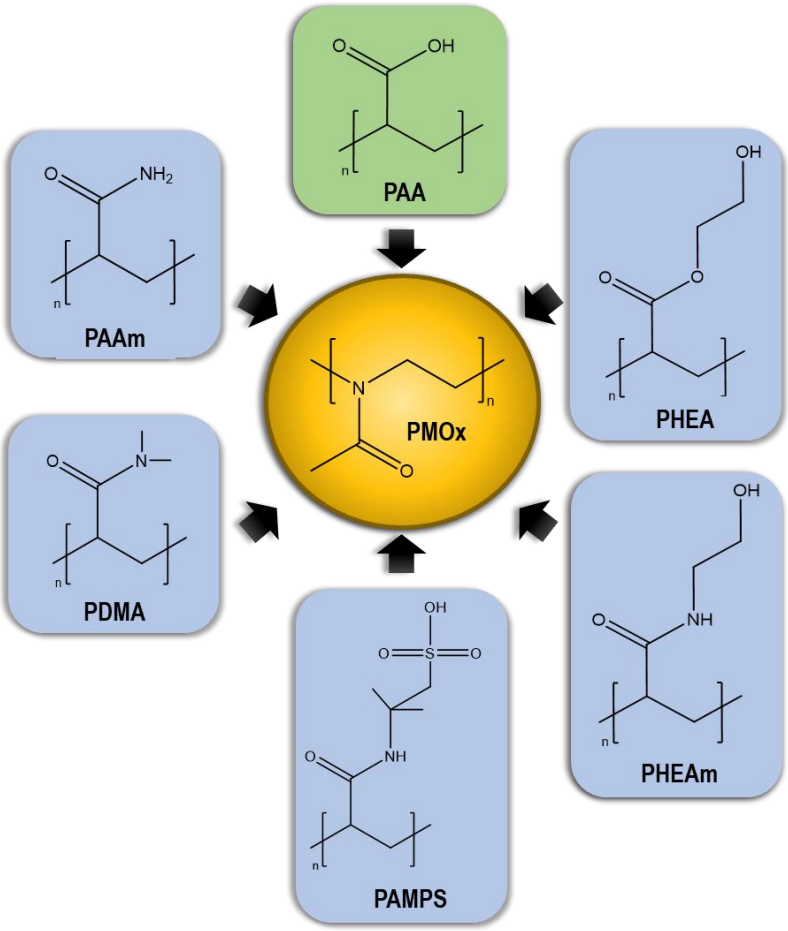

Figure 26: *Investigated double network hydrogels systems based on poly(2-methyl-2-oxazoline) and polyacrylates.*[131]

As seen in Table 6, the compositions of the different DNHs vary in the weight content of the secondary network. This variation is due to the differing swelling ratios of the PMOx network in the respective acrylate monomer solutions. In the cases of PAAm and PAMPS, saturated aqueous solutions were used, while all other double networks were prepared by swelling in the pure liquid monomer (see Table 11 in experimental section). This explains the lower content of PAMPS and PAAm in the DNHs compared to those swollen in the pure monomer. The polyacrylate derivatives with higher molecular weight (PHEA and PHEAm) lead with more than 80 wt% to the highest content of the secondary network. The DNH $PMOx_{50}$/PAMPS was found to be too fragile to be tested and was excluded from further investigation. All other DNHs were investigated by using tensile and compression tests (Figure 27 and Table 6).

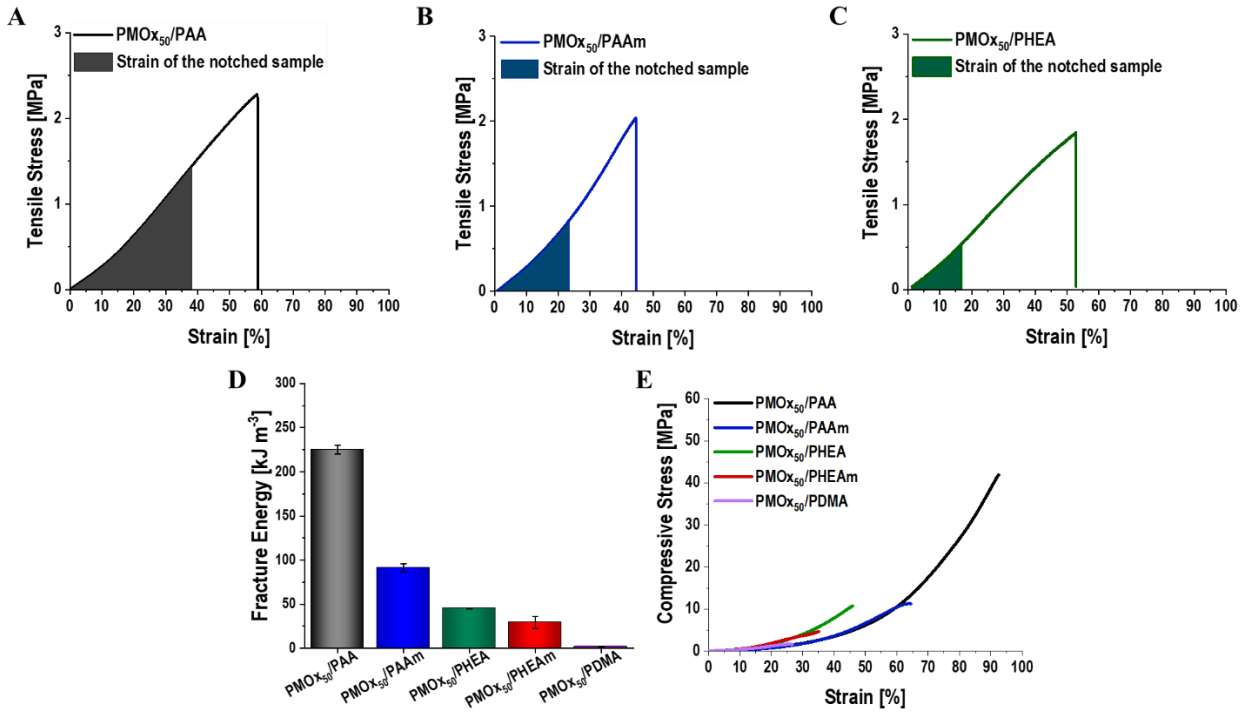

Figure 27: *Tensile stress-strain curve of A) PMOx$_{50}$/PAA, B) PMOx$_{50}$/PAAm, and C) PMOx$_{50}$/PHEA. The filled areas represent the fracture energy at the breaking strain of the notched sample. D) Fracture energy values and E) compressive curves of all tested DNHs. All experiments were performed in water at room temperature. The values in Figure 27-D are expressed as mean ± SD (n = 3-4).*[131]

Table 6: *Overview of the water content and mechanical properties of the different double network hydrogels based on PMOx$_{50}$ and different polyacrylates. The values are expressed as mean ± SD (n = 3-4).*[131]

Double network Hydrogel		Second Network Content [%]	Water Content [%]	Tensile Modulus [MPa]	Tensile Strength [MPa]	Fracture Energy [kJ m^{-3}]	Compressive Modulus [MPa]	Compressive Strength [MPa]
1. Network	2. Network							
PMOx$_{50}$	PAA	74.0 ± 5.0	61.4 ± 0.4	2.7 ± 0.1	2.4 ± 0.1	225.1 ± 5.2	4.5 ± 0.4	42.0 ± 8.0
PMOx$_{50}$	PAAm	64.3 ± 1.7	73.0 ± 1.0	3.1 ± 0.2	2.3 ± 0.4	91.1 ± 4.7	4.8 ± 0.4	12.7 ± 0.3
PMOx$_{50}$	PDMA	70.2 ± 1.6	72.5 ± 0.6	1.6 ± 0.8	0.10 ± 0.01	1.8 ± 0.2	4.3 ± 0.2	1.6 ± 0.1
PMOx$_{50}$	PHEA	86.0 ± 0.1	60.0 ± 2.0	2.7 ± 0.1	1.7 ± 0.4	45.1 ± 0.4	5.7 ± 0.5	10.3 ± 1.3
PMOx$_{50}$	PHEAm	78.4 ± 1.3	76.3 ± 0.5	2.5 ± 0.9	0.9 ± 0.1	29.3 ± 6.6	4.7 ± 0.8	5.7 ± 0.6
PMOx$_{50}$	PAMPS	54.0 ± 0.1	82.4 ± 2.5	-	-	-	-	-

As seen in Table 6, the tensile and compressive moduli of all investigated PMOx-based DNHs are in the same range. This can be explained by considering that the moduli were determined from the initial slope in the stress-strain-curve or at low stress levels (0.3 MPa) in the

compression test, respectively. In both cases, no significant deformation occurs and thus the breaking and reforming of hydrogen bonds is negligible. The moduli of the DNHs are predominantly controlled by the pre-stretched primary PMOx. In addition, the water content values are not strongly differing being in a range of 60 and 76 % in all cases, with the exception of $PMOx_{50}$/PAMPS, which is too brittle to be handled.

The tensile strength and the fracture energy values of the PMOx-based DNHs reveal a stronger influence of the nature of the secondary polyacrylate network (see Table 6 and Figure 27-A, D). DNHs with PAAm and PHEA show a stress-strain curve that is in terms of breaking strength and elongation to break rather similar to that of $PMOx_{50}$/PAA all showing around 2 MPa tensile strength. In contrast, $PMOx_{50}$/PHEAm can only be strained to ca. 20% and breaks at 1 MPa and $PMOx_{50}$/PDMA is strainable to less than 10% and breaks at below 0.1 MPa (stress-strain curves shown in Attachments Figure 36). This clearly indicates that not only hydrogen bonds are essential in the strain-stress resistance of the DNHs, but also the structure of the polyacrylate side groups is critical to achieve high tensile strength.[131]

The fracture energy values reveal that the polyacrylate network structure significantly influences the toughness of the DNHs. The fracture energy, measured using notched samples, addresses the dynamic crack propagation of an unstable crack. In other words, it assesses the stability of the induced crack in the sample. As evident from the fracture energies shown in Figure 27-D and Table 6, PAA as secondary network shows the highest inhibition of crack propagation (fracture energy of 225 kJ m^{-3}). The DNHs with PHEA and PAAm as secondary network, which show elongation to break of 50 and 45%, respectively, become rather fragile, when a notch was cut in the samples, indicating that the double network cannot reform its hydrogen bonds quickly enough to dissipate the energy at the crack. Nevertheless, the fracture energy values of the $PMOx_{50}$/PHEA DNH (45 kJ m^{-3}) and $PMOx_{50}$/PAAm (91 kJ m^{-3}) are still rather high compared to the single network hydrogels (< 1 kJ m^{-3}).

The influence of the nature of the second network on the mechanics of PMOx-based DNHs is even more pronounced in the compression tests (Figure 27-E). The compressive strength of the PHEA- and the PAAm-based DNHs is of 10.3 MPa and 12.7 MPa, nearly 4 times lower than that of $PMOx_{50}$/PAA. The reason for this is the significantly lower compressibility compared to the latter network, despite the similarity of the compression modulus values between the

DNHs. The DNH composed of PMOx and PHEAm shows lower compressibility and compression strength (5.7 MPa) than the two other hydrogen bonds forming DNHs. Using PDMA as secondary network, which has two methyl groups instead of two hydrogens on the nitrogen, results in a PMOx-based DNH a compressive strength of less than 1 MPa. This is because no hydrogen or other sacrificial bonds can be formed between the PMOx and PDMA network, as both are only proton acceptors. These results clearly show that hydrogen bonds between the two networks are responsible for the improved mechanical compressive strength of the DNHs based on PMOx.

Altogether, none of the alternative secondary networks outperforms the high strength of $PMOx_{50}$/PAA DNHs in tension and compression mode. We presume that the latter DNH is not only stabilized by hydrogen bonds between the carbonyl groups of PMOx and the carboxylic acid group of PAA, but also by strong hydrogen bonds within the PAA network. These double hydrogen bonds are according to HUANG et al. more than 3 times stronger than single hydrogen bonds formed between hydroxyl or amide protons and carbonyl groups,[158] which are the ones formed by PAAm, PHEA, and PHEAm.

In order to understand the effect of the side chain of the POx network on the interaction between the primary and secondary networks, DNHs based on poly(2-ethyl-2-oxazoline) PEtOx with a polymerization degree of 50 were prepared. In this case, only PAA, PAAm and PHEA as secondary network were evaluated, because they show the best performance when combined with the PMOx-based network. The composition of the synthesized PEtOx-based DNHs (Table 7) was found to be similar to the respective PMOx-based DNHs (Table 6). Figure 28 and Table 7 summarize the results of the tensile and compressive mechanical test.

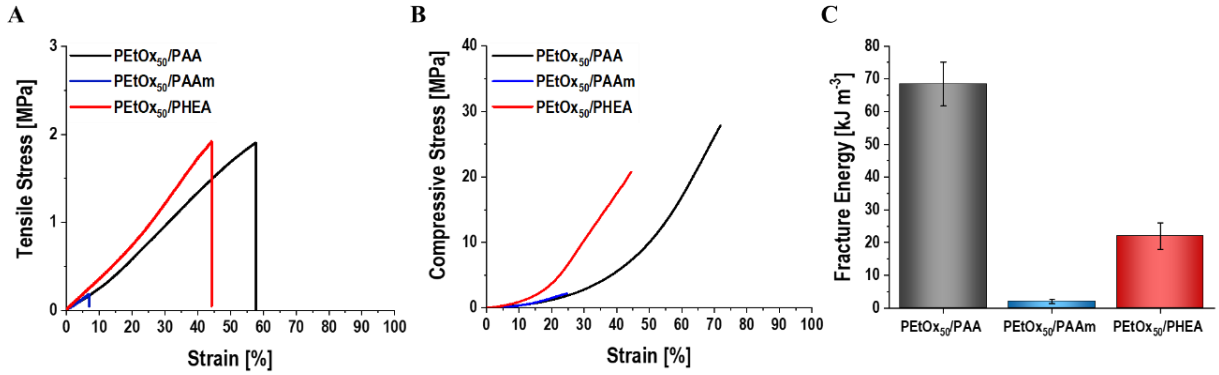

Figure 28: *A) Tensile stress-strain curves and B) compressive stress-strain curves and C) fracture energies of DNHs based on PEtOx$_{50}$ and PAA, PAA and PHEA in water at ambient temperature. The values in Figure 28-C are expressed as mean ± SD (n = 3-4).*[131]

Table 7: *Overview of the water content and mechanical performance of the different double network hydrogels based on PEtOx$_{50}$. The values are expressed as mean ± SD (n = 3-4).*[131]

Double network Hydrogel		2.Network Content [%]	Water Content [%]	Tensile Modulus [MPa]	Tensile Strength [MPa]	Fracture Energy [kJ m^{-3}]	Compressive Modulus [MPa]	Compressive Strength [MPa]
1. Network	2. Network							
PEtOx$_{50}$	PAA	74.0 ± 4.0	56.5 ± 2.4	2.5± 0.3	1.6 ± 0.5	68.4 ± 6.7	4.1 ± 0.6	29.4 ± 3.9
PEtOx$_{50}$	PAAm	60.7 ± 0.4	70.2 ± 1.5	2.0 ± 1.0	0.2 ± 0.1	2.0 ± 0.6	6.0 ± 0.7	4.1 ± 1.7
PEtOx$_{50}$	PHEA	79.0± 2.0	54.0 ± 2.0	4.2 ± 0.6	1.9 ± 0.4	22.0 ± 4.0	7.9 ± 1.3	19.0 ± 3.0

The PEtOx-based DNHs with PAA, PHEA, and PAAm exhibit similar tensile and compressive and tensile moduli compared to the respective PMOx DNHs. The stress-strain curve in Figure 28-A shows that the PEtOx$_{50}$/PAA hydrogel performs similar to the respective PMOx DNH. However, the notched sample of PEtOx/PAA shows a two-fold shorter elongation to break than PMOx$_{50}$/PAA, resulting in an almost three-fold lower fracture energy. The PEtOx$_{50}$/PHEA DNH is behaves altogether similar to the respective PMOx DNH when subjected to strain. The greatest influence of the POx side chain was found for the PEtOx$_{50}$/PAAm, both fracture energy and strain to break of this DNH drops by more than 10 times compared to PMOx$_{50}$/PAAm.

The effect of the POx side group is even more pronounced in the compression test. The PEtOx$_{50}$/PAA DNH exhibits the best mechanical performance of all three DNHs. However, the values of the compressive strength (29.4 ± 3.9 MPa) compared to the value of PMOx$_{50}$/PAA (42.0 ± 8.0 MPa) is considerably lower. Compared to the respective PMOx-based DNH,

$PEtOx_{50}$/PHEA shows increased stiffness and the compressive strength. $PEtOx_{50}$/PHEA DNH fractures at 21 MPa, which is double the value of the respective $PMOx_{50}$/PHEA (10.3 MPa). Thus, PHEA seems to form stronger hydrogen bonding to PEtOx than to PMOx, which is the opposite of PAA and can be explained by the longer side chains of PHEA. In contrast to the strengthening effect of PHEA as secondary network for PEtOx-based DNH compared to the respective PMOx-based DNH, the compressive strength of $PEtOx_{50}$/PAAm DNH of 2 MPa is five times lower than that of the respective PMOx-DNH.

These results show how the variation of the POx side group greatly influences the mechanical performance of DNHs synthesized with different types of acrylates. According to parameters shown above, an increase of the length of the POx side groups results in at least higher compression strength, as long as the second polyacrylate network contains hydrogen donors on longer spacers. It is worth noting that the PAAm containing DNHs have a significantly lower acrylate content (60-64 wt%) than for example the PAA-based DNHs (74 wt%). This is due to the preparation procedure that requires the use of an aqueous AAm solution. It is likely that POx/PAAm DNHs can be significantly increased in strength and toughness if a higher loading with PAAm is ensured.

PMOx/PHEAm DNHs have a high acrylate content but have lower toughness and strength then the other investigated PMOx-based DNHs. This is somewhat surprising, because PHEAm is reported to be a high-performing secondary polymer network in other DNHs.[164-165] The polymer is containing amide and hydroxyl groups that can serve as both hydrogen-bonding donors and acceptors that strengthen the noncovalent interactions within hydrogel network.[166-167] These bonds enable PHEAm to form different hydrogen bonds at different distances with the primary polymer network in a DNH. Thus, should result in higher toughness at least (Figure 29).

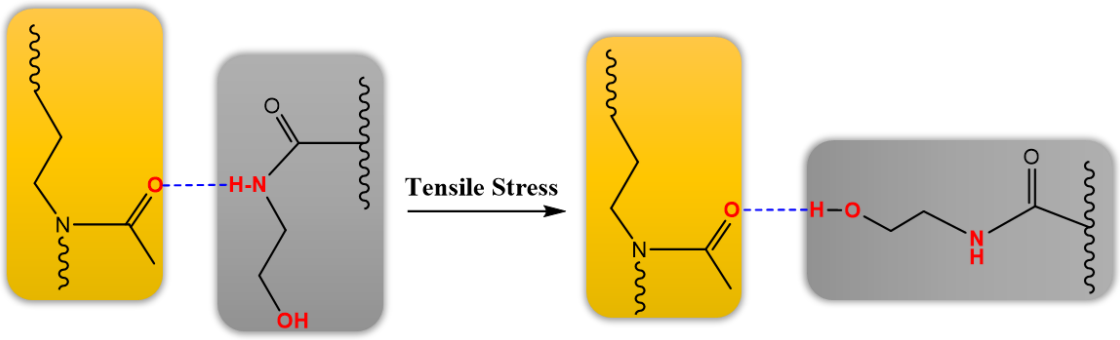

Figure 29: *Dynamics of the hydrogen bond interaction between the PMOx and PHEAm polymeric networks upon tensile stress.*[48,131]

It was presumed that PHEAm as a secondary network might not have the suited geometry to form strong hydrogen bonds with the PMOx network due to the flexibility of the side group. Thus, we hypothesized that the addition of a fraction of a stronger binding monomer as comonomer would force binding between PHEAm and the POx-network. To test this, PHEAm-*co*-PAA and PHEAm-*co*-PAAm in different monomer ratios were used as secondary network for cross-linked PMOx. The DNH based on $PMOx_{50}$/P(HEAm-*co*-AA) were found to be too brittle to measure mechanical properties. In contrast, $PMOx_{50}$/P(HEAm-*co*-AAm) DNH show a promising mechanical performance.

The water content and the mechanical properties of the DNHs $PMOx_{50}$/P(HEAm-*co*-AAm) with different AAm/HEAm ratios are summarized in Figures 30 and 31, and in Table 8.

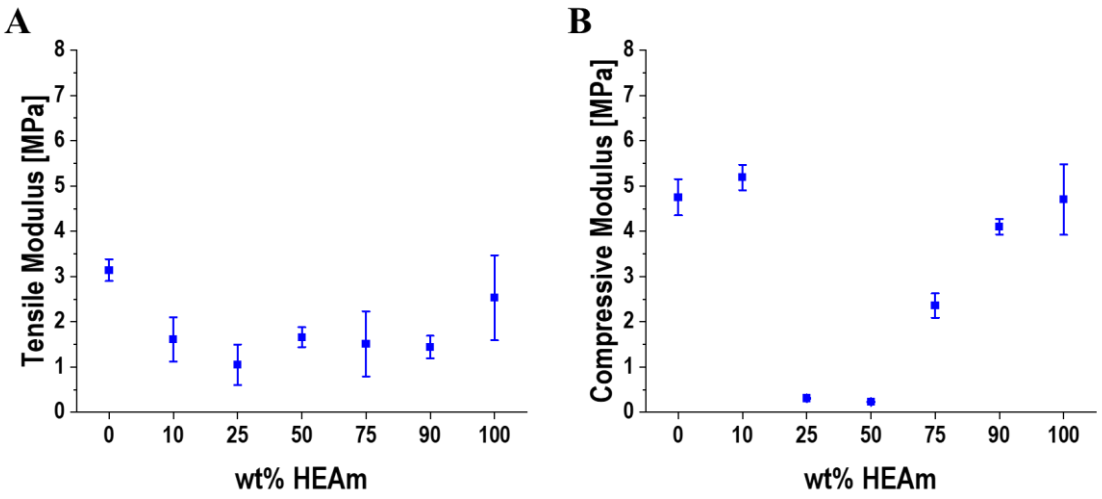

Figure 30: *Tensile A) and compressive B) moduli of $PMOx_{50}$/P(HEAm-co-AAm) DNHs in comparison to $PMOx_{50}$/PAAm and $PMOx_{50}$/PHEAm. All experiments are performed in water at ambient temperature. The values in Figure 30-D are expressed as mean ± SD (n = 3-4).*[48,131]

As seen in Figure 30, mixing two monomers in the secondary networks affords a softening of all resulting DNHs compared to $PMOx_{50}$/PAAm and $PMOx_{50}$/PHEAm. While the Youngs modulus of the copolymer DNHs is about half of their respective homopolymer DNHs, the compressive modulus decreases most in the case of PHEAm contents 35 and 50 wt%, where the compressive stiffness is more than 10 times lower. These results show that mixing two different monomers results in a decrease of interactions between the PMOx and the side chains of the secondary network. We hypothesise that this is due to longer side chain of PHEAm that offers a higher distance between the interconnecting networks and thus the shorter hydrogen forming side groups of PAAm cannot reach the carbonyl function of PMOx. Thus, when increasing the HEAm content from 10 to 50 wt%, this effect becomes more pronounced and the number of PHEAm side groups that form hydrogen bonds is lower than that of the hompolymer DNH $PMOx_{50}$/PHEAm. Increasing the amount of HEAm to 75 wt% results in a higher number of hydrogen bonds between PMOx and the PHEAm side groups and thus an increased stiffness. Moreover, the addition of HEAm as 10 and 90 wt% are not significantly influential to the compressive modulus, because the low number of non-matching groups is not disturbing the structure of the dominant functional side groups at minor deformation.[131]

Table 8: *Overview of the water content and mechanical performance of the double network hydrogels based on $PMOx_{50}$ and P(HEAm-co-AAm). The values are expressed as mean ± SD (n = 3-4).*[48,131]

DN 2. Co-Network	2. Co-Network Content [%]	Water Content [%]	Tensile Strength [MPa]	Fracture Energy [kJ m^{-3}]	Compressive Strength [MPa]
$HEAm_{10\%}$-*co*-$AAm_{90\%}$	77.0 ± 2.3	76.4 ± 0.6	0.9 ± 0.2	69.1 ± 0.6	2.1 ± 0.3
$HEAm_{25\%}$-*co*-$AAm_{75\%}$	78.6 ± 2.0	79.7 ± 2.5	0.5 ± 0.3	63.1 ± 4.9	9.5 ± 1.4
$HEAm_{50\%}$-*co*-$AAm_{50\%}$	77.2 ± 3.4	76.2 ± 0.9	0.88 ±0.02	92.0 ± 5.1	10.4 ± 0.7
$HEAm_{75\%}$-*co*-$AAm_{25\%}$	77.1 ± 2.1	76.8 ± 2.6	1.1 ± 0.3	52.1 ± 9.2	3.4 ± 0.4
$HEAm_{90\%}$-*co*-$AAm_{10\%}$	79.4 ± 1.9	76.7 ± 3.2	1.4 ± 0.2	415.0 ± 43.3	10.5 ± 0.5

A different scenario was found for the compressive strength. Adding 10% of HEAm to AAm leads to a more than 6-fold drop in compressive strength compared to $PMOx_{50}$/PAAm (from 12.7 MPa for $PMOx_{50}$/PAAm to 2.1 MP for $PMOx_{50}$/P($HEAm_{10\%}$-*co*-$AAm_{90\%}$). In contrast, 10% AAm in HEAm results in nearly double the compressive strength compared to $PMOx_{50}$/PHEAm (from 5.7 MPa for $PMOx_{50}$/PHEAm to 10.5 MP for $PMOx_{50}$/P($HEAm_{90\%}$-*co*-$AAm_{10\%}$). Thus, the minor amount of different functional in the secondary copolymer network plays a strong role for larger deformations. However, the compressive strength in not exceeding that of $PMOx_{50}$/PAAm in any composition of copolymer DNHs (Table 8).

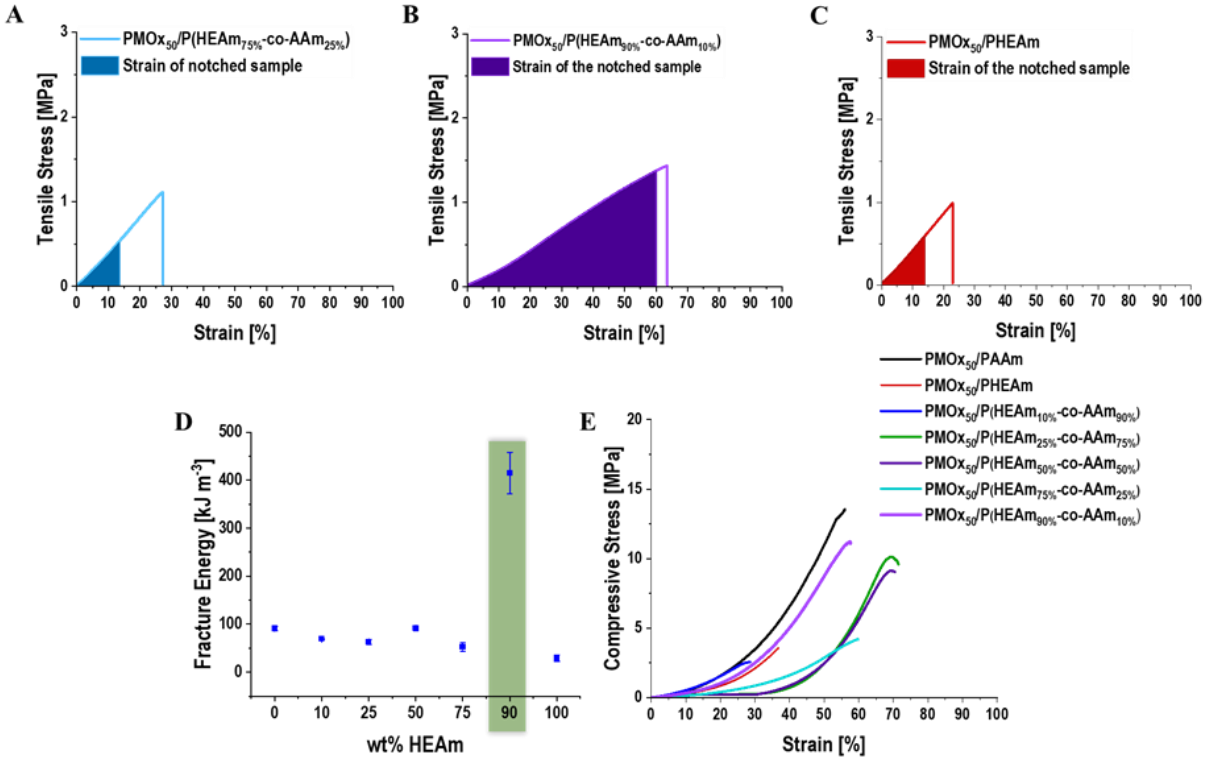

Figure 31: *Tensile stress-strain curve of A) PMOx$_{50}$/P(HEAm$_{75\%}$-co-AAm$_{25\%}$), B) PMOx$_{50}$/P(HEAm$_{90\%}$-co-AAm$_{10\%}$) and C) PMOx$_{50}$/PHEAm. The filled areas represent the fracture energy at the breaking strain of the notched sample. D) Fracture energy values and E) compressive curves of all tested PMOx$_{50}$/P(HEAm-co-AAm) DNHs. All experiments are performed in water at ambient temperature. The values in Figure 31-D are expressed as mean ± SD (n = 3-4).*[48,131]

Finally, the strain fracture energy of the copolymer DNHs reveals that the toughness is gradually decreasing for higher content of HEAm, with the exception of the composition of HEAm:AAm of 90:10. In the latter case, the fracture is about 400 kJ m^{-3}, which is 6 times higher than that of PMOx$_{50}$/PHEAm. Remarkably, the notched sample of the PMOx$_{50}$/P(HEAm$_{90\%}$-*co*-AAm$_{10\%}$) shows the same strain-to-break as the unnotched sample (Figure 31-B). Comparing the stress-strain curve of PMOx$_{50}$/P(HEAm$_{90\%}$-*co*-AAm$_{10\%}$) (Figure 31-B) to PMOx$_{50}$/PAA (Figure 27-A) reveals that the combination of PHEAm and PAAm in the secondary network of PMOx-based DNHs almost doubles the fracture energy and thus the toughness compared to respective PAA system. Thus, the mechanism proposed in Figure 29 seems valid and the possibility of forming hydrogen bonds at different distances between the two networks indeed improves the tensile toughness of the DNH.[131]

The requirement of the small amount (10 wt% accounts for 6.4 mol%) of AAm might be explained by the slightly higher water content (79%) of the DNH compared to the rather fragile pure $PMOx_{50}$/PHEAm (76%). The higher water content leads to an increased swelling ratio ($S = m_{(swollen)}/m_{(dry)}$, from 4.2 to 4.8) which increases the distance between PHEAm and PMOx by approximately 5%. This could be the optimal ratio required for the improved toughness and is supported when considering that the fracture energy of PMOx/PHEAm DNH is ten times lower than that of $PMOx_{50}$/P($HEAm_{90\%}$-*co*-$AAm_{10\%}$) (Figure 31-C and Table 8). A further increase of 25 wt% AAm does result in a dramatic drop of fracture energy (Figure 31-A and D), which is caused by a lower density of the HEAm groups in the DNH. These results clearly show that mixing monomers in acrylate phase is a beneficial way to optimize the properties of $PMOx_{50}$ based DNH.

4.4 Conclusion

This chapter addresses the question of how the mechanical properties of POx_{50}-based DNHs with different polyacrylate networks can be tuned through systematic variations of the chemical nature in both networks. It could be established that the double network structure is a major requirement for achieving good mechanical properties, such as high compressive strength, in the hydrogels. The secondary network for POx-based DNHs evidently needs to be a proton donor to sufficiently dissipate energy. The high compression strength of $PMOx_{50}$/PAA was found to be caused by the strong hydrogen bonds formed within the PAA network and this could not be achieved by any other POx-based DNH. Furthermore, the POx side chain is an important factor in the resulting mechanical properties of the respective hydrogels. An increase of the side chain of POx, from methyl to ethyl groups, changes the interactions with the secondary polyacrylate network in a way that longer proton donating side chains on the acrylate are required to reach the carbonyl group of the POx network. Thus, the interactions between the two networks is very sensitive to the smallest changes in the structure of the side groups. This was found to be even more pronounced when mixing monomers in the secondary polyacrylate network. The addition of a small fraction of AAm (10 wt%) to HEAm (90 wt%) leads to a PMOx-based DNH with 10-times higher toughness, more than the double the tensile strength, and almost double compressive strength compared to $PMOx_{50}$/PHEAm. In terms of tensile toughness this DNH even exceeds the overall best performing $PMOx_{50}$/PAA. Thus, fine tuning of POx-based DNH is a versatile and promising way to obtain high performing DNHs

for biomedical applications beyond artificial cartilage for skin substitutes and supporting structures for bone regeneration. Finally, such DNHs are also interesting candidates for pressure resistant desalination membranes or even as actors for energy harvesting materials.[131]

4.5 Experimental Section/Methods

The Experimental section and methods are based on previous studies by the author Benitez-Duif et.al.[17,131]

-***Materials*:** Chloroform (Fischer Scientific) was distilled from activated aluminum oxide (Merck) under reduced pressure and under argon atmosphere stored. The monomers 2-methyl-2-oxazolin (MOx) and 2-ethyl-2-oxazoline (EtOx) were obtained from Acros Organics, these were distilled over CaH_2 (Acros Organics). *Trans*-1,4-dibromo-2-butene (DBB, Acros Organics) was recrystallized twice from n-heptane (Fischer Scientific). N,N-Dimethylaminopropylmethacrylamid (DMAP-MAA, Sigma-Aldrich) was under reduced pressure distilled. All distilled chemicals were under argon atmosphere and at -20°C stored[17]. Acrylic acid (AA, 98% extra pure, Acros Organics), Acrylamide (AAm, VWR), N,N-Dimethylacrylamide (DMA, 99%, Sigma Aldrich), 2-Hydroxyethyl acrylate (HEA, 97%, TCI-Europe)[71], N-(2-Hydroxyethyl)acrylamide (HEAm, >98%, TCI-Europe)[71], Irgacure 2959 (IG2959, >98%, TCI-Europe), Irgacure 651 (IG651, Ciba Specialty Chemicals), Tetraethylene glycol dimethacrylate, (TEGDMA, Sigma-Aldrich), methanol (Fischer Scientific), N,N-methylene-bis-acrylamide (MBAm, 99%, Merck), diethyl ether (Honeywell Riedel-de-Haën™).[48,131]

-***Synthesis of poly(2-oxazoline) macromonomers with DMAP-MAA end groups:*** The synthesis of telechelic $PMOx_{50}$ and $PEtOx_{50}$ was performed according to previously works of Tiller et al.[17,69] The cationic ring opening polymerization of 2-methyl-2-oxazolin (MOx) and 2-ethyl-2-oxazoline (EtOx) with DBB as initiator was carried out in dry chloroform (20 mL) under argon atmosphere in an industrial microwave reactor. Since the polymerization time and temperature depends on the degree of polymerization and monomer´s type, the polymerization time and temperature for the two different polymers are in Table 9 listed. The living ends of all polymers were terminated with N,N-Dimethylaminopropylmethacrylamid (DMAP-MAA) in a 10-fold molar excess (respect to the mole of initiator) at 49 °C for 72 h. The resulting polymeric

product was purified by precipitating the polymers three times in ice-cold diethyl ether and then dialyzed against mixture of methanol/H_2O (1:1) using benzoylated cellulose membranes (1000 MWCO). The methanol was first removed under reduced pressure and the remaining aqueous solution was dried by lyophilization.[17,131]

Table 9: *Composition and polymerization conditions for the synthesis of PMOx and PEtOx with DMAP-MAA end groups.*[131]

Polymer	m_{DBB} [g]	$V_{Monomer}$[a)] [mL]	Time [h]	Temperature [°C]	$V_{DMAP-MAA}$[b)] [mL]
$PMOx_{50}$	0.3	6	2.5	105	2.5
$PEtOx_{50}$	0.21	5	2.5	110	1.8

[a)]Volume of monomer (MOx or EtOx); [b)] Volume of DMAP-MAA to functionalization of PMOx and PEtOx.

-Determination of the degree of polymerization and functionalization of poly(2-oxazoline) with DMAP-MAA end groups: The degree of polymerization (DP) of the synthesized poly(2-methyl-2-oxazoline) and poly(2-ethyl-2-oxazoline) and degree of functionalization (F, in %) with DMAP-MAA as end groups were determinated using ^1H NMR spectroscopy(Agilent AV500/AV400 spectrometer at 25 °C with $CDCl_3$ as the solvent). The molecular weight (M_n) and dispersity (Đ) of the polymers were evaluated through size exclusion chromatography (SEC). The SEC analysis was carried out using a Viscotek GPCMax system with a refractive index detector at 55 °C, employing a saline solution of N,N-dimethylformamide (DMF + LiBr, 20 mmol) as the eluent. Calibration was performed with poly(styrene) standards (Viscotek).[17,131]

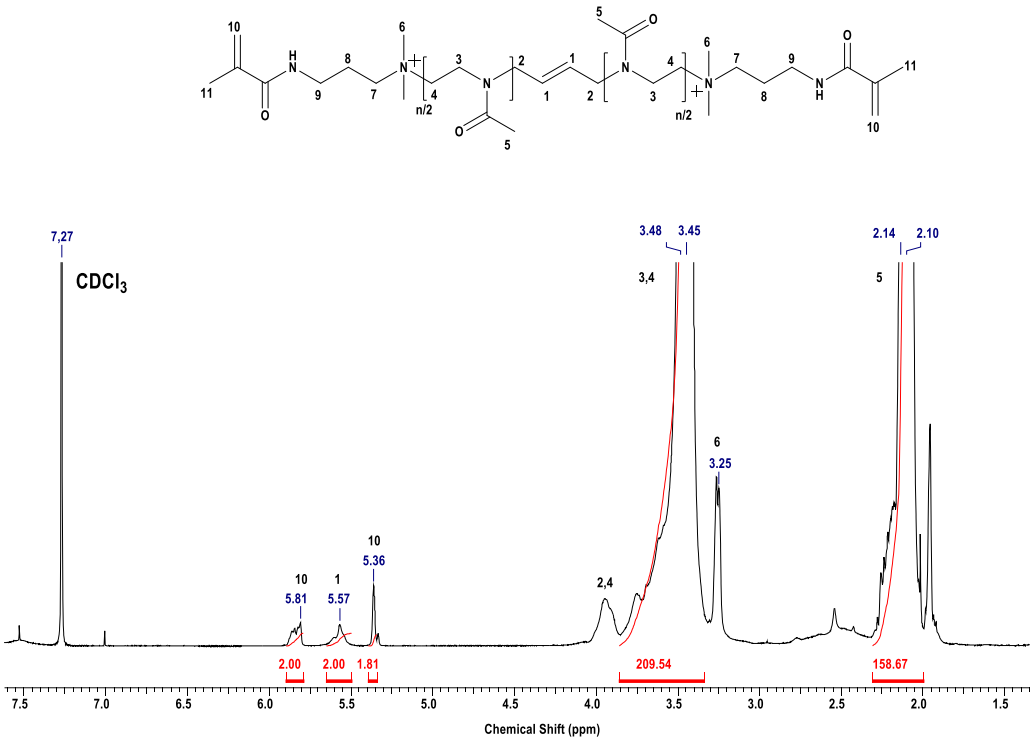

Figure 32: *[1]H-NMR spectrum of $PMOx_{50}$ functionalized with DMAP-MAA end groups in $CDCl_3$ at 400 MHz.*[48,131]

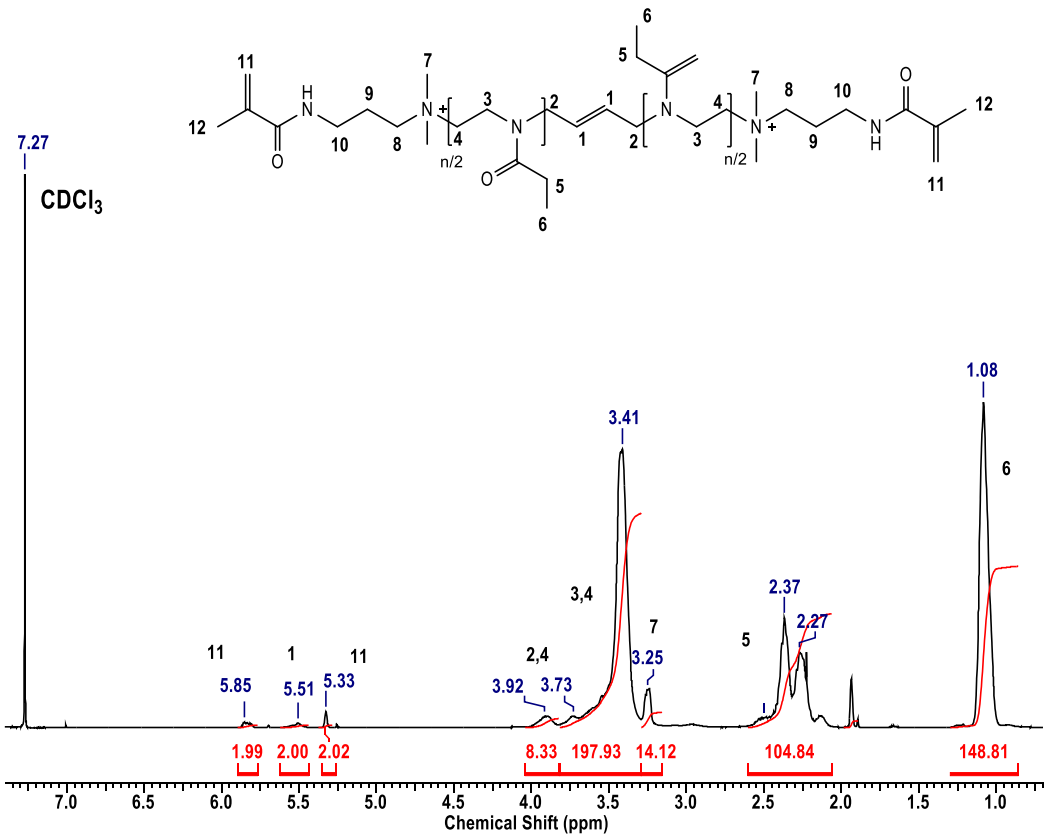

Figure 33: *[1]H-NMR spectrum of $PEtOx_{50}$ functionalized with DMAP-MAA end groups in $CDCl_3$ at 400 MHz.*[131]

Table 10: *Analytical data of the synthetized POx with DMAP-MAA end groups.*[48,131]

Polymer	$DP_{,NMR}$ [-]	$M_{n,NMR}$ [g mol^{-1}]	$M_{n,SEC}$ [g mol^{-1}]	Đ [-]	F-$_{DMAP-MAA}$[a)] [%]
$PMOx_{50}$	53	4820	4739	1.19	95
$PEtOx_{50}$	50.4	5391	5370	1.14	99

[a)]Degree of funtionalization of POX with DMAP-MAA end groups.

***-Fabrication of the POx and Polyacrylate double network hydrogels*:** The double-networks hydrogels composed of POx and different acrylate monomeres were synthesized using a two-step polymerization method. This method was initially developed by GONG et al.[31] and was also detailed in our previous work.[17,131]

The first POx hydrogel network was prepared from an aqueous solution of 34 wt% macromonomer POx with DMAP-MAA end groups and photoinitiator IG2959 (4.6 wt% respect to the macromonomer). This precursor solution was placed between two microscope slides, which were previously coated with poly(propylene)-tape and separated by 1.05 mm thick spacers for the compression-tested samples. Spacers with 0.35 mm thickness were used for tensile-tested hydrogels, so that these could be fixed between the clamps of the tensile tester. Then, it reacted in an UV curing chamber (Emmi-Classic automatic, 36 W, λ = 340 nm) for 36 min (switching each side every 2 min). Upon the exposure to the UV light, the macromonomer underwent a free-radical induced polymerization to form a stable POx primary network (1N). Afterwards the POx network was soaked in DI water over night, in order to remove the unreacted macromonomers and impurities.[17]

In order to incorporate the polyacrylate (PA) secondary network, the first network was carefully removed from the water and immersed in the respective acrylate solution overnight. The different acrylate solutions contained a photoinitiator (IG2959 or IG651) and a crosslinking agent (TEGDMA or MBAm). Table 11 shows the weight percentages of the components in the different acrylate solutions. The initiator content is proportional to the total amount of acrylate monomer, while the crosslinking agent content is determined by a mole ratio of approximately 2100 between the total monomer amount and the crosslinking agent. For acrylamide (AAm) and 2-acrylamido-2-methylpropane sulfonic acid (AMPS) as solid monomers, dissolution in water was necessary followed by an adjustment of the molar ratio monomer-crosslinking agent.

The swollen hydrogel was placed between two glass plates and cured under a UV source for 20 minutes, alternating sides every 2 minutes. The final POx/PA double network (DN) hydrogel was removed from the glass plates and washed thoroughly with water for 48 h. All washed DN hydrogels were dried at room temperature and stored. The cleaned samples were swollen in water at least 48 h before the measurements.[131]

Table 11: *Composition of the different acrylate second network solutions.*[48,71,131,168]

Acrylate	Monomer Content in Solution [wt%]	Initiator	Initiator Content [wt%]	Crosslinking Agent	Crosslinking Agent [wt%]
AA	100	IG651	0.24	TEGDMA	0.22
AAm	50[a)]	IG2959	0.24	MBAm	0.24
HEA	100	IG651	0.24	TEGDMA	0.12
HEAm	100	IG651	0.24	TEGDMA	0.13
DMA	100	IG651	0.24	TEGDMA	0.16
AMPS	20 [a)]	IG2959	0.24	MBAm	0.06
$HEAm_{90\%}$-co-$AAm_{10\%}$	100	IG2959	0.24	TEGDMA	0.14
$HEAm_{75\%}$-co-$AAm_{25\%}$	100	IG2959	0.24	TEGDMA	0.15
$HEAm_{50\%}$-co-$AAm_{50\%}$	67 [a)]	IG2959	0.24	MBAm	0.08
$HEAm_{25\%}$-co-$AAm_{75\%}$	57 [a)]	IG2959	0.24	MBAm	0.09
$HEAm_{10\%}$-co-$AAm_{90\%}$	53 [a)]	IG2959	0.24	MBAm	0.10

[a)] Solid content of AAm, AMPs and HEAm-PAAm in aqueous solution. Initiator and crosslinking agent content are in relation to the total amount of acrylate monomer.

-Determination of the water content: Between 3 and 4 dry hydrogel samples with 6 mm diameter were immersed in deionized water until equilibrium was reached, which corresponds to a swelling time of at least 48 h. Subsequently, the swelled hydrogels were dried under vacuum at 50 °C for 48 h.[17,131] To determinate the water content (WC) the wet (m_g) and dry (after swelling, m_d) weights of the DN hydrogels were measured and calculated as follows:

$$\mathrm{WC\ (wt\%)} = \frac{m_g - m_d}{m_g} \times 100 \qquad (1)$$

-Determination of the Polyacrylate content in the double-network: The polyacrylate second network content in the double network was calculated from the dry weight of the POx based

first network (m_{1N}) before its swelling in the acrylic acid monomer solution and the dry weight of the resulting POx/PAA hydrogel (m_{DN}) after the washed process[17,131]:

$$PA\ (\%) = \frac{m_{DN} - m_{1N}}{m_{DN}} \times 100 \quad (2)$$

-***Tensile mechanical test:*** The stress-strain-curves were recorded at room temperature using an Instron 3340 tensile tester with a cell with load 1 kN. At least four swollen DNH samples of different double networks with average dimensions of 4.55 mm x 29.9 mm x 0.76 mm (width x length x thickness) were fixed between the clamps with help of sandpaper resulting in effective lengths (l_o) between 7 and 18 mm. The experiment was performed at a crosshead speed of 5% min^{-1} until failure of the sample. During the whole experiment, the samples were kept hydrated with water using a spray bottle. The tensile modulus was obtained from the initial slope of the stress-strain curve. The determination of the fracture energy was determined based on previous works of TILLER et al.[79,129] Three additional samples, with the same dimensions as mentioned above, were notched in the center. The notch length corresponds to one third of the sample´s width. The tensile test of the notched samples was performed until failure as described above. This experiment allows to determine the strain at which the notch turn into a running crack.[131] The corresponding fracture energy (Γ, in J m^{-3}) of the samples was calculated as follows:

$$\Gamma = \int_0^{\varepsilon_c} \sigma(\varepsilon) d\varepsilon \quad (4)$$

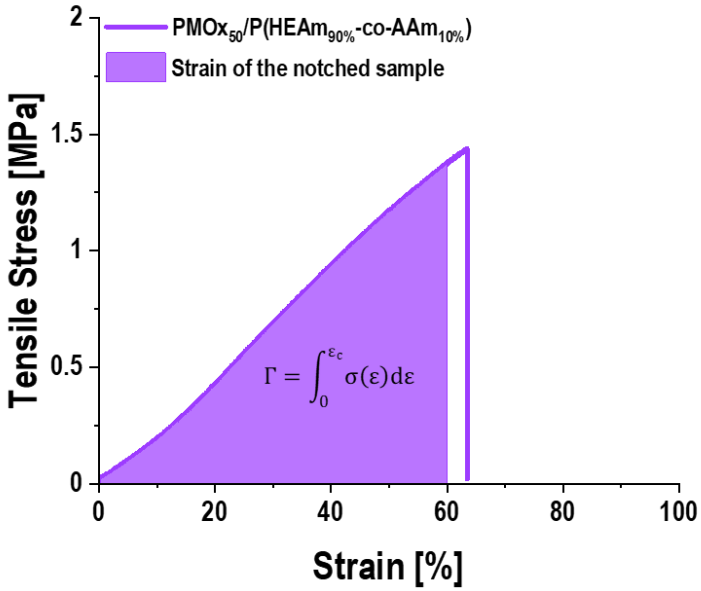

Figure 34: *Stress –strain curve of DN based on $PMOx_{50}$/P($HEAm_{90\%}$-co-$AAm_{10\%}$)and the area calculated from the strain of the notched sample.*[48,131]

-Compressive mechanical test: The compressive behavior of $PMOx_{50}$/PAA and native cartilage were evaluated with an Instron 5967 tester with a cell load of 30 kN at room temperature. Five circular samples with diameter of 12 mm and thickness between 1.8 and 2.2 mm were tested. The sample was placed in the compression cell, covered with swelling media (H_2O) and compressed with an initial preload of 1N. All samples were compressed with a compressive strain rate of 0.5 mm min^{-1} until failure. Compressive stress-strain-curves were recorded. Compressive modulus values were obtained from the slope at 0.2-0.3 MPa compressive stress.[17,131]

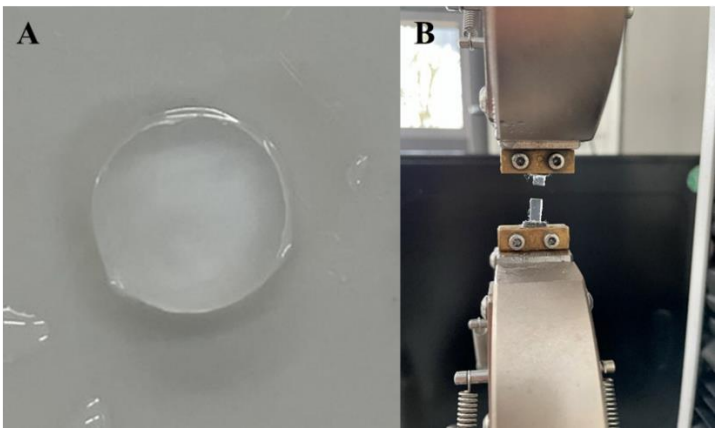

Figure 35: *DN $PMOx_{50}$/PAAm in compression form (A) and after tensile test (B).*[48,131]

-Statistical Analysis: All values were expressed as mean ± standard deviation (SD). The results were analyzed statistically using a one-way ANOVA, followed by a Tukey post-hoc test. In all cases, the significance was set at $p \leq 0.05$. Statistical analysis was carried out using OriginPro 2020b Software.[17,131]

4.6 ATTACHMENTS

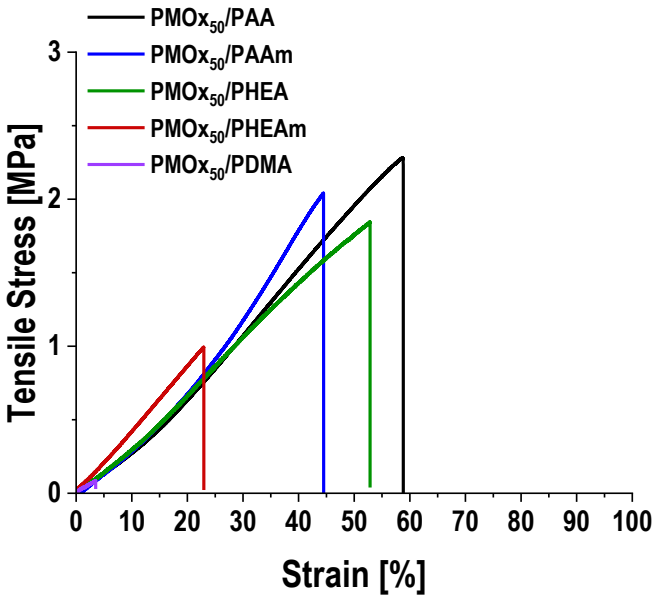

Figure 36: *Stress –strain curve of DN based on $PMOx_{50}$ and PAA, PAAm, PHEA, PHEAm and PDMA.*[131]

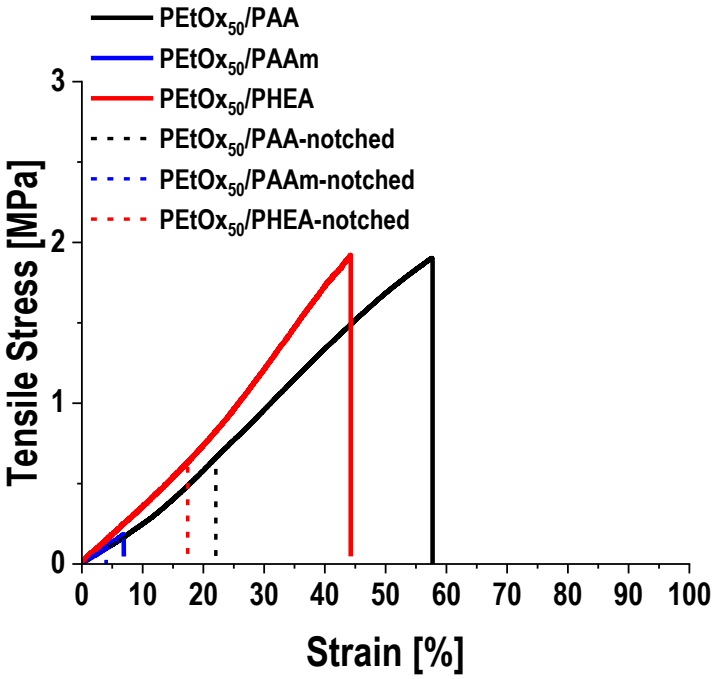

Figure 37: *Stress–strain curve of DN based on PEtOx$_{50}$ and PAA, PAAm, PHEA and the respectively notched samples.*

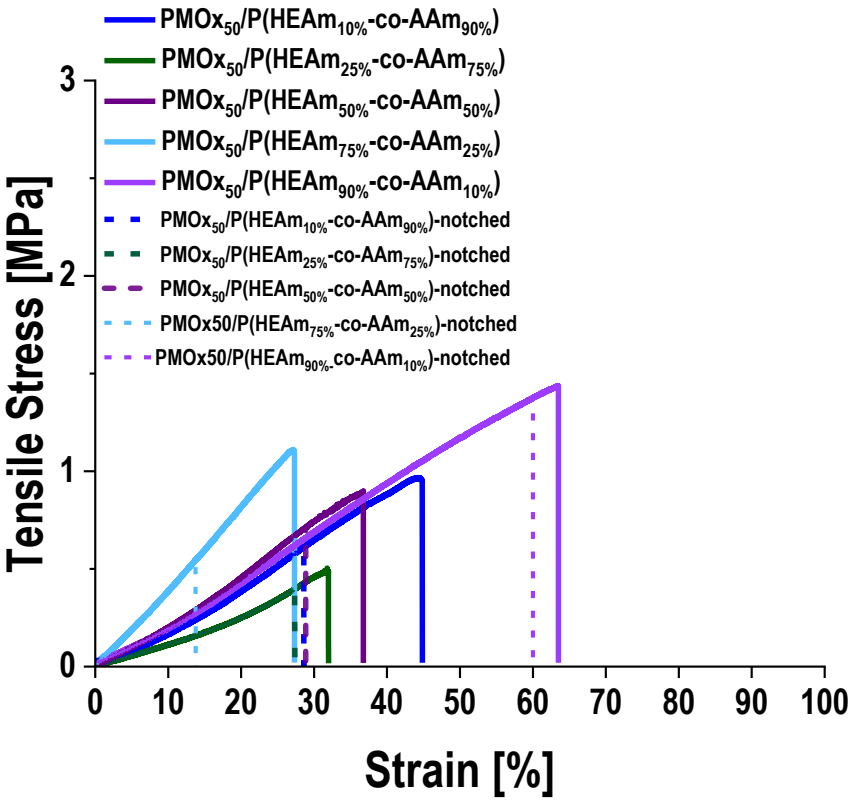

Figure 38: *Stress–strain curve of DN based on PMOx$_{50}$ /P(HEAm-co-AAm) and the notched samples.*[48,131]

5. pH-Stable Double Network Hydrogels with Enhanced Mechanical Integrity Across a Wide pH Range

Some findings presented in this chapter were based on preliminary results of M. SANTHIRASEGARAN´s Master´s thesis.[168]

5.1 ABSTRACT

Double network hydrogels (DNHs) are a renowned class material for their outstanding and tunable mechanical properties, making them highly suitable for diverse biomedical applications such as implants. Implanted hydrogels often encounter varying pH conditions within different tissues or in response to inflammation and infection. Hydrogels materials that maintain their structure and functionality across these conditions are essential for successful implementation and tissue regeneration. In this chapter, we present the development and characterization of DNHs that exhibit remarkable stability and mechanical integrity across a broad pH range of 3.4 to 10.5. These DNHs are composed of a first network based on poly(2-methyl-2-oxazoline) and a second network of poly(acrylic acid-*co*-acryl amide) P(AA-*co*-AAm). A ratio of 90 wt% PAA and 10 wt% PAAm in the second network enabled the pH stabilization of the hydrogel. Comprehensive testing, including compressive tests and tensile strength assessments, demonstrated that these hydrogels maintain their robustness and structural integrity from acidic to alkaline conditions. This study marks a significant step towards the broader applicability of DNHs in environments with fluctuating pH conditions.

5.2 INTRODUCTION

Double network hydrogels have demonstrated exceptional toughness, strength, and versatility in their composition. These unique material properties position them as valuable candidates for applications in biomedical engineering, environmental science, and various industrial sectors.[169] Although high strength and stiffness are required in many practical applications, the use of materials as biomaterials for implants often requires meeting the mechanical properties of the natural tissue. One recent example of such a material is articular cartilage, which has a complex structure and specific mechanical features that must be matched by the potential artificial substitute. Therefore, it is also important to evaluate the material performance in

conditions similar to the original environment of the tissue in the human body, such as ion and salt concentrations. This implies that the implanted material often encounters varying pH conditions within different tissues or in response to inflammation or infection.[170-171] Therefore, hydrogel materials that maintain their integrity across these conditions are essential for successful tissue implantation.

Most of the double network hydrogel systems with cartilage-like properties that have been reported are based on at least one polyelectrolyte component, such as poly(2-acrylamido-2-methylpropane sulfonic acid) (PAMPS)[45,76,85] and poly(acrylic acid) (PAA).[17] The incorporation of acidic or ionic groups in the hydrogel network is beneficial for enhancing the water uptake, which is required to mimic the water content of natural tissues. These groups also form hydrogen bonds or ionic interactions between the involved polymer networks, which can act as sacrificial bonds for the energy dissipation process. The swelling and mechanical performance of hydrogel systems containing polymer networks with acidic groups, such as poly(acrylic acid), are highly dependent on the pH environment.[169,172-173] At pH values above the acid exponent (pKa) of acrylic acid (pKa = 4.7),[174] the dissociation of the acid groups leads to an inevitable loss of mechanical performance.[90] This makes it crucial to ensure the stability of these materials under tissue-relevant conditions.

To address the challenge of developing pH-resistant hydrogels with polyelectrolyte components, we reported double network hydrogels (DNHs) based on poly(2-methyl-2-oxazoline) (PMOx) and poly(acrylic acid) (PAA) with articular cartilage-like performance (as also described in Chapter 3).[17] One of the most remarkable features of the $PMOx_{50}$/PAA DNH is the strong pKa shift of PAA from 4.7 to above 7.4. This pKa shift was attributed to the stabilization of the carboxylic acid groups of PAA against protonation up to pH 7.4, due to the formation of hydrogen bonds between PAA and the PMOx network. However, the compressive strength of the $PMOx_{50}$/PAA DNH decreases significantly at pH 7.6, suggesting a vulnerability of the material under slightly alkaline conditions, which could limit its performance in biological environments where pH fluctuations occur. This highlights the need to improve the stability of the PAA carboxylic groups at higher pH levels. One potential approach to achieve this is by introducing additional components to reinforce this stabilization. Findings in Chapter 4 underscored the potential of incorporating comonomers in the second network to significantly

enhance hydrogen-bonding interactions, leading to superior mechanical properties and fracture resistance, while also contributing to the pH stabilization.

Building upon these insights, the present study aims to design a double network hydrogel that maintains high pH-resistance even in alkaline conditions by copolymerizing the second network, PAA, with polyacrylamide (PAAm), resulting in $PMOx_{50}$/P(AA-*co*-AAm) DNHs. The approach to forming pH-resistant materials with ionic components is important for enhancing their applicability and performance in various fields where environmental pH conditions can vary significantly.

5.3 Results and Discussion

Goal of this study was to develop a double network hydrogel with enhanced pH resistance, ensuring stable yet excellent mechanical performance across a wide range of pH values. To achieve this, we assume that the addition of a comonomer to the secondary network in the original system could be optimal. This suggestion is based on observations gained in Chapter 4, where the critical role of molecular structure, functional groups, side chains, and the spatial arrangement between interacting networks in forming strong or weak hydrogen bonds was discussed. These factors were shown to significantly influence water uptake capability and mechanical behavior. A key highlight of the study was the development of a double network hydrogel (DNH) based on $PMOx_{50}$/P($HEAm_{90\%}$-*co*-$AAm_{10\%}$). By incorporating 10% acrylamide (AAm) as a comonomer, it was possible to achieve extraordinary fracture energy values. This was due to the formation of dynamic hydrogen bonds, which effectively dissipated energy under tensile stress.

Given these findings, it would be interesting to explore whether the addition of a comonomer capable of forming dynamic and strong hydrogen bonds could enhance the stability of hydrogels containing ionic components such as acrylic acid, particulary at higher pH values. Previous experiments showed that adding PHEAm, which offers both strong hydrogen bond donors and acceptors, did not yield in stable hydrogels when combined with poly(acrylic acid) (PAA), making it unsuitable for further testing. This finding also suggested that the ideal comonomer for acrylic acid (AA) in such systems should share similar spatial geometry and a non-ionic nature such as AAm. Acrylamide is widely used in double network hydrogels for cartilage-repair applications due to its elasticity and its ability to form hydrogen-bonding

interactions in different hydrogels systems.[85,175] Moreover, the combination of AAm and AA is well-known not only for producing ionic and hydrogen bond-reinforced double network hydrogels[22,176-177] but also for creating Hydrogen-Bonded (HB) multilayer systems,[178] where stability across physiologically relevant pH range is essential. Therefore, we propose that the addition of AAm as comonomer into the secondary network could further enhance the stability the DNH-PMOx$_{50}$/PAA, even in alkaline pH ranges.

In this study, double network hydrogels (DNHs) composed of a primary network of poly(2-methyl-2-oxazoline) (PMOx) with a degree of polymerization of 50, and various compositions of poly(acrylic acid-*co*-acrylamide) (PAA-*co*-PAAm) as the secondary network were investigated. The synthesis of the telechelic PMOx$_{50}$ and the double network hydrogels followed the same methods previously described in this work in Chapter 3 and 4. The main objective of this study was to examine the influence of pH and salt concentration on the mechanical performance of these hydrogels by varying the ration between PAA: PAAm in the second network, using the previously reported PMOx$_{50}$/PAA DNHs as reference. To achieve this, the samples were tested in two different environments: distilled water and phosphate-buffered saline (PBS) solutions with pH values ranging from 7.4 to 10. The experimental conditions in distilled water served as a control to observe the mechanical performance of the DNHs in the absence of ionic interactions. In contrast, the PBS solutions provided a range of physiological and slightly alkaline conditions to simulate the possible environments these hydrogels might encounter in biomedical applications like in implants.

A series of swelling and mechanical tests, including tensile stress-strain and compressive strength evaluations, were conducted to measure the performance of these hydrogels under these conditions. These tests aimed to identify the optimal compositions of PAA-*co*-PAAm in the secondary network for maintaining hydrogel stability and functionality across a wide range of pH and salt concentrations. The water uptake capability is a crucial feature of hydrogel materials, reflecting the stability of the networks dimension. The water content across different pH conditions provides insights into the swelling behavior of the synthetized double network hydrogels, as shown in Figure 39.

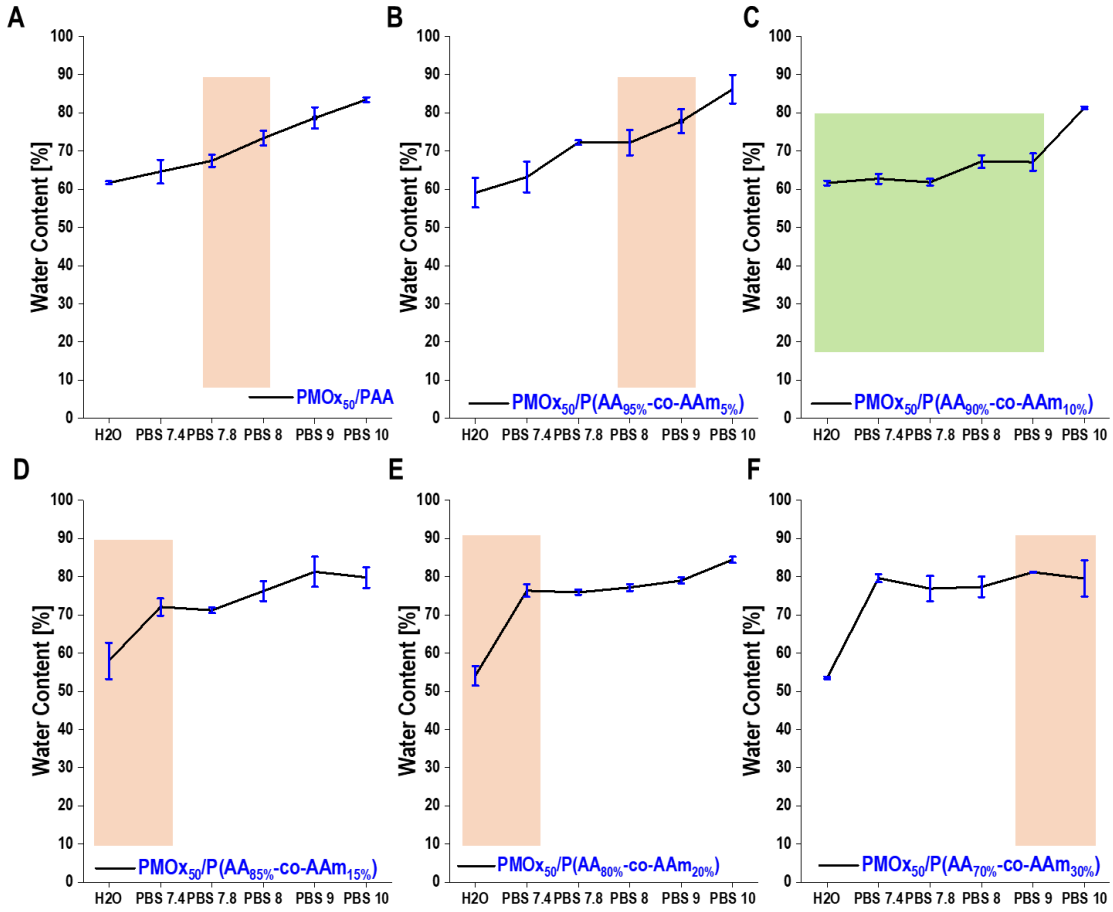

Figure 39: *Water content of DNHs based on A) $PMOx_{50}$/PAA, B) $PMOx_{50}$/P($AA_{95\%}$-co-$AAm_{5\%}$), C) $PMOx_{50}$/P($AA_{90\%}$-co-$AAm_{10\%}$), D) $PMOx_{50}$/P($AA_{85\%}$-co-$AAm_{15\%}$), E) $PMOx_{50}$/P($AA_{80\%}$-co-$AAm_{20\%}$) and F) $PMOx_{50}$/P($AA_{70\%}$-co-$AAm_{30\%}$)in different swelling media. Values are expressed as mean ± SD (n =4).*

DNHs containing 0 wt% and 5 wt% polyacrylamide (PAAm) show a linear an increase of the water content by increasing pH values of the PBS solution. No significant difference of the water content between water and PBS 7.4 was observed, indicating that the salt concentration does not significantly influence their swelling behavior. In contrast, DNHs with PAAm content ranging from 15 wt% to 30 wt% exhibit a sharp increase in water content when transitioning from distilled water to PBS at pH 7.4. This suggests that, for these compositions, the salt concentration has a more substantial impact on swelling behavior than the pH value. Notably, the hydrogel with a secondary network composition of 90 wt% poly(acrylic acid) (PAA) and 10 wt% PAAm exhibits water content values between 62 and 67 wt% up to pH values up to 9.0. This specific ratio appears to balance the hydrophilic nature of PAA and the structural contributions of PAAm, resulting in a hydrogel that maintains its integrity and consistent swelling behavior in varying pH environments.

One of the most important characteristics of biomaterials designed to mimic load-bearing tissues, such as articular cartilage, is high compressive strength. The articular cartilage tissue typically exhibits water content values up to 85 wt% while being able to withstand compressive stresses ranging from 14 to 59 MPa.[14-15,17] This combination of a high water content and a substantial compressive strength is one of the unique features of articular cartilage, making it exceptionally challenging to replicate in synthetic biomaterials. In the Figure 40 shows the correlation between water content and compressive strength at different swelling conditions.

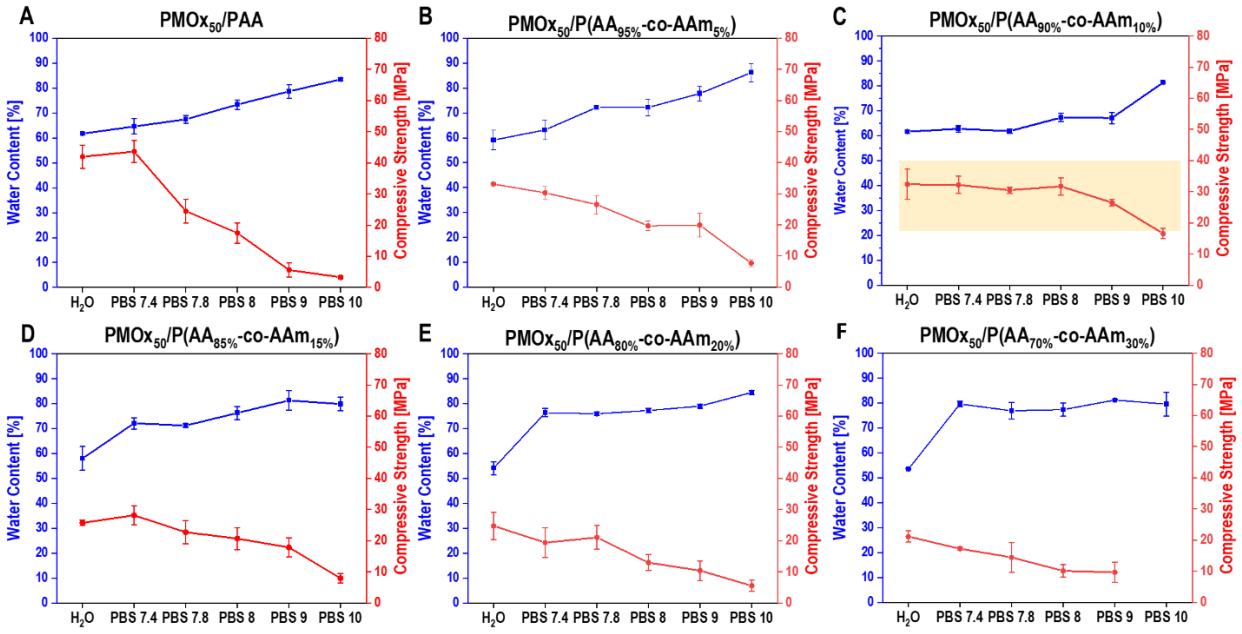

Figure 40: *Water content and compressive strength of DNHs based on A) $PMOx_{50}$/PAA, B) $PMOx_{50}$/P($AA_{95\%}$-co-$AAm_{5\%}$), C) $PMOx_{50}$/P($AA_{90\%}$-co-$AAm_{10\%}$), D) $PMOx_{50}$/P($AA_{85\%}$-co-$AAm_{15\%}$), E) $PMOx_{50}$/P($AA_{80\%}$-co-$AAm_{20\%}$)and F) $PMOx_{50}$/P($AA_{70\%}$-co-$AAm_{30\%}$) in different swelling media. Values are expressed as mean ± SD (n =3- 4).*

In the Figure 40, it is noticeable, that the water content of the different hydrogel at different pH values correlates inversely with their compressive strength. As the water content increases, the compressive strength of the DNHs generally decreases, underscoring the negative effect of water absorption on the mechanical performance of these materials. In comparison to the reference $PMOx_{50}$/PAA, which exhibits a drastic loss of the compressive strength at pH values above 7.4, DNHs containing PAAm as co-network show a more gradual reduction in compressive performance. This behavior indicates that the incorporation of PAAm, like PMOx, contributes to stabilizing the protonation of the carboxylic acid groups in PAA, thereby

enhancing the mechanical stability of the hydrogel network under alkaline conditions. However, this also indicates that the stability of these hydrogels depends on the interactions formed between the polymer networks in the DNHs, which are influenced by the AAm content, salt concentration, and pH levels.

In particular, hydrogels containing 10wt% PAAm as copolymer exhibit exceptional performance, maintaining compressive strength values between 30 to 40 MPa at pH values up to 9.0. Even at pH values above 9.0, these hydrogels retain a compressive strength of approximately 20 MPa, which remains within the range of literature values reported for the compressive strength of articular cartilage (14-59 MPa). This suggest that 90 wt% PAA with 10 wt% PAAm is the optimal ratio, which provides a favorable balance between the water uptake and compressive mechanical strength. Based on these results, the DNHs $PMOx_{50}/P(AA_{90\%}$-*co*-$AAm_{10\%})$ were further investigated for a better understanding of the factor contributing to their exceptional pH resilience.

To explore the dynamics of the interactions between the networks, the $PMOx_{50}/P(AA_{90\%}$-*co*-$AAm_{10\%})$ hydrogels were subjected to tensile testing. This method allows comprehending the dynamics of the interactions between the networks involved. Additionally, these hydrogels were tested at pH 3.4, which is below the pKa of PAA (4.7). Testing at this lower pH was important to determine the behavior of this hydrogels in a broad pH range. The results are presented in Figure 41.

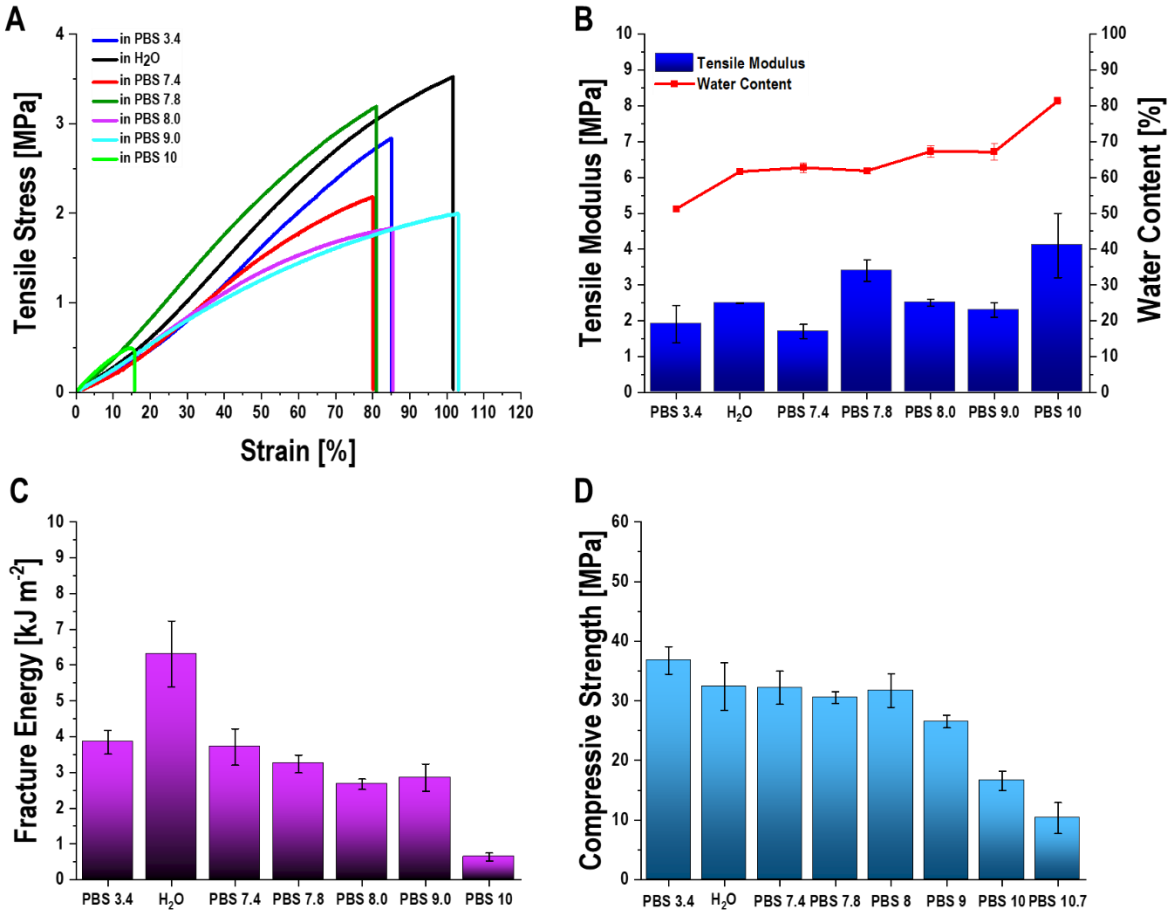

Figure 41: *A) tensile stress-strain curve, B) tensile modulus vs water content, C) fracture energy and D) compressive strength of DNHs based on PMOx$_{50}$/P(AA$_{90\%}$-co-AAm$_{10\%}$) in different swelling media. Values of Figure 41-B, C, D are expressed as mean ± SD (n =3- 4).*[168]

The tensile-stress curves shown in Figure 41-A were used as a starting point to determine the tensile modulus and fracture energy values. Generally, it can be observed that the addition of 10% AAm into the system the elasticity of the system improve, having strain values at break up to 100% compared to the reference PMOx$_{50}$/PAA (50 % strain), giving the system elasticity which is characteristic of polyacrylamide hydrogels systems.[179] It is also evident that the tensile behavior of the DNHs decreases above pH values of 8.0, particularly in terms of tensile strength. Notably, the hydrogels swollen in distilled water exhibit better tensile stress performance than those in PBS, with fracture energy reaching up to 6500 J m^{-2}, similar to the PMOx$_{50}$/PAA reference (6900 J m^{-2}). It could be attributed to the presence of salts in the PBS solution, which weakens PAAm´s ability to form the hydrogen bonds, thereby limiting the formation of strong and reversible hydrogen-bonding interactions that dissipate the energy.

Under compressive stress, no significant difference in the behavior of the DNHs is observed up to PBS pH 8.0. The fracture energy tends to decrease in conditions that disrupt hydrogen bonding, such as changing the swelling medium from water to salt-containing media like PBS, and at higher pH levels. At lower pH levels (e.g., PBS pH 3.4), better mechanical performance was expected because the carboxylic acid groups of PAA are mostly protonated, allowing for stronger hydrogen bonding interactions between PMOx, PAA, and PAAm, which enhances network cohesion. However, the results indicate that salt content is also a key factor to consider, as it reduces the dynamics of hydrogen bonds under tensile stress. Despite this, the hydrogels exhibit steady behavior in salt-containing media up to pH values of 9.0.

At the end of this study, we attempted to use FTIR (Fourier-Transform Infrared Spectroscopy) to identify possible hydrogen bonding interactions within the double network hydrogels. The hydrogels were first swollen in their respective media for approximately 48 hours, and then carefully dried at room temperature to avoid damaging the interactions between the components; the Figure 42 illustrates the FTIR spectra of the DNH $PMOx_{50}$/P($AA_{90\%}$-*co*-$AAm_{10\%}$) at different swelling media.

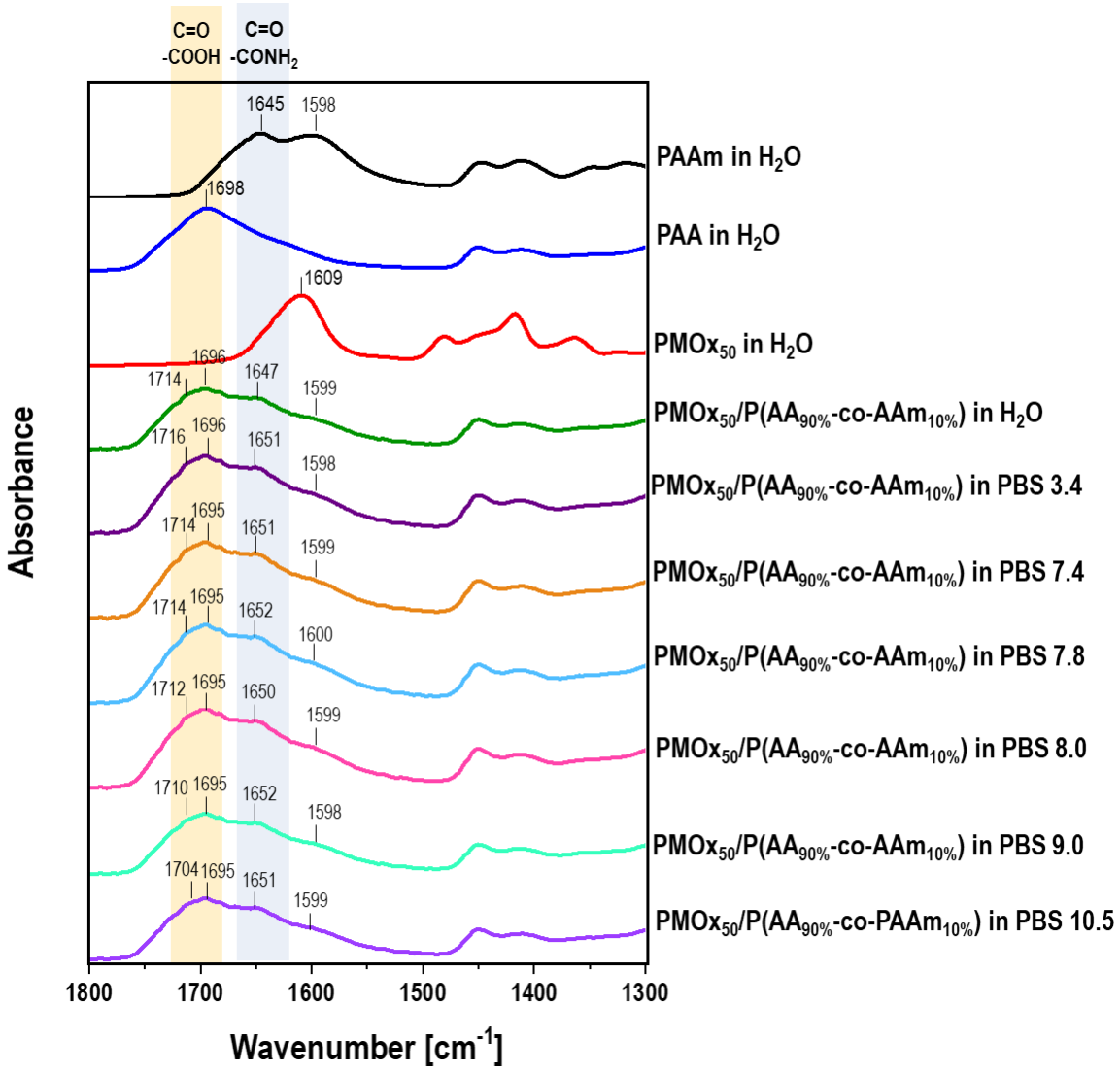

Figure 42: *FTIR-spectra of the single networks, PAAm, PAA and PMOx$_{50}$, and PMOx$_{50}$/P(AA$_{90\%}$-co-AAm$_{10\%}$) double network hydrogels in H$_2$O and in PBS at pH-values between 3.4 and 10.5.*

The formation of PAAm in the double network hydrogel PMOx$_{50}$/P(AA$_{90\%}$-*co*-AAm$_{10\%}$) is indicated by peaks between 1647 and 1651 cm^{-1}, corresponding to the C=O stretch of PAAm (amide I).[180-181] The characteristic peaks corresponding to the stretching vibration of the carbonyl groups (C=O) in PAA typically appear between 1700 and 1725 cm^{-1}, reflecting the protonated carboxyl acid groups of PAA.[180,182] As a startpoint, the PAA single network shows the ν(C=O) at 1698 cm^{-1} (see Figure 42), while the original DNH PMOx$_{50}$/PAAm exhibits this peak at 1705 cm^{-1} in water (refer to Figure 15). Upon the addition of 10% AAm, a broadening of this peak is observed, registering signals between 1695 and 1716 cm^{-1}, suggesting the coexistence of different interactions for these carbonyl groups.

Initially, this confirms the presence of PAA protonated carboxyl groups across the different swelling media. However, at pH 3.4, where protonation does not occur due to PAA´s pKa of 4.7, the C=O peak shifts from 1714 cm^{-1} to 1704 cm^{-1} when the sample is swollen at pH 10.5. This shift correlates with the mechanical performance of $PMOx_{50}$/P($AA_{90\%}$-*co*-$AAm_{10\%}$) under different pH conditions (Figure 41), where a significant drop in the performance is observed at pH 10. The persistence of protonated carboxyl groups, despite the increase in pH and salt concentration, suggest a stabilizing effect provided by the introduction of AAm. This is a noteworthy observation, as the reference system without AAm showed a significant loss in performance at pH values above 7.6 (Figure 14).

Additionally, the superposition and shifted of the C=O peaks of PAA and PAAm in the double network hydrogel, indicate hydrogen-bonding interactions.[183] A shift to lower wavenumber (red shift) in the C=O stretching vibration of PAA, from 1698 cm^{-1} to 1695 cm^{-1}, is observed across all swelling media, further supporting the formation of hydrogen-bonding interactions in the double-network.

Finally, while the carbonyl peaks of PMOx are expected around 1908 cm^{-1}, these signals could not be clearly distinguished due to overlapping peaks from other components, complicating the analysis in this region.

To explain the remarkable performance and pH resilience of this hydrogel system by incorporation of 10 wt% AAm, the following mechanism is suggested: When not all carboxylate groups of PAA in the network structure have a proton-binding partner, they are more easily deprotonated at lower pH values or in response to changes in salt concentration, compared to the groups involved in stable hydrogen bonds. By replacing the excess non-binding carboxylates with another hydrogen donor monomer, such as AAm, greater stabilization of the DNHs is achieved at high pH values. This leads to an even higher pKa shift for PAA than with original $PMOx_{50}$/PAA system.

The swelling behavior of the hydrogels with varying AAm content revealed that 10 wt% acrylamide is necessary to effectively pair with the majority of the carboxylic acid groups of PAA, thereby inhibiting their deprotonation. The incorporation of PAAm into the secondary network significantly contributes to the stabilization of the hydrogel structure by promoting

additional hydrogen-bonding interactions between the amide groups of PAAm and the protonated carboxylic acid groups of PAA. These formed hydrogen bonds enhance reversible interactions within the network, allowing it to dissipate energy under mechanical stress while also maintaining stability across various swelling conditions. As a result, this system successfully shifts the PAA´s pKa from an initial value of 4.7 to 7.4 in $PMOx_{50}$/PAA, and even up to pH 9 in salt-containing media in $PMOx_{50}$/P($AA_{90\%}$-*co*-$AAm_{10\%}$).

5.4 Conclusion

This part of the work aimed to developed double network hydrogels (DNHs) containing $PMOx_{50}$ and PAA that are resilient across a wide pH range, while addressing the limitations of the use of PAA due its protonation in pH values above 4.7. The previously reported $PMOx_{50}$/PAA system served as reference for understanding the mechanisms to stabilize the PAA by shifting its pKa from 4.7 to 7.4. With this knowledge and the understanding gained on the use of comonomers in the double network structure to enhance the mechanical performance, PAAm was used due its very well-known donor and acceptor functionalities, which allow to form stable hydrogen bonding interactions.

The optimized composition, specifically $PMOx_{50}$/P($AA_{90\%}$-*co*-$AAm_{10\%}$), exhibited excellent compressive strength and fracture energy, exceeding that of articular cartilage, even under highly acidic and alkaline conditions, as summarized in Figure 43. The incorporation of 10 wt% AAm enhances stability by forming additional hydrogen bonding interactions and improving energy dissipation under mechanical stress. These interactions enable the hydrogels to withstand mechanical impacts while preserving their structural integrity in environments with fluctuating pH levels, such as those found in tissue implants or regeneration. This makes $PMOx_{50}$/P($AA_{90\%}$-*co*-$AAm_{10\%}$) DNHs promising materials for use in tissue engineering and regenerative medicine.

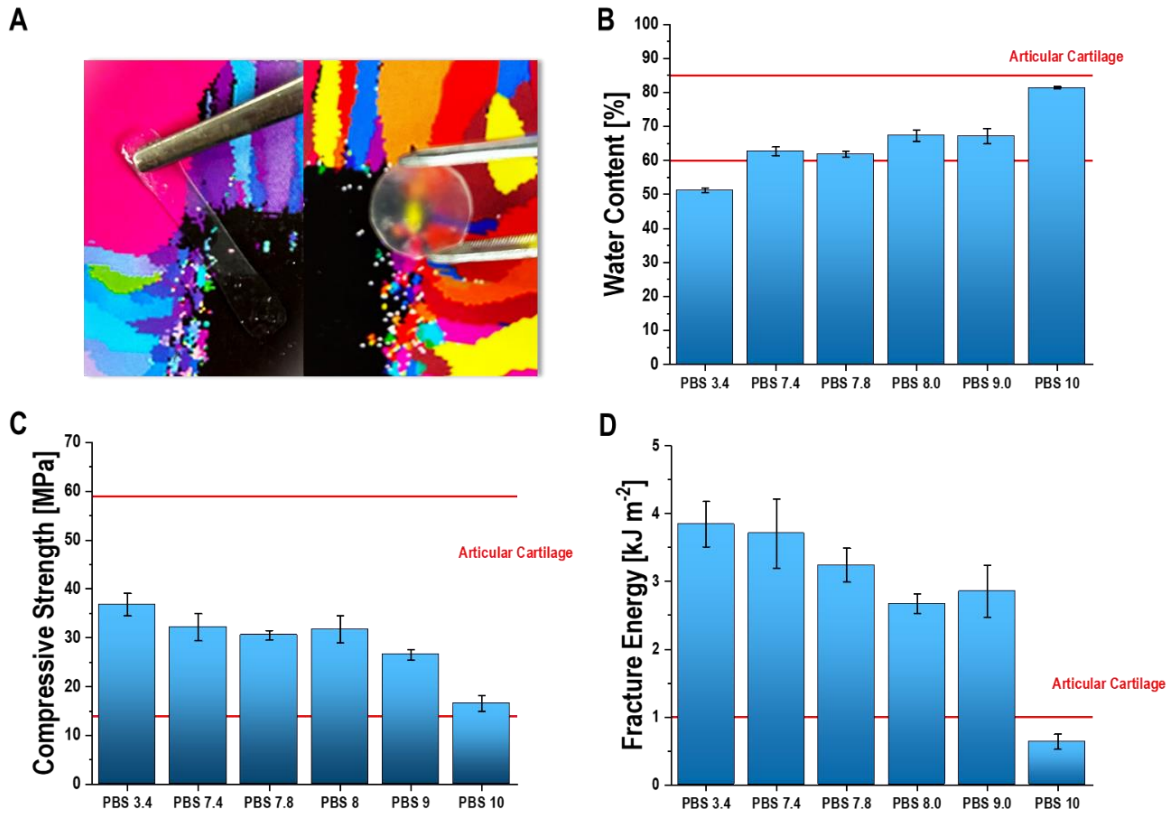

Figure 43: *Graphical summary of $PMOx_{50}/P(AA_{90\%}$-co-$AAm_{10\%})$ DN hydrogels features; A) swollen DN-$PMOx_{50}/P(AA_{90\%}$-co-$AAm_{10\%})$ in tensile and compressive form, B) water content, C) compressive strength and D) fracture energy at different PBS pH-values. The red lines represent the values of the native articular cartilage. Values of Figure 42-B, C, D are expressed as mean ± SD (n =3-4).*

5.5 Experimental Section/Methods

The Experimental section and methods are based on the previous study by the author Benitez-Duif et.al.[17]

-***Materials*:** Chloroform (Fischer Scientific) was distilled from activated aluminum oxide (Merck) under reduced pressure und under argon atmosphere stored. The monomers 2-methyl-2-oxazolin (MOx) was obtained from Acros Organics, these were distilled over CaH_2 (Acros Organics). *Trans*-1,4-dibromo-2-butene (DBB, Acros Organics) was recrystallized twice from n-heptane (Fischer Scientific). N,N-Dimethylaminopropylmethacrylamid (DMAP-MAA, Sigma-Aldrich) was under reduced pressure distilled. All distilled chemicals were under argon atmosphere and at -20°C stored[17]. Acrylic acid (AA, 98% extra pure, Acros Organics),

Acrylamide (AAm, VWR), Irgacure 2959 (IG2959, >98%, TCI-Europe), Irgacure 651 (IG651, Ciba Specialty Chemicals), Tetraethylene glycol dimethacrylate (TEGDMA, Sigma-Aldrich), N,N-methylene-bis-acrylamide (MBAm, 99%, Merck), methanol (Fischer Scientific), diethyl ether (Honeywell Riedel-de-Haën™). The high concentrated phosphate buffered saline (10xPBS, Fischer Scientific) was diluted for the measurements with distilled water to a 1xsolution (1xPBS) with a pH value of 7.41. The pH value of the different PBS solutions were adjusted with 1.0 M NaOH and 1.0 M HCl.

-Synthesis of poly(2-oxazoline) macromonomers with DMAP-MAA end groups: The synthesis of telechelic PMOx was performed according to previously works of TILLER et al.[17, 69] The cationic ring opening polymerization of 2-methyl-2-oxazolin (MOx, 5 mL) with DBB (0.25 g) as initiator was carried out in dry chloroform (20 mL) under argon atmosphere in an industrial microwave reactor. After a polymerization time of 2.5 h at 105 °C, the living ends of the resulting polymer were terminated with 2.1 mL of N,N-Dimethylaminopropylmethacrylamid (DMAP-MAA) in a 10-fold molar excess (respect to the initiator) at 49 °C for 72 h. The resulting polymeric product was purified by precipitating the polymers three times in ice-cold diethyl ether and then dialyzed against mixture of methanol/H_2O (1:1) using benzoylated cellulose membranes (1000 MWCO). The methanol was first removed under reduced pressure and the remaining aqueous solution was dried by lyophilization.[17]

-Determination of the degree of polymerization and functionalization of poly(2-oxazoline) with DMAP-MAA end groups: The degree of polymerization (DP) of the synthesized poly(2-methyl-2-oxazoline) and degree of functionalization (F, in %) with DMAP-MAA as end groups were determinated using ^{1}H NMR spectroscopy(Agilent AV500/AV400 spectrometer at 25 °C with $CDCl_3$ as the solvent). The molecular weight (M_n) and dispersity (Đ) of the polymer were evaluated through size exclusion chromatography (SEC). The SEC analysis was carried out using a Viscotek GPCMax system with a refractive index detector at 55 °C, employing a saline solution of N,N-dimethylformamide (DMF + LiBr, 20 mmol) as the eluent. Calibration was performed with poly(styrene) standards (Viscotek).[17]

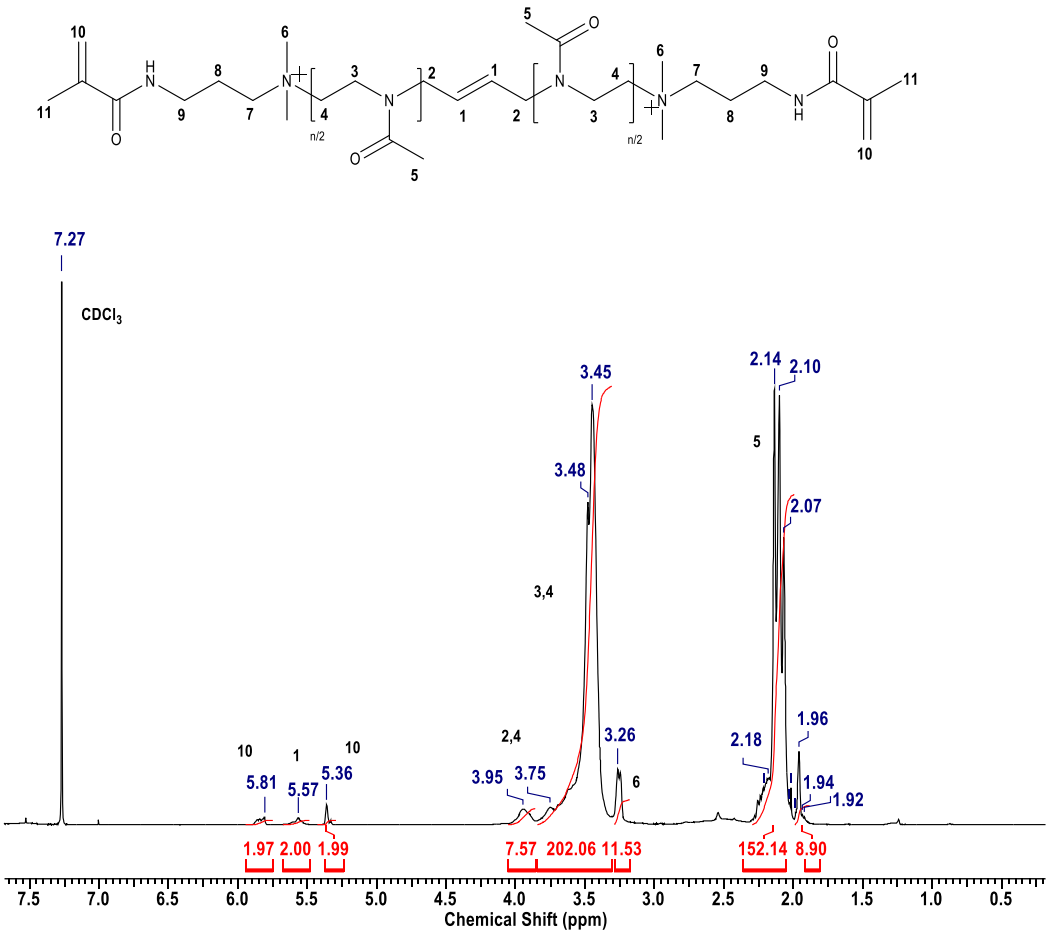

Figure 44: *^{1}H-NMR spectrum of $PMOx_{50}$ with DMAP-MAA end groups in $CDCl_3$ at 400 MHz.*

Table 12: *Analytical data of the synthetized POx with DMAP-MAA end groups.*[48]

Polymer	DP,NMR [-]	$M_{n,NMR}$ [g mol^{-1}]	$M_{n,SEC}$ [g mol^{-1}]	Đ [-]	F-DMAP-MAA[a)] [%]
$PMOx_{50}$	51	4656	5416	1.16	99

[a)]Degree of funtionalization of POX with DMAP-MAA end groups.

***-Fabrication of the POx/PAA-PAAm double network hydrogels*:** The double-networks hydrogels based on POx/PAA were synthesized via the two-step polymerization method, which was first developed by GONG et al.[31] The primary hydrogel network was prepared from an aqueous solution with 34 wt% macromonomer POx with DMAP-MAA end groups and photoinitiator IG2959 (4.6 wt% respect to the macromonomer). This precursor solution was placed between two microscope slides, which were previously coated with poly(propylene)-tape and separated by 1.05 mm thick spacers for the compression-tested samples. Spacers with

0.35 mm thickness were used for tensile-tested hydrogels, so that these could be fixed between the clamps of the tensile tester. Then, it reacted in an UV curing chamber (Emmi-Classic automatic, 36 W, λ = 340 nm) for 36 min (switching each side every 2 min). Upon the exposure to the UV light, the macromonomer underwent a free-radical induced polymerization to form a stable POx primary network (1N). Afterwards the POx network was soaked in DI water over night, in order to remove the unreacted macromonomers and impurities.[17]

In order to incorporate the poly(acrylic acid) (PAA) and polyacrylamide (PAAm) based second co-network, the first network was carefully removed from the water and immersed in the different solutions based on acrylic acid (AA) and acryl amide (AAm) over night (see Table 13). The co-acrylate solutions contain photoinitiator IG651 (0.24 wt% with respect to the total acrylate amount) and tetraethylene glycol dimethacrylate (TEGDMA) as crosslinking agent (0.19 wt% with respect to AA-*co*-AAm). Afterwards, the swollen hydrogel was placed between the two glass plates and cured under UV source for another 20 min (switching each side every 2 min). The final POx/P(AA-*co*-AAm) double network (DN) hydrogel was removed from the glass plates and washed thoroughly with water for at least 48 h. All washed DN hydrogels were dried at room temperature and given in the corresponding swelling media, H_2O and 1xPBS (pH 3.4, 7.4, 7.8, 8.0, 9.0, 10.0 and 10.5), at least 48 h before the measurements.

Table 13: *Composition of the different acrylate second network solutions.*[168]

Acrylate	Monomer Content in Solution [wt%]	Initiator	Initiator Content* [wt%]	Crosslinking Agent	Crosslinking Agent* [wt%]
$AA_{95\%}$-*co*-$AAm_{5\%}$	100	IG651	0.24	TEGDMA	0.79
$AA_{90\%}$-*co*-$AAm_{10\%}$	100	IG651	0.24	TEGDMA	0.79
$AA_{85\%}$-*co*-$AAm_{15\%}$	100	IG651	0.24	TEGDMA	0.79
$AA_{80\%}$-*co*-$AAm_{20\%}$	100	IG651	0.24	TEGDMA	0.79
$AA_{70\%}$-*co*-$AAm_{30\%}$	100	IG651	0.24	TEGDMA	0.79

Initiator and crosslinking agent content are in relation to the total amount of acrylate monomer.

-Determination of the water content: Between 3 and 4 dry hydrogel samples with 6 mm diameter were immersed in deionized water until equilibrium was reached, which corresponds to a swelling time of at least 48 h. Subsequently, the swelled hydrogels were dried under

vacuum at 50 °C for 48 h[17]. To determine the water content (WC) the wet (m_g) and dry (after swelling, m_d) weights of the DN hydrogels were measured and calculated as follows:

$$\text{WC (wt\%)} = \frac{m_g - m_d}{m_g} \times 100 \quad (1)$$

-Determination of the Polyacrylate content in the double-network: The polyacrylate (PA) or second network content in the double network was calculated from the dry weight of the POx based first network (m_{1N}) before its swelling in the comonomer solution and the dry weight of the resulting POx/PAA-*co*-PAAm hydrogel (m_{DN}) after the washed process, results are presented in Table 14.

$$\text{PA (\%)} = \frac{m_{DN} - m_{1N}}{m_{DN}} \times 100 \quad (2)$$

Table 14: *Content of the second network PAA-PAAm in PMOx$_{50}$/P(AA-co-AAm).*

DNH	2. Network Content (PA) [%]
PMOx$_{50}$/P(AA$_{95\%}$-*co*-AAm$_{5\%}$)	80.4 ± 1.3
PMOx$_{50}$/P(AA$_{90\%}$-*co*-AAm$_{10\%}$)	80.6 ± 1.7
PMOx$_{50}$/P(AA$_{85\%}$-*co*-AAm$_{15\%}$)	84.0 ± 1.0
PMOx$_{50}$/P(AA$_{80\%}$-*co*-AAm$_{20\%}$)	83.4 ± 3.4
PMOx$_{50}$/P(AA$_{70\%}$-*co*-AAm$_{30\%}$)	86.7 ± 1.6

-Tensile mechanical test: The tensile stress-strain-curves were recorded at room temperature using an Instron 3340 tensile tester with a cell with load 1 kN. At least four swelled dog-bone tensile samples of different double-networks with average dimensions of 4.55 mm x 29.9 mm x 0.76 mm (width x length x thickness) were fixed between the clamps with help of sandpaper resulting in effective lengths (l_o) between 15 and 18 mm. The experiment was performed at a crosshead speed of 5% min^{-1} until failure of the sample. During the whole experiment, the samples were kept hydrated with the corresponding swelling media using a spray bottle. The tensile modulus was obtained from the initial slope of the stress-strain curve.[17] Fracture energy was determined based on previously works of TILLER et al.[79,129] Three additional samples, with the same dimensions as mentioned above, were notched in the center. The notch length

corresponds to one third of the sample´s width. The tensile test of the notched samples was performed until failure as described above. This experiment allows to determine the strain at which the notch turn into a running crack. The corresponding fracture energy (Γ, in J m^{-2}) of the samples was calculated as follows:

$$\Gamma = l_o \times \int_0^{\varepsilon_c} \sigma(\varepsilon) d\varepsilon \qquad (3)$$

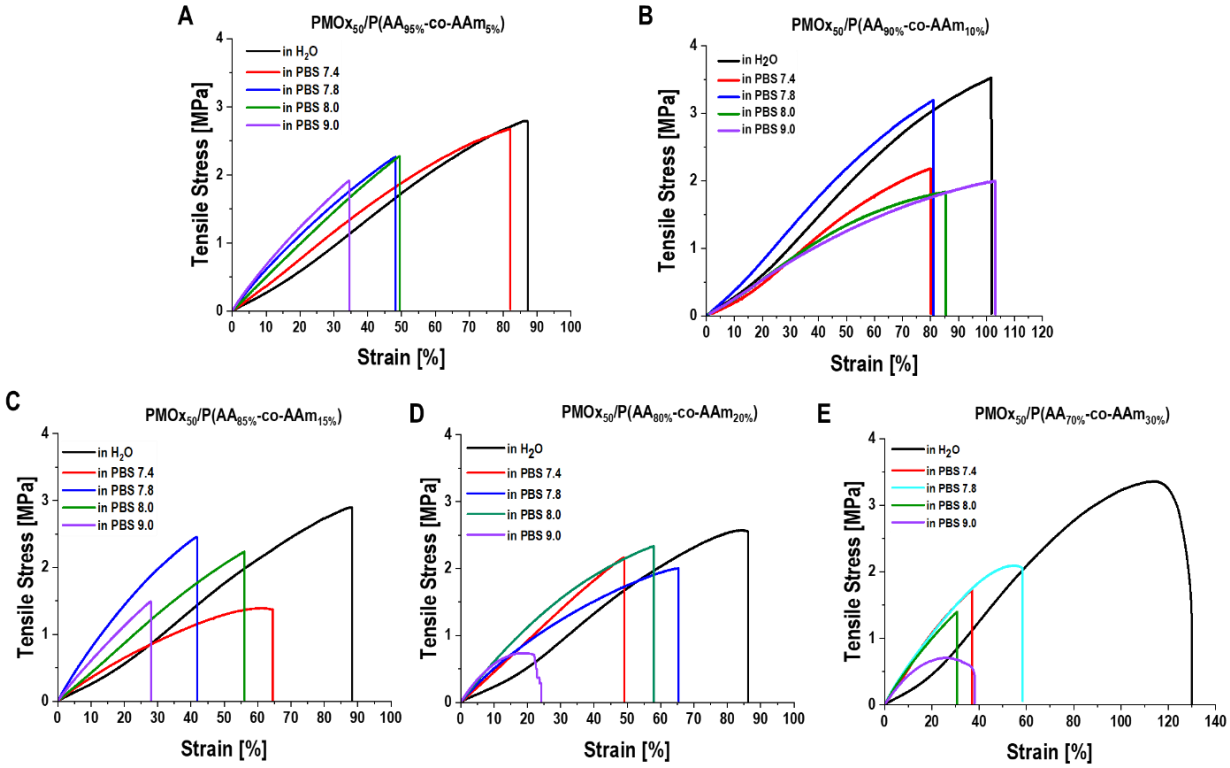

Figure 45: *Tensile stress-strain curve of DNHs based on A) PMOx$_{50}$/P(AA$_{95\%}$-co-AAm$_{5\%}$), B) PMOx$_{50}$/P(AA$_{90\%}$-co-AAm$_{10\%}$),[168] C) PMOx$_{50}$/P(AA$_{85\%}$-co-AAm$_{15\%}$), D) PMOx$_{50}$/P(AA$_{80\%}$-co-AAm$_{20\%}$)[168] and E) PMOx$_{50}$/P(AA$_{70\%}$-co-AAm$_{30\%}$) in different swelling media.*

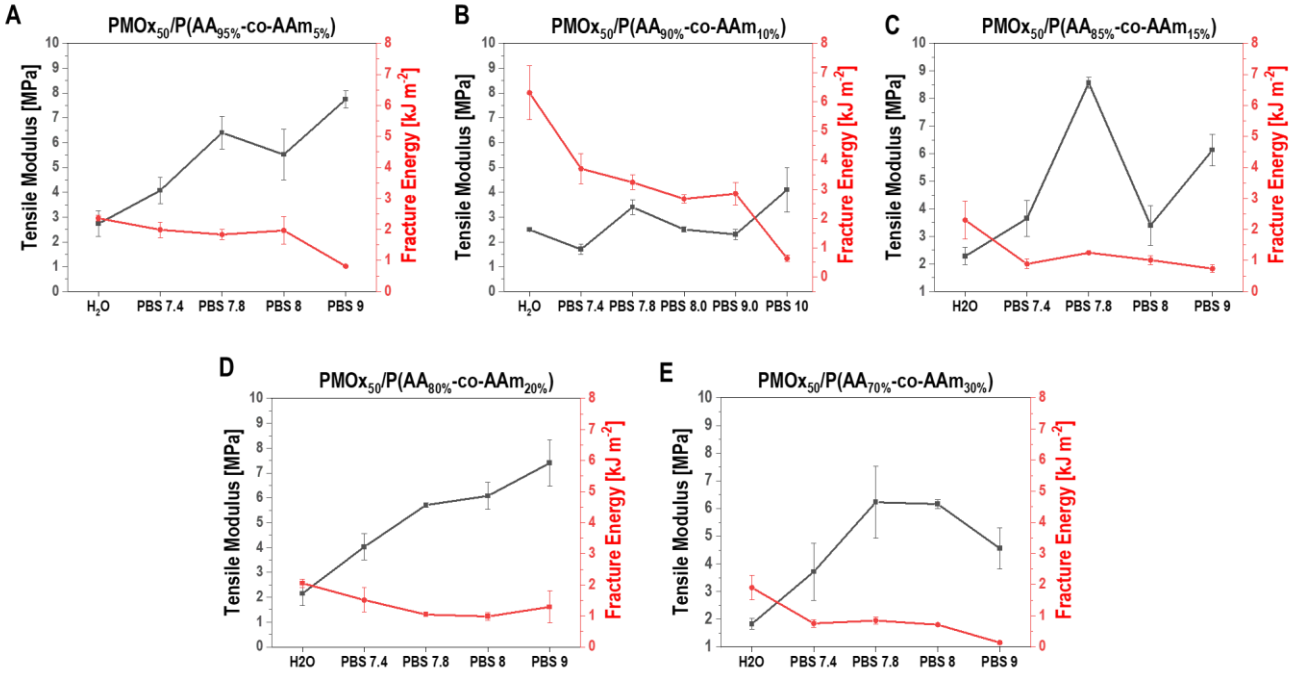

Figure 46: *Tensile modulus and fracture energy of DNHs based on A) PMOx$_{50}$/P(AA$_{95\%}$-co-AAm$_{5\%}$), B) PMOx$_{50}$/P(AA$_{90\%}$-co-AAm$_{10\%}$)[168], C) PMOx$_{50}$/P(AA$_{85\%}$-co-AAm$_{15\%}$), D) PMOx$_{50}$/P(AA$_{80\%}$-co-AAm$_{20\%}$)[168] and E) PMOx$_{50}$/P(AA$_{70\%}$-co-AAm$_{30\%}$) in different swelling media. Values are expressed as mean ± SD (n =3-4).*

-Compressive mechanical test: The compressive behavior of PMOx$_{50}$/PAA-PAAm was evaluated with an Instron 5967 tester with a cell load of 30 kN at room temperature. Five circular samples with diameter of 12 mm and thickness between 1.8 und 2.2 mm were tested. The sample was placed in the compression cell, covered with swelling media, H_2O and 1xPBS (pH 3.4, 7.4, 7.8, 8.0, 9.0, 10.0 and 10.5), and compressed with an initial preload of 1N. All samples were compressed with a compressive strain rate of 0.5 mm min^{-1} until failure. Compressive stress-strain-curves were recorded. Compressive modulus values were obtained from the slope at 0.2-0.3 MPa compressive stress.[17]

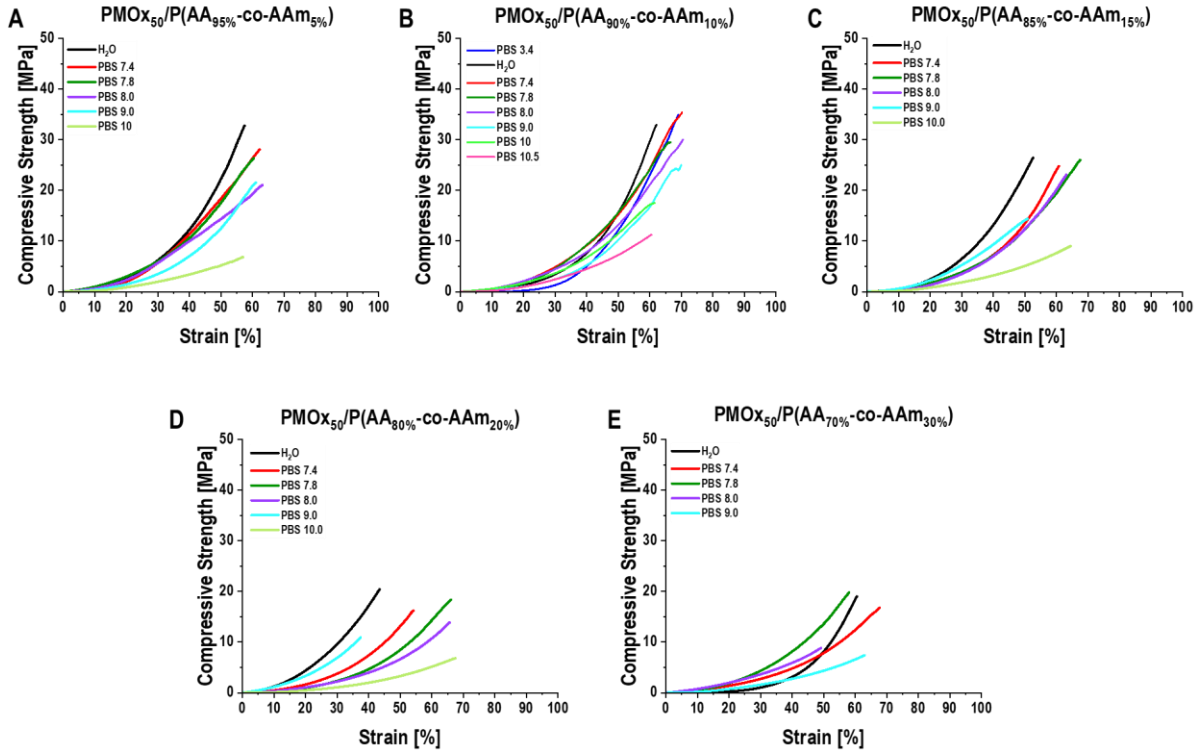

Figure 47: *Compressive stress-strain curve of DNHs Tensile modulus and fracture energy of DNHs based on A) $PMOx_{50}/P(AA_{95\%}\text{-co-}AAm_{5\%})$, B) $PMOx_{50}/P(AA_{90\%}\text{-co-}AAm_{10\%})$,[168] C) $PMOx_{50}/P(AA_{85\%}\text{-co-}AAm_{15\%})$, D) $PMOx_{50}/P(AA_{80\%}\text{-co-}AAm_{20\%})$[168] and E) $PMOx_{50}/P(AA_{70\%}\text{-co-}AAm_{30\%})$ in different swelling media.*

-***Statistical Analysis:*** All values were expressed as mean ± standard deviation (SD). The results were analyzed statistically using a one-way ANOVA, followed by a Tukey post-hoc test. In all cases, the significance was set at $p \leq 0.05$. Statistical analysis was carried out using OriginPro 2020b Software.[17]

5.6 ATTACHMENTS

Table 15: *Summary of the tensile and compressive properties of DNHs based on $PMOx_{50}$/P(AA-co-AAm) in different swelling media.*

DNH	Swelling Media	Water Content [%]	Tensil Modulus [MPa]	Tensile Strength [MPa]	Fracture energy [J/m^2]	Compressive Modulus [MPa]	Compressive Strength [MPa]
$PMOx_{50}$/P($AA_{95\%}$-*co*-$AAm_{5\%}$)	H2O	59.1 ± 3.9	2.7 ± 0.5	2.6 ± 0.3	2361± 93	5.7 ± 0.4	33.1 ± 0.4
	PBS 7.4	63.2 ± 4.0	4.1 ± 0.5	2.3± 1.1	1990 ± 249	5.7 ± 1.1	30.3 ± 2.0
	PBS 7.8	72.2 ± 0.6	6.4 ± 0.7	2.0 ± 0.4	1836 ± 159	8.6 ± 3.1	26.6 ± 2.9
	PBS 8	72.2 ± 3.3	5.5 ± 1.0	1.8 ± 0.6	1968 ± 451	7.9 ± 3.0	19.7 ± 1.5
	PBS 9	77.8 ± 3.1	7.7 ± 0.4	2.0 ± 0.6	816 ± 28	5.3 ± 0.4	19.9 ± 3.9
	PBS 10	86.2 ± 3.7				5.6 ± 1.1	7.7 ± 1.1
$PMOx_{50}$/P($AA_{90\%}$-*co*-$AAm_{10\%}$)[168]	PBS 3.4	51.2 ± 0.7	1.9 ± 0.5	2.3 ± 0.5	3843 ± 334	5.1 ± 0.6	36.8 ± 2.3
	H2O	61.6 ± 0.6	2.50 ± 0.01	2.9 ± 0.9	6308 ± 922	5.1 ± 0.2	32.4 ± 4.9
	PBS 7.4	62.7 ± 1.3	1.7 ± 0.2	1.9 ± 0.4	3709 ± 510	5.8 ± 0.7	32.2 ± 2.8
	PBS 7.8	61.8 ± 0.9	3.4 ± 0.3	3.1 ± 0.3	3240 ± 248	4.9 ± 0.8	31.0 ± 1.0
	PBS 8	67.3 ± 1.7	2.5 ± 0.1	1.7 ± 0.2	2673 ± 146	4.7 ± 0.1	31.7 ± 2.8
	PBS 9	67.1 ± 2.3	2.3 ± 0.2	1.7 ± 0.4	2853 ± 382	4.7 ± 0.4	26.5 ± 1.1
	PBS 10	81.3 ± 0.3	4.1 ± 0.9	0.6 ± 0.2	637 ± 112	5.6 ± 0.2	16.6 ± 1.6
	PBS 10.7	78.8 ± 5.9	-	-	-	5.2 ± 0.7	10.4 ± 2.6
$PMOx_{50}$/P($AA_{85\%}$-*co*-$AAm_{15\%}$)	H2O	58.0 ± 4.8	2.3± 0.3	2.7 ± 0.6	2301 ± 615	5.8 ± 0.3	25.7 ± 0.9
	PBS 7.4	72.1 ± 2.3	3.7 ± 0.7	1.2 ± 0.3	888 ± 154	7.1 ± 1.1	28.2 ± 3.0
	PBS 7.8	71.2 ± 0.7	8.6 ± 0.2	1.7 ± 0.7	1249 ± 15	5.5 ± 0.3	22.7 ± 3.7
	PBS 8	76.3 ± 2.6	3.4 ± 0.7	1.6 ± 0.5	1013 ± 138	6.1 ± 0.3	20.7± 3.5
	PBS 9	81.3 ± 3.9	6.1 ± 0.6	1.7 ± 0.8	738 ± 119	7.0± 0.5	17.9 ± 3.1
	PBS 10	79.8 ± 2.7	-	-	-	5.1 ± 0.9	7.9 ± 1.6
$PMOx_{50}$/P($AA_{80\%}$-*co*-$AAm_{20\%}$)[168]	H2O	54.1 ± 2.6	2.2± 0.5	2.7± 0.2	2055 ± 134	7.1 ± 1.1	24.8 ± 4.4
	PBS 7.4	76.4 ± 1.7	4.0 ± 0.5	1.7 ± 0.6	1513 ± 394	6.8 ± 0.5	19.4 ± 4.8
	PBS 7.8	75.9 ± 0.7	5.7 ± 0.1	1.6 ± 0.4	1046 ± 30	4.6 ± 0.6	21.0 ± 4.0
	PBS 8	77.2 ± 0.9	6.1 ± 0.6	2.1 ± 0.4	985 ± 119	5.1± 0.2	13.0 ± 2.6
	PBS 9	79.0 ± 0.8	7.4± 1.0	1.0 ± 0.3	1289 ± 519	7.8 ± 1.1	10.4 ± 3.2
	PBS 10	84.5 ± 0.8				3.7 ± 0.1	5.6 ± 1.7

$PMOx_{50}/P(AA_{70\%}$-*co*-$AAm_{30\%})$	H2O	53.5 ± 0.3	1.8 ± 0.2	3.5 ± 0.3	1904 ± 386	4.6 ± 1.5	21.1 ± 1.8
	PBS 7.4	79.6 ± 1.1	3.7 ± 1.0	0.9 ± 0.8	614 ± 254	6.3 ± 0.8	17.2 ± 0.6
	PBS 7.8	76.9 ± 3.3	6.2 ± 1.3	1.2 ± 0.8	366 ± 68	3.2 ± 0.1	14.5 ± 4.8
	PBS 8	77.3 ± 2.7	6.2 ± 0.2	1.5 ± 0.1	713 ± 33	77.34 ± 2.69	77.34 ± 2.69
	PBS 9	81.2 ± 0.1	4.6 ± 0.7	0.6 ± 0.1	138 ± 37	6.5 ± 0.3	10.1± 2.0
	PBS 10	79.6 ± 4.8	-	-	-	4.9 ± 0.4	9.7 ± 3.2

6. Conclusions and Outlook.

In this study, tough double network hydrogels (DNHs) based on poly(2-oxazoline) (POx) and polyacrylates were successfully developed, achieving innovative results in hydrogel performance and properties. These findings demonstrate the potential of DNHs for diverse applications, particularly for replicating complex tissues like articular cartilage.

The first part of this research focused on the development of novel poly(2-methyl-2-oxazoline) (PMOx)/poly(acrylic acid) (PAA) double network hydrogels using a two-step synthesis method. The resulting materials exhibited remarkable compressive strength, reaching up to 60 MPa, a low coefficient of friction, and a water content of 66 wt%, along with viscoelastic properties comparable to native articular cartilage. The DNHs demonstrated stability across various physiologically relevant environments, including water, egg white (as a synovial fluid substitute), and PBS buffer, and maintained integrity in conditions with pH levels ranging from 7.4 to 7.8. This exceptional mechanical performance and environmental stability are attributed to the formation of hydrogen bonds within and between both networks, the pKa shift induced by the POx, and the sacrificial bonds acting as toughening mechanisms. Furthermore, these hydrogels showed superior performance compared to other cartilage-like hydrogels and displayed good cytocompatibility, positioning them as promising candidates for biomedical applications where stable mechanical properties are essential.

The second part of the study investigated the tunability of POx_{50}-based DNHs by systematically varying the chemical structures of both networks. The findings confirmed that the double network architecture is critical for achieving robust mechanical properties, particularly when the secondary network acts as a proton donor, enhancing energy dissipation through hydrogen bonding interactions. The $PMOx_{50}$/PAA DNHs demonstrated exceptional compressive strength due to the formation of strong hydrogen bonds within PMOx and PAA, and between PAA network itself. Additionally, this study revealed that small modifications to the side chains of POx and polyacrylates can significantly affect the mechanical properties, suggesting a new approach to optimizing material performance by adjusting side chain length and functional groups. Further experimentation with co-network systems showed that adding 10 wt% acrylamide (AAm) to the

second network, composed of N-(2-hydroxyethyl)acrylamide (HEAm), significantly enhanced toughness and tensile strength, surpassing other POx-based DNHs. These results emphasize the importance of network configuration in double network systems and highlight the versatility of POx-based DNHs, which can be tailored for various applications.

In the final part of this work, the knowledge gained throughout the study was applied to develop DNHs based on $PMOx_{50}$ and PAA. Recognizing that PAA's ability to protonate is a limiting factor at pH values above 7.4, we aimed to create hydrogels resilient to a broader pH range for potential use in tissue replacement. Consequently, we successfully developed DNHs that maintained mechanical stability and integrity across a wide pH range (3.4 to 10.5). The optimized combination of PMOx and PAA-*co*-PAAm networks resulted in hydrogels suitable for biomedical implants and tissue regeneration in environments with fluctuating pH levels, such as those affected by inflammation or infection.

This thesis represents a significant advancement in the development of DNHs based on poly(2-oxazoline) within this research group, establishing a foundation for further exploration and optimization of these materials. Future work could focus on exploring other POx derivatives with varying side chains and functional groups to fine-tune the mechanical properties and responsiveness of DNHs. Additionally, expanding the range of secondary networks to include other types of proton donors and functionalities that introduce different interactions, which contribute to toughening mechanisms, could enhance the performance and versatility of these hydrogels for specific applications.

For applications such as cartilage tissue repair, further studies are needed to assess the biocompatibility, biodegradability, and *in vitro/ vivo* performance of these DNHs in more complex biological environments. Such investigations would provide valuable insights not only into their potential as implant materials, but also into optimizing and understanding their design to achieve a required performance.

While this work focused on developing DNH materials with pH-resilience, future studies could explore the combination of different polyacrylate and poly(2-oxazoline) derivate to create

materials with self-healing featured and smart/stimuli-responsive behaviors. In future studies, this material system could be further developed and applied as pH-responsive actuator for drug delivery and in non-biomedical applications, such as pressure-resistant desalination membranes or as materials for energy harvesting. With their tunable properties, the developed POx-based DNHs hold significant promise for advancing both biomedical and environmental technologies.

7. References

1. Li, J.; Zhang, H.; Han, Y.; Hu, Y.; Geng, Z.; Su, J., Targeted and responsive biomaterials in osteoarthritis. *Theranostics* **2023,** *13* (3), 931-954.

2. Wong, A. Y. L.; Samartzis, D.; Maher, C., The global burden of osteoarthritis: past and future perspectives. *The Lancet Rheumatology* **2023,** *5* (9), e496-e497.

3. Steinmetz, J. D.; Culbreth, G. T.; Haile, L. M.; Rafferty, Q.; Lo, J.; Fukutaki, K. G.; Cruz, J. A.; Smith, A. E.; Vollset, S. E.; Brooks, P. M.; Cross, M.; Woolf, A. D.; Hagins, H.; Abbasi-Kangevari, M.; Abedi, A.; Ackerman, I. N.; Amu, H.; Antony, B.; Arabloo, J.; Aravkin, A. Y.; Argaw, A. M.; Artamonov, A. A.; Ashraf, T.; Barrow, A.; Bearne, L. M.; Bensenor, I. M.; Berhie, A. Y.; Bhardwaj, N.; Bhardwaj, P.; Bhojaraja, V. S.; Bijani, A.; Briant, P. S.; Briggs, A. M.; Butt, N. S.; Charan, J.; Chattu, V. K.; Cicuttini, F. M.; Coberly, K.; Dadras, O.; Dai, X.; Dandona, L.; Dandona, R.; de Luca, K.; Denova-Gutiérrez, E.; Dharmaratne, S. D.; Dhimal, M.; Dianatinasab, M.; Dreinhoefer, K. E.; Elhadi, M.; Farooque, U.; Farpour, H. R.; Filip, I.; Fischer, F.; Freitas, M.; Ganesan, B.; Gemeda, B. N. B.; Getachew, T.; Ghamari, S.-H.; Ghashghaee, A.; Gill, T. K.; Golechha, M.; Golinelli, D.; Gupta, B.; Gupta, V. B.; Gupta, V. K.; Haddadi, R.; Hafezi-Nejad, N.; Halwani, R.; Hamidi, S.; Hanif, A.; Harlianto, N. I.; Haro, J. M.; Hartvigsen, J.; Hay, S. I.; Hebert, J. J.; Heidari, G.; Hosseini, M.-S.; Hosseinzadeh, M.; Hsiao, A. K.; Ilic, I. M.; Ilic, M. D.; Jacob, L.; Jayawardena, R.; Jha, R. P.; Jonas, J. B.; Joseph, N.; Kandel, H.; Karaye, I. M.; Khan, M. J.; Kim, Y. J.; Kolahi, A.-A.; Korzh, O.; Koteeswaran, R.; Krishnamoorthy, V.; Kumar, G. A.; Kumar, N.; Lee, S.-w.; Lim, S. S.; Lobo, S. W.; Lucchetti, G.; Malekpour, M.-R.; Malik, A. A.; Mandarano-Filho, L. G. G.; Martini, S.; Mentis, A.-F. A.; Mesregah, M. K.; Mestrovic, T.; Mirrakhimov, E. M.; Misganaw, A.; Mohammadpourhodki, R.; Mokdad, A. H.; Momtazmanesh, S.; Morrison, S. D.; Murray, C. J. L.; Nassereldine, H.; Netsere, H. B.; Neupane Kandel, S.; Owolabi, M. O.; Panda-Jonas, S.; Pandey, A.; Pawar, S.; Pedersini, P.; Pereira, J.; Radfar, A.; Rashidi, M.-M.; Rawaf, D. L.; Rawaf, S.; Rawassizadeh, R.; Rayegani, S.-M.; Ribeiro, D.; Roever, L.; Saddik, B.; Sahebkar, A.; Salehi, S.; Sanchez Riera, L.; Sanmarchi, F.; Santric-Milicevic, M. M.; Shahabi, S.; Shaikh, M. A.; Shaker, E.; Shannawaz, M.; Sharma, R.; Sharma, S.; Shetty, J. K.; Shiri, R.; Shobeiri, P.; Silva, D. A. S.; Singh, A.; Singh, J. A.; Singh, S.; Skou, S. T.; Slater, H.; Soltani-Zangbar, M. S.; Starodubova, A. V.; Tehrani-Banihashemi, A.; Valadan Tahbaz, S.;

Valdez, P. R.; Vo, B.; Vu, L. G.; Wang, Y.-P.; Yahyazadeh Jabbari, S. H.; Yonemoto, N.; Yunusa, I.; March, L. M.; Ong, K. L.; Vos, T.; Kopec, J. A., Global, regional, and national burden of osteoarthritis, 1990–2020 and projections to 2050: a systematic analysis for the Global Burden of Disease Study 2021. *The Lancet Rheumatology* **2023,** *5* (9), e508-e522.

4. Vega, S.; Kwon, M.; Burdick, J. A., Recent advances in hydrogels for cartilage tissue engineering. *European Cells and Materials* **2017,** *33*, 59-75.

5. Du, D.; Hsu, P.; Zhu, Z.; Zhang, C., Current surgical options and innovation for repairing articular cartilage defects in the femoral head. *Journal of Orthopaedic Translation* **2020,** *21*, 122-128.

6. Armiento, A. R.; Stoddart, M. J.; Alini, M.; Eglin, D., Biomaterials for articular cartilage tissue engineering: Learning from biology. *Acta Biomaterialia* **2018,** *65*, 1-20.

7. Liu, Y.; Wu, Y.; Zhou, L.; Wang, Z.; Dai, C.; Ning, C.; Tan, G., A Dual-Bonded Approach for Improving Hydrogel Implant Stability in Cartilage Defects. *Materials (Basel)* **2017,** *10* (2).

8. Ingavle, G. C.; Frei, A. W.; Gehrke, S. H.; Detamore, M. S., Incorporation of aggrecan in interpenetrating network hydrogels to improve cellular performance for cartilage tissue engineering. *Tissue engineering. Part A* **2013,** *19* (11-12), 1349-59.

9. Atwal, A.; Dale, T. P.; Snow, M.; Forsyth, N. R.; Davoodi, P., Injectable hydrogels: An emerging therapeutic strategy for cartilage regeneration. *Advances in Colloid and Interface Science* **2023,** *321*, 103030.

10. Huang, J.; Xiong, J.; Wang, D.; Zhang, J.; Yang, L.; Sun, S.; Liang, Y., 3D Bioprinting of Hydrogels for Cartilage Tissue Engineering. *Gels (Basel, Switzerland)* **2021,** *7* (3).

11. Wada, S.; Kitamura, N.; Nonoyama, T.; Kiyama, R.; Kurokawa, T.; Gong, J. P.; Yasuda, K., Hydroxyapatite-coated double network hydrogel directly bondable to the bone: Biological and biomechanical evaluations of the bonding property in an osteochondral defect. *Acta Biomaterialia* **2016,** *44*, 125-134.

12. Zhou, J.; Li, Q.; Tian, Z.; Yao, Q.; Zhang, M., Recent advances in 3D bioprinted cartilage-mimicking constructs for applications in tissue engineering. *Materials Today Bio* **2023,** *23*, 100870.

13. Arakaki, K.; Kitamura, N.; Fujiki, H.; Kurokawa, T.; Iwamoto, M.; Ueno, M.; Kanaya, F.; Osada, Y.; Gong, J. P.; Yasuda, K., Artificial cartilage made from a novel double-network hydrogel: In vivo effects on the normal cartilage and ex vivo evaluation of the friction property. *Journal of Biomedical Materials Research Part A* **2010,** *93A* (3), 1160-1168.

14. Yang, F.; Zhao, J.; Koshut, W. J.; Watt, J.; Riboh, J. C.; Gall, K.; Wiley, B. J., A Synthetic Hydrogel Composite with the Mechanical Behavior and Durability of Cartilage. *Advanced Functional Materials* **2020,** *30* (36), 2003451.

15. Kerin, A. J.; Wisnom, M. R.; Adams, M. A., The compressive strength of articular cartilage. *Proceedings of the Institution of Mechanical Engineers, Part H: Journal of Engineering in Medicine* **1998,** *212* (4), 273-280.

16. Rauner, N.; Meuris, M.; Zoric, M.; Tiller, J. C., Enzymatic mineralization generates ultrastiff and tough hydrogels with tunable mechanics. *Nature* **2017,** *543* (7645), 407-410.

17. Benitez-Duif, P. A.; Breisch, M.; Kurka, D.; Edel, K.; Gökcay, S.; Stangier, D.; Tillmann, W.; Hijazi, M.; Tiller, J. C., Ultrastrong Poly(2-Oxazoline)/Poly(Acrylic Acid) Double-Network Hydrogels with Cartilage-Like Mechanical Properties. *Advanced Functional Materials* **2022,** *32* (44), 2204837.

18. Krishnan, Y.; Grodzinsky, A. J., Cartilage diseases. *Matrix Biol* **2018,** *71-72*, 51-69.

19. Warnecke, D.; Meßemer, M.; de Roy, L.; Stein, S.; Gentilini, C.; Walker, R.; Skaer, N.; Ignatius, A.; Dürselen, L., Articular cartilage and meniscus reveal higher friction in swing phase than in stance phase under dynamic gait conditions. *Scientific Reports* **2019,** *9* (1), 5785.

20. Beddoes, C. M.; Whitehouse, M. R.; Briscoe, W. H.; Su, B., Hydrogels as a Replacement Material for Damaged Articular Hyaline Cartilage. *Materials (Basel)* **2016,** *9* (6), 443.

21. Forster, H.; Fisher, J., The influence of continuous sliding and subsequent surface wear on the friction of articular cartilage. *Proceedings of the Institution of Mechanical Engineers. Part H, Journal of engineering in medicine* **1999,** *213* (4), 329-45.

22. Zhou, L.; Pei, X.; Fang, K.; Zhang, R.; Fu, J., Super tough, ultra-stretchable, and fast recoverable double network hydrogels physically crosslinked by triple non-covalent interactions. *Polymer* **2020,** *192*, 122319.

23. Baumann, C. A.; Hinckel, B. B.; Bozynski, C. C.; Farr, J., Articular Cartilage: Structure and Restoration. In *Joint Preservation of the Knee: A Clinical Casebook*, Yanke, A. B.; Cole, B. J., Eds. Springer International Publishing: Cham, 2019; pp 3-24.

24. Cvek, M.; Zahoranova, A.; Mrlik, M.; Sramkova, P.; Minarik, A.; Sedlacik, M., Poly(2-oxazoline)-based magnetic hydrogels: Synthesis, performance and cytotoxicity. *Colloids and Surfaces B: Biointerfaces* **2020,** *190*, 110912.

25. Aerts, A.; Vovchenko, M.; Elahi, S. A.; Viñuelas, R. C.; De Maeseneer, T.; Purino, M.; Hoogenboom, R.; Van Oosterwyck, H.; Jonkers, I.; Cardinaels, R.; Smet, M., A Spontaneous In Situ Thiol-Ene Crosslinking Hydrogel with Thermo-Responsive Mechanical Properties. *Polymers* **2024,** *16* (9), 1264.

26. Rana, H. H.; Park, J. H.; Ducrot, E.; Park, H.; Kota, M.; Han, T. H.; Lee, J. Y.; Kim, J.; Kim, J.-H.; Howlett, P.; Forsyth, M.; MacFarlane, D.; Park, H. S., Extreme properties of double networked ionogel electrolytes for flexible and durable energy storage devices. *Energy Storage Materials* **2019,** *19*, 197-205.

27. Chen, Q.; Chen, H.; Zhu, L.; Zheng, J., Engineering of Tough Double Network Hydrogels. *Macromolecular Chemistry and Physics* **2016,** *217* (9), 1022-1036.

28. Chen, Q.; Chen, H.; Zhu, L.; Zheng, J., Fundamentals of double network hydrogels. *Journal of Materials Chemistry B* **2015,** *3* (18), 3654-3676.

29. Petelinšek, N.; Mommer, S., Tough Hydrogels for Load-Bearing Applications. *Advanced Science* **2024,** *11* (12), 2307404.

30. Narasimhan, B. N.; Deijs, G. S.; Manuguri, S.; Ting, M. S. H.; Williams, M. A. K.; Malmström, J., A comparative study of tough hydrogen bonding dissipating hydrogels made with different network structures. *Nanoscale Advances* **2021,** *3* (10), 2934-2947.

31. Gong, J. P.; Katsuyama, Y.; Kurokawa, T.; Osada, Y., Double-Network Hydrogels with Extremely High Mechanical Strength. *Advanced Materials* **2003,** *15* (14), 1155-1158.

32. Hu, X.; Vatankhah-Varnoosfaderani, M.; Zhou, J.; Li, Q.; Sheiko, S. S., Weak Hydrogen Bonding Enables Hard, Strong, Tough, and Elastic Hydrogels. *Advanced Materials* **2015,** *27* (43), 6899-6905.

33. Wang, X.; Zhao, F.; Pang, B.; Qin, X.; Feng, S., Triple network hydrogels (TN gels) prepared by a one-pot, two-step method with high mechanical properties. *RSC Advances* **2018,** *8* (13), 6789-6797.

34. Zhang, W.; Chen, S.; Jiang, W.; Zhang, Q.; Liu, N.; Wang, Z.; Li, Z.; Zhang, D., Double-network hydrogels for biomaterials: Structure-property relationships and drug delivery. *European Polymer Journal* **2023,** *185*, 111807.

35. Nakajima, T.; Sato, H.; Zhao, Y.; Kawahara, S.; Kurokawa, T.; Sugahara, K.; Gong, J. P., A Universal Molecular Stent Method to Toughen any Hydrogels Based on Double Network Concept. *Advanced Functional Materials* **2012,** *22* (21), 4426-4432.

36. Xu, X.; Jerca, V. V.; Hoogenboom, R., Bioinspired double network hydrogels: from covalent double network hydrogels via hybrid double network hydrogels to physical double network hydrogels. *Materials Horizons* **2021,** *8* (4), 1173-1188.

37. Huang, X.; Li, J.; Luo, J.; Gao, Q.; Mao, A.; Li, J., Research progress on double-network hydrogels. *Materials Today Communications* **2021,** *29*, 102757.

38. Yu, F.; Cui, T.; Yang, C.; Dai, X.; Ma, J., κ-Carrageenan/Sodium alginate double-network hydrogel with enhanced mechanical properties, anti-swelling, and adsorption capacity. *Chemosphere* **2019,** *237*, 124417.

39. Fitzgerald, M. M.; Bootsma, K.; Berberich, J. A.; Sparks, J. L., Tunable Stress Relaxation Behavior of an Alginate-Polyacrylamide Hydrogel: Comparison with Muscle Tissue. *Biomacromolecules* **2015,** *16* (5), 1497-1505.

40. Chen, Q.; Zhu, L.; Zhao, C.; Wang, Q.; Zheng, J., A Robust, One-Pot Synthesis of Highly Mechanical and Recoverable Double Network Hydrogels Using Thermoreversible Sol-Gel Polysaccharide. *Advanced Materials* **2013,** *25* (30), 4171-4176.

41. Sun, H.; Zhang, M.; Liu, M.; Yu, Y.; Xu, X.; Li, J., Fabrication of Double-Network Hydrogels with Universal Adhesion and Superior Extensibility and Cytocompatibility by One-Pot Method. *Biomacromolecules* **2020,** *21* (12), 4699-4708.

42. Mozaffari, E.; Tanhaei, B.; Khajenoori, M.; Movaghar Khoshkho, S., Unveiling the swelling behavior of κ-carrageenan hydrogels: Influence of composition and physiological environment on drug delivery potential. *Journal of Industrial and Engineering Chemistry* **2024**.

43. Chen, F.-L.; Pearce, E. M.; Kwei, T. K., Intermacromolecular complexes by in situ polymerization. *Polymer* **1988,** *29* (12), 2285-2289.

44. Xu, X. W.; Jerca, V. V.; Hoogenboom, R., Bioinspired double network hydrogels: from covalent double network hydrogels via hybrid double network hydrogels to physical double network hydrogels. *Materials Horizons* **2021,** *8* (4), 1173-1188.

45. Means, A. K.; Shrode, C. S.; Whitney, L. V.; Ehrhardt, D. A.; Grunlan, M. A., Double Network Hydrogels that Mimic the Modulus, Strength, and Lubricity of Cartilage. *Biomacromolecules* **2019,** *20* (5), 2034-2042.

46. Wang, Q.; Hou, R.; Cheng, Y.; Fu, J., Super-tough double-network hydrogels reinforced by covalently compositing with silica-nanoparticles. *Soft Matter* **2012,** *8* (22), 6048-6056.

47. Matsuda, T.; Kawakami, R.; Namba, R.; Nakajima, T.; Gong, J. P., Mechanoresponsive self-growing hydrogels inspired by muscle training. *Science* **2019,** *363* (6426), 504-508.

48. Weckes, S. Synthese und Charakterisierung von Co-Doppelnetzwerken auf der Basis von Poly(2-Methyl-2-Oxazolin). Master thesis, TU Dortmund, 2023.

49. Xu, Z.; Chen, Y.; Cao, Y.; Xue, B., Tough Hydrogels with Different Toughening Mechanisms and Applications. *International journal of molecular sciences* **2024,** *25* (5), 2675.

50. Zhu, N.; Yang, B.; Li, S.; Yang, H.; Miao, Y.; Cong, Y.; Zhang, R.; Fu, J., Dynamic and structural studies on synergetic energy dissipation mechanisms of single-, double-, and triple-network hydrogels sequentially crosslinked by multiple non-covalent interactions. *Polymer* **2022,** *250*, 124868.

51. Hu, S.; Fang, Y.; Liang, C.; Turunen, M.; Ikkala, O.; Zhang, H., Thermally trainable dual network hydrogels. *Nature Communications* **2023,** *14* (1), 3717.

52. Huang, G.; Wang, P.; Cai, Y.; Jiang, K.; Li, H., Tough, self-healing double network hydrogels crosslinked via multiple dynamic non-covalent bonds for strain sensor. *Journal of Polymer Science* **2023,** *61* (15), 1675-1687.

53. Zhu, J.; Guan, S.; Hu, Q.; Gao, G.; Xu, K.; Wang, P., Tough and pH-sensitive hydroxypropyl guar gum/polyacrylamide hybrid double-network hydrogel. *Chemical Engineering Journal* **2016,** *306*, 953-960.

54. Li, T.; Zhang, X.; Xia, B.; Ma, P.; Chen, M.; Du, M.; Wang, Y.; Dong, W., Hybrid double-network hydrogels with excellent mechanical properties. *New Journal of Chemistry* **2020,** *44* (38), 16569-16576.

55. He, Z.; Yuan, W., Adhesive, Stretchable, and Transparent Organohydrogels for Antifreezing, Antidrying, and Sensitive Ionic Skins. *ACS Applied Materials & Interfaces* **2021,** *13* (1), 1474-1485.

56. Wang, Y. J.; Li, C. Y.; Wang, Z. J.; Zhao, Y.; Chen, L.; Wu, Z. L.; Zheng, Q., Hydrogen bond-reinforced double-network hydrogels with ultrahigh elastic modulus and shape memory property. *Journal of Polymer Science Part B: Polymer Physics* **2018,** *56* (19), 1281-1286.

57. Li, L.; Wu, P.; Yu, F.; Ma, J., Double network hydrogels for energy/environmental applications: challenges and opportunities. *Journal of Materials Chemistry A* **2022,** *10* (17), 9215-9247.

58. Yu, F.; Yang, P.; Yang, Z.; Zhang, X.; Ma, J., Double-network hydrogel adsorbents for environmental applications. *Chemical Engineering Journal* **2021,** *426*, 131900.

59. Wei, W.; Ma, Y.; Yao, X.; Zhou, W.; Wang, X.; Li, C.; Lin, J.; He, Q.; Leptihn, S.; Ouyang, H., Advanced hydrogels for the repair of cartilage defects and regeneration. *Bioactive Materials* **2021,** *6* (4), 998-1011.

60. Yang, J.; Li, Y.; Zhu, L.; Qin, G.; Chen, Q., Double network hydrogels with controlled shape deformation: A mini review. *Journal of Polymer Science Part B: Polymer Physics* **2018,** *56* (19), 1351-1362.

61. Haque, M. A.; Kurokawa, T.; Gong, J. P., Super tough double network hydrogels and their application as biomaterials. *Polymer* **2012,** *53* (9), 1805-1822.

62. Ogawa, M.; Kitamura, N.; Kurokawa, T.; Arakaki, K.; Tanaka, Y.; Gong, J. P.; Yasuda, K., Poly(2-acrylamido-2-methylpropanesulfonic acid) gel induces articular cartilage regeneration in vivo: Comparisons of the induction ability between single- and double-network gels. *Journal of Biomedical Materials Research Part A* **2012,** *100A* (9), 2244-2251.

63. Gong, J.; Katsuyama, Y.; Kurokawa, T.; Osada, Y., Double-Network Hydrogels with Extremely High Mechanical Strength. *Adv. Mater.* **2003,** *15*, 1155.

64. Das, A.; Babu, A.; Chakraborty, S.; Van Guyse, J. F. R.; Hoogenboom, R.; Maji, S., Poly(N-isopropylacrylamide) and Its Copolymers: A Review on Recent Advances in the Areas of Sensing and Biosensing. *Advanced Functional Materials* **2024,** *34* (37), 2402432.

65. Romanovska, A.; Schmidt, M.; Brandt, V.; Tophoven, J.; Tiller, J. C., Controlling the function of bioactive worm micelles by enzyme-cleavable non-covalent inter-assembly cross-linking. *Journal of Controlled Release* **2024,** *368*, 15-23.

66. de la Rosa, V. R., Poly(2-oxazoline)s as materials for biomedical applications. *Journal of Materials Science: Materials in Medicine* **2014,** *25* (5), 1211-1225.

67. Grube, M.; Leiske, M. N.; Schubert, U. S.; Nischang, I., POx as an Alternative to PEG? A Hydrodynamic and Light Scattering Study. *Macromolecules* **2018,** *51* (5), 1905-1916.

68. Hijazi, M.; Schmidt, M.; Xia, H.; Storkmann, J.; Plothe, R.; Santos, D. D.; Bednarzick, U.; Krumm, C.; Tiller, J. C., Investigations on the thermoresponsive behavior of copoly(2-oxazoline)s in water. *Polymer* **2019,** *175*, 294-301.

69. Wilhelm, S. A.; Maricanov, M.; Brandt, V.; Katzenberg, F.; Tiller, J. C., Amphiphilic polymer conetworks with ideal and non-ideal swelling behavior demonstrated by small angle X-ray scattering. *Polymer* **2022,** *242*, 124582.

70. Benski, L.; Viran, I.; Katzenberg, F.; Tiller, J. C., Small-Angle X-Ray Scattering Measurements on Amphiphilic Polymer Conetworks Swollen in Orthogonal Solvents. *Macromolecular Chemistry and Physics* **2021,** *222* (1), 2000292.

71. Kurka, D. Untersuchung der mechanischen Eigenschaften von Doppelnetzwerk-Hydrogelen auf Basis von Poly(2-oxazolinen) in Abhängigkeit des zweiten Netzwerkes. Master thesis, TU Dortmund, 2021.

72. Gökcay, S. Synthese und Charakterisierung von Doppelnetzwerk-Hydrogelen auf Basis von Poly(2-Methyl-2-oxazolin)/Poly(Acrylsäure). Master thesis, TU Dortmund, 2021.

73. Edel, K. M. Untersuchung der mechanischen Eigenschaften von Doppelnetzwerken auf Basis von Poly(2-methyl-2-oxazolin)/Poly(acrylsäure) in Abhängigkeit des Quellmittels. Bachelor thesis, TU Dortmund, 2020.

74. Hunter, D. J.; Bierma-Zeinstra, S., Osteoarthritis. *Lancet (London, England)* **2019,** *393* (10182), 1745-1759.

75. Hunter, D. J.; March, L.; Chew, M., Osteoarthritis in 2020 and beyond: a Lancet Commission. *The Lancet* **2020,** *396* (10264), 1711-1712.

76. Means, A. K.; Grunlan, M. A., Modern Strategies To Achieve Tissue-Mimetic, Mechanically Robust Hydrogels. *ACS Macro Letters* **2019,** *8* (6), 705-713.

77. Trachsel, L.; Johnbosco, C.; Lang, T.; Benetti, E. M.; Zenobi-Wong, M., Double-Network Hydrogels Including Enzymatically Crosslinked Poly-(2-alkyl-2-oxazoline)s for 3D Bioprinting of Cartilage-Engineering Constructs. *Biomacromolecules* **2019,** *20* (12), 4502-4511.

78. Strassburg, A.; Petranowitsch, J.; Paetzold, F.; Krumm, C.; Peter, E.; Meuris, M.; Köller, M.; Tiller, J. C., Cross-Linking of a Hydrophilic, Antimicrobial Polycation toward a Fast-Swelling, Antimicrobial Superabsorber and Interpenetrating Hydrogel Networks with Long Lasting Antimicrobial Properties. *ACS Applied Materials and Interfaces* **2017,** *9* (42), 36573-36582.

79. Milovanovic, M.; Mihailowitsch, L.; Santhirasegaran, M.; Brandt, V.; Tiller, J. C., Enzyme-induced mineralization of hydrogels with amorphous calcium carbonate for fast synthesis of ultrastiff, strong and tough organic–inorganic double networks. *Journal of Materials Science* **2021,** *56* (27), 15299-15312.

80. Meng, Y.; Ye, L.; Coates, P.; Twigg, P., In Situ Cross-Linking of Poly(vinyl alcohol)/Graphene Oxide–Polyethylene Glycol Nanocomposite Hydrogels as Artificial Cartilage Replacement: Intercalation Structure, Unconfined Compressive Behavior, and Biotribological Behaviors. *The Journal of Physical Chemistry C* **2018,** *122* (5), 3157-3167.

81. Beck, E. C.; Barragan, M.; Tadros, M. H.; Gehrke, S. H.; Detamore, M. S., Approaching the compressive modulus of articular cartilage with a decellularized cartilage-based hydrogel. *Acta Biomaterialia* **2016,** *38*, 94-105.

82. Gong, J. P., Why are double network hydrogels so tough? *Soft Matter* **2010,** *6* (12), 2583-2590.

83. Azuma, C.; Yasuda, K.; Tanabe, Y.; Taniguro, H.; Kanaya, F.; Nakayama, A.; Chen, Y. M.; Gong, J. P.; Osada, Y., Biodegradation of high-toughness double network hydrogels as potential materials for artificial cartilage. *Journal of Biomedical Materials Research Part A* **2007,** *81A* (2), 373-380.

84. Yasuda, K.; Ping Gong, J.; Katsuyama, Y.; Nakayama, A.; Tanabe, Y.; Kondo, E.; Ueno, M.; Osada, Y., Biomechanical properties of high-toughness double network hydrogels. *Biomaterials* **2005,** *26* (21), 4468-4475.

85. Arnold, M. P.; Daniels, A. U.; Ronken, S.; García, H. A.; Friederich, N. F.; Kurokawa, T.; Gong, J. P.; Wirz, D., Acrylamide Polymer Double-Network Hydrogels: Candidate Cartilage Repair Materials with Cartilage-Like Dynamic Stiffness and Attractive Surgery-Related Attachment Mechanics. *Cartilage* **2011,** *2* (4), 374-383.

86. Ronken, S.; Wirz, D.; Daniels, A. U.; Kurokawa, T.; Gong, J. P.; Arnold, M. P., Double-network acrylamide hydrogel compositions adapted to achieve cartilage-like dynamic stiffness. *Biomechanics and Modeling in Mechanobiology* **2013,** *12* (2), 243-248.

87. Cheng, Y.; Hu, Y.; Xu, M.; Qin, M.; Lan, W.; Huang, D.; Wei, Y.; Chen, W., High strength polyvinyl alcohol/polyacrylic acid (PVA/PAA) hydrogel fabricated by Cold-Drawn method for cartilage tissue substitutes. *Journal of Biomaterials Science, Polymer Edition* **2020,** *31* (14), 1836-1851.

88. Bichara, D. A.; Bodugoz-Sentruk, H.; Ling, D.; Malchau, E.; Bragdon, C. R.; Muratoglu, O. K., Osteochondral defect repair using a polyvinyl alcohol-polyacrylic acid (PVA-PAAc) hydrogel. *Biomedical Materials (Bristol, England)* **2014,** *9* (4), 045012.

89. Pourbashir, S.; Shahrousvand, M.; Ghaffari, M., Preparation and characterization of semi-IPNs of polycaprolactone/poly (acrylic acid)/cellulosic nanowhisker as artificial articular cartilage. *International Journal of Biological Macromolecules* **2020,** *142*, 298-310.

90. Myung, D.; Koh, W.; Ko, J.; Hu, Y.; Carrasco, M.; Noolandi, J.; Ta, C. N.; Frank, C. W., Biomimetic strain hardening in interpenetrating polymer network hydrogels. *Polymer* **2007,** *48* (18), 5376-5387.

91. Zhao, X.; Liang, J.; Shan, G.; Pan, P., High strength of hybrid double-network hydrogels imparted by inter-network ionic bonds. *Journal of Materials Chemistry B* **2019,** *7* (2), 324-333.

92. Myung, D.; Waters, D.; Wiseman, M.; Duhamel, P.-E.; Noolandi, J.; Ta, C. N.; Frank, C. W., Progress in the development of interpenetrating polymer network hydrogels. *Polymers for Advanced Technologies* **2008,** *19* (6), 647-657.

93. You, J.; Xie, S.; Cao, J.; Ge, H.; Xu, M.; Zhang, L.; Zhou, J., Quaternized Chitosan/Poly(acrylic acid) Polyelectrolyte Complex Hydrogels with Tough, Self-Recovery, and Tunable Mechanical Properties. *Macromolecules* **2016,** *49* (3), 1049-1059.

94. Hartmann, L.; Watanabe, K.; Zheng, L. L.; Kim, C. Y.; Beck, S. E.; Huie, P.; Noolandi, J.; Cochran, J. R.; Ta, C. N.; Frank, C. W., Toward the development of an artificial cornea: improved

stability of interpenetrating polymer networks. *Journal of biomedical materials research. Part B, Applied biomaterials* **2011,** *98* (1), 8-17.

95. Liu, T.; Jiao, C.; Peng, X.; Chen, Y.-N.; Chen, Y.; He, C.; Liu, R.; Wang, H., Super-strong and tough poly(vinyl alcohol)/poly(acrylic acid) hydrogels reinforced by hydrogen bonding. *Journal of Materials Chemistry B* **2018,** *6* (48), 8105-8114.

96. Zheng, L. L.; Vanchinathan, V.; Dalal, R.; Noolandi, J.; Waters, D. J.; Hartmann, L.; Cochran, J. R.; Frank, C. W.; Yu, C. Q.; Ta, C. N., Biocompatibility of poly(ethylene glycol) and poly(acrylic acid) interpenetrating network hydrogel by intrastromal implantation in rabbit cornea. *Journal of biomedical materials research. Part A* **2015,** *103* (10), 3157-65.

97. Naficy, S.; Razal, J. M.; Whitten, P. G.; Wallace, G. G.; Spinks, G. M., A pH-sensitive, strong double-network hydrogel: Poly(ethylene glycol) methyl ether methacrylates–poly(acrylic acid). *Journal of Polymer Science Part B: Polymer Physics* **2012,** *50* (6), 423-430.

98. He, T.; Jańczewski, D.; Guo, S.; Man, S. M.; Jiang, S.; Tan, W. S., Stable pH responsive layer-by-layer assemblies of partially hydrolysed poly(2-ethyl-2-oxazoline) and poly(acrylic acid) for effective prevention of protein, cell and bacteria surface attachment. *Colloids and Surfaces B: Biointerfaces* **2018,** *161*, 269-278.

99. Kozlovskaya, V.; Shamaev, A.; Sukhishvili, S. A., Tuning swelling pH and permeability of hydrogel multilayer capsules. *Soft Matter* **2008,** *4* (7), 1499-1507.

100. Li, Y.; Pan, T.; Ma, B.; Liu, J.; Sun, J., Healable Antifouling Films Composed of Partially Hydrolyzed Poly(2-ethyl-2-oxazoline) and Poly(acrylic acid). *ACS Applied Materials & Interfaces* **2017,** *9* (16), 14429-14436.

101. Su, C.; Sun, J.; Zhang, X.; Shen, D.; Yang, S., Hydrogen-Bonded Polymer Complex Thin Film of Poly(2-oxazoline) and Poly(acrylic acid). *Polymers* **2017,** *9* (8), 363.

102. Mathivanan, N.; Paramasivam, G.; Vergaelen, M.; Rajendran, J.; Hoogenboom, R.; Sundaramurthy, A., Hydrogen-Bonded Multilayer Thin Films and Capsules Based on Poly(2-n-

propyl-2-oxazoline) and Tannic Acid: Investigation on Intermolecular Forces, Stability, and Permeability. *Langmuir* **2019,** *35* (45), 14712-14724.

103. Krumm, C.; Konieczny, S.; Dropalla, G. J.; Milbradt, M.; Tiller, J. C., Amphiphilic polymer conetworks based on end group cross-linked poly(2-oxazoline) homo- and triblock copolymers. *Macromolecules* **2013,** *46* (9), 3234-3245.

104. Schoenfeld, I.; Dech, S.; Ryabenky, B.; Daniel, B.; Glowacki, B.; Ladisch, R.; Tiller, J. C., Investigations on diffusion limitations of biocatalyzed reactions in amphiphilic polymer conetworks in organic solvents. *Biotechnology and Bioengineering* **2013,** *110* (9), 2333-2342.

105. Sittko, I.; Kremser, K.; Roth, M.; Kuehne, S.; Stuhr, S.; Tiller, J. C., Amphiphilic polymer conetworks with defined nanostructure and tailored swelling behavior for exploring the activation of an entrapped lipase in organic solvents. *Polymer* **2015,** *64*, 122-129.

106. Knauss, R.; Schiller, J.; Fleischer, G.; Kärger, J.; Arnold, K., Self-diffusion of water in cartilage and cartilage components as studied by pulsed field gradient NMR. *Magnetic Resonance in Medicine* **1999,** *41* (2), 285-292.

107. Liess, C.; Lüsse, S.; Karger, N.; Heller, M.; Glüer, C. C., Detection of changes in cartilage water content using MRI T2-mapping in vivo. *Osteoarthritis and Cartilage* **2002,** *10* (12), 907-913.

108. Akizuki, S.; Mow, V. C.; Müller, F.; Pita, J. C.; Howell, D. S.; Manicourt, D. H., Tensile properties of human knee joint cartilage: I. Influence of ionic conditions, weight bearing, and fibrillation on the tensile modulus. *Journal of orthopaedic research : official publication of the Orthopaedic Research Society* **1986,** *4* (4), 379-92.

109. Natoli, R. M.; Revell, C. M.; Athanasiou, K. A., Chondroitinase ABC treatment results in greater tensile properties of self-assembled tissue-engineered articular cartilage. *Tissue engineering. Part A* **2009,** *15* (10), 3119-28.

110. Cook, S. G.; Guan, Y.; Pacifici, N. J.; Brown, C. N.; Czako, E.; Samak, M. S.; Bonassar, L. J.; Gourdon, D., Dynamics of Synovial Fluid Aggregation under Shear. *Langmuir* **2019,** *35* (48), 15887-15896.

111. Faryna, A.; Goldenberg, K., Joint Fluid. In *Clinical Methods: The History, Physical, and Laboratory Examinations*, ed.; Walker, H. K.; Hall, W. D.; Hurst, J. W., Eds. Butterworths Copyright © 1990, Butterworth Publishers, a division of Reed Publishing.: Boston, 1990; p 774.

112. Jahn, S.; Seror, J.; Klein, J., Lubrication of Articular Cartilage. *Annual review of biomedical engineering* **2016,** *18*, 235-58.

113. Fu, L.; Sun, X.; He, W.; Cai, C.; Onishi, A.; Zhang, F.; Linhardt, R. J.; Liu, Z., Keratan sulfate glycosaminoglycan from chicken egg white. *Glycobiology* **2016,** *26* (7), 693-700.

114. Hayashi, M.; Kadomatsu, K.; Kojima, T.; Ishiguro, N., Keratan sulfate and related murine glycosylation can suppress murine cartilage damage in vitro and in vivo. *Biochemical and Biophysical Research Communications* **2011,** *409* (4), 732-7.

115. Liu, Z.; Zhang, F.; Li, L.; Li, G.; He, W.; Linhardt, R. J., Compositional analysis and structural elucidation of glycosaminoglycans in chicken eggs. *Glycoconjugate journal* **2014,** *31* (8), 593-602.

116. Brand, R. A., Joint contact stress: A reasonable surrogate for biological processes? *Iowa Orthop J* **2005,** *25*, 82-94.

117. Guilak, F., The slippery slope of arthritis. *Arthritis & Rheumatism* **2005,** *52* (6), 1632-1633.

118. Lawless, B. M.; Sadeghi, H.; Temple, D. K.; Dhaliwal, H.; Espino, D. M.; Hukins, D. W. L., Viscoelasticity of articular cartilage: Analysing the effect of induced stress and the restraint of bone in a dynamic environment. *J Mech Behav Biomed Mater* **2017,** *75*, 293-301.

119. Grabowska, B.; Holtzer, M., Structural examination of the cross-linking reaction mechanism of polyacrylate binding agents. *Archives of Metallurgy and Materials* **2009**, 427-437.

120. Milovanovic, M.; Isselbaecher, N.; Brandt, V.; Tiller, J. C., Improving the Strength of Ultrastiff Organic–Inorganic Double-Network Hydrogels. *Chemistry of Materials* **2021,** *33* (21), 8312-8322.

121. Fik, C. P.; Konieczny, S.; Pashley, D. H.; Waschinski, C. J.; Ladisch, R. S.; Salz, U.; Bock, T.; Tiller, J. C., Telechelic Poly(2-oxazoline)s with a biocidal and a polymerizable terminal as collagenase inhibiting additive for long-term active antimicrobial dental materials. *Macromolecular Bioscience* **2014,** *14* (11), 1569-1579.

122. Hijazi, M.; Krumm, C.; Cinar, S.; Arns, L.; Alachraf, W.; Hiller, W.; Schrader, W.; Winter, R.; Tiller, J. C., Entropically driven Polymeric Enzyme Inhibitors by End-Group directed Conjugation. *Chemistry - A European Journal* **2018,** *24* (18), 4523-4527.

123. Konieczny, S.; Fik, C. P.; Averesch, N. J. H.; Tiller, J. C., Organosoluble enzyme conjugates with poly(2-oxazoline)s via pyromellitic acid dianhydride. *Journal of Biotechnology* **2012,** *159* (3), 195-203.

124. Konieczny, S.; Krumm, C.; Doert, D.; Neufeld, K.; Tiller, J. C., Investigations on the activity of poly(2-oxazoline) enzyme conjugates dissolved in organic solvents. *Journal of Biotechnology* **2014,** *181*, 55-63.

125. Shah, R. F.; Martinez, A. M.; Pedoia, V.; Majumdar, S.; Vail, T. P.; Bini, S. A., Variation in the Thickness of Knee Cartilage. The Use of a Novel Machine Learning Algorithm for Cartilage Segmentation of Magnetic Resonance Images. *J Arthroplasty* **2019,** *34* (10), 2210-2215.

126. Shepherd, D. E.; Seedhom, B. B., Thickness of human articular cartilage in joints of the lower limb. *Ann Rheum Dis* **1999,** *58* (1), 27-34.

127. Little, C. J.; Bawolin, N. K.; Chen, X., Mechanical Properties of Natural Cartilage and Tissue-Engineered Constructs. *Tissue Engineering Part B: Reviews* **2011,** *17* (4), 213-227.

128. Oloyede, A.; Flachsmann, R.; Broom, N. D., The dramatic influence of loading velocity on the compressive response of articular cartilage. *Connective tissue research* **1992,** *27* (4), 211-24.

129. Milovanovic, M.; Rauner, N.; Civelek, E.; Holtermann, T.; Jid, O. E.; Meuris, M.; Brandt, V.; Tiller, J. C., Enzyme-Induced Ferrification of Hydrogels for Toughening of Functional Inorganic Compounds. *Macromolecular Materials and Engineering* **2022,** *n/a* (n/a), 2200051.

130. Wells, C.; Walker, M., Evaluation of the acute and medically complex patient. *Geriatric Physical Therapy* **2012**, 153-182.

131. Benitez-Duif, P. A.; Weckes, S.; Pinto Ferreira, R. M.; Kurka, D.; Tiller, J. C., Insights on the influence of functional side groups on the mechanical performance of Poly(2-oxazoline)/Poly(acrylate) double network hydrogels. *Polymer* **2025,** *319*, 128014.

132. Rana, M. M.; De la Hoz Siegler, H., Evolution of Hybrid Hydrogels: Next-Generation Biomaterials for Drug Delivery and Tissue Engineering. *Gels (Basel, Switzerland)* **2024,** *10* (4), 216.

133. Mantha, S.; Pillai, S.; Khayambashi, P.; Upadhyay, A.; Zhang, Y.; Tao, O.; Pham, H. M.; Tran, S. D., Smart Hydrogels in Tissue Engineering and Regenerative Medicine. *Materials (Basel)* **2019,** *12* (20).

134. Monnery, B. D.; Hoogenboom, R., Thermoresponsive hydrogels formed by poly(2-oxazoline) triblock copolymers. *Polymer Chemistry* **2019,** *10* (25), 3480-3487.

135. Thai, N. L. B.; Beaman, H. T.; Perlman, M.; Obeng, E. E.; Du, C.; Monroe, M. B. B., Chitosan Poly(vinyl alcohol) Methacrylate Hydrogels for Tissue Engineering Scaffolds. *ACS Applied Bio Materials* **2024**.

136. Hanko, M.; Bruns, N.; Tiller, J. C.; Heinze, J., Optical biochemical sensor for determining hydroperoxides in nonpolar organic liquids as archetype for sensors consisting of amphiphilic conetworks as immobilisation matrices. *Analytical and Bioanalytical Chemistry* **2006,** *386* (5), 1273-1283.

137. Tobis, J.; Thomann, Y.; Tiller, J. C., Synthesis and characterization of chiral and thermo responsive amphiphilic conetworks. *Polymer* **2010,** *51* (1), 35-45.

138. Dech, S.; Cramer, T.; Ladisch, R.; Bruns, N.; Tiller, J. C., Solid−Solid Interface Adsorption of Proteins and Enzymes in Nanophase-Separated Amphiphilic Conetworks. *Biomacromolecules* **2011,** *12* (5), 1594-1601.

139. Dech, S.; Wruk, V.; Fik, C. P.; Tiller, J. C., Amphiphilic polymer conetworks derived from aqueous solutions for biocatalysis in organic solvents. *Polymer* **2012,** *53* (3), 701-707.

140. Savin, G.; Bruns, N.; Thomann, Y.; Tiller, J. C., Nanophase separated amphiphilic microbeads. *Macromolecules* **2005,** *38* (18), 7536-7539.

141. Fodor, C.; Stumphauser, T.; Thomann, R.; Thomann, Y.; Iván, B., Poly(N-vinylimidazole)-l-poly(propylene glycol) amphiphilic conetworks and gels: molecularly forced blends of incompatible polymers with single glass transition temperatures of unusual dependence on the composition. *Polymer Chemistry* **2016,** *7* (34), 5375-5385.

142. Erdodi, G.; Kennedy, J. P., Amphiphilic conetworks: Definition, synthesis, applications. *Progress in Polymer Science* **2006,** *31* (1), 1-18.

143. Apostolides, D. E.; Patrickios, C. S.; Sakai, T.; Guerre, M.; Lopez, G.; Améduri, B.; Ladmiral, V.; Simon, M.; Gradzielski, M.; Clemens, D.; Krumm, C.; Tiller, J. C.; Ernould, B.; Gohy, J.-F., Near-Model Amphiphilic Polymer Conetworks Based on Four-Arm Stars of Poly(vinylidene fluoride) and Poly(ethylene glycol): Synthesis and Characterization. *Macromolecules* **2018,** *51* (7), 2476-2488.

144. Song, G.; Zhang, L.; He, C.; Fang, D.-C.; Whitten, P. G.; Wang, H., Facile Fabrication of Tough Hydrogels Physically Cross-Linked by Strong Cooperative Hydrogen Bonding. *Macromolecules* **2013,** *46* (18), 7423-7435.

145. Zhang, X. N.; Wang, Y. J.; Sun, S.; Hou, L.; Wu, P.; Wu, Z. L.; Zheng, Q., A Tough and Stiff Hydrogel with Tunable Water Content and Mechanical Properties Based on the Synergistic Effect of Hydrogen Bonding and Hydrophobic Interaction. *Macromolecules* **2018,** *51* (20), 8136-8146.

146. Milovanovic, M.; Unruh, M. T.; Brandt, V.; Tiller, J. C., Forming amorphous calcium carbonate within hydrogels by enzyme-induced mineralization in the presence of N-(phosphonomethyl)glycine. *Journal of Colloid and Interface Science* **2020,** *579*, 357-368.

147. Nonoyama, T.; Gong, J. P., Double-network hydrogel and its potential biomedical application: A review. *Proceedings of the Institution of Mechanical Engineers, Part H: Journal of Engineering in Medicine* **2015,** *229* (12), 853-863.

148. Kim, J.; Park, J.; Choe, G.; Jeong, S.-I.; Kim, H.-S.; Lee, J. Y., A Gelatin/Alginate Double Network Hydrogel Nerve Guidance Conduit Fabricated by a Chemical-Free Gamma Radiation for Peripheral Nerve Regeneration. *Advanced Healthcare Materials n/a* (n/a), 2400142.

149. Banerjee, H.; Ren, H., Optimizing Double-Network Hydrogel for Biomedical Soft Robots. *Soft Robotics* **2017,** *4* (3), 191-201.

150. Milovanovic, M.; Tabakoglu, F.; Saki, F.; Pohlkoetter, E.; Buga, D.; Brandt, V.; Tiller, J. C., Organic-inorganic double networks as highly permeable separation membranes with a chiral selector for organic solvents. *Journal of Membrane Science* **2023,** *668*, 121190.

151. Liu, S.; Zhong, Y.; Zhang, X.; Pi, M.; Wang, X.; Zhu, R.; Cui, W.; Ran, R., Highly Deformable, Conductive Double-Network Hydrogel Electrolytes for Durable and Flexible Supercapacitors. *ACS Applied Materials & Interfaces* **2022,** *14* (13), 15641-15652.

152. Zhang, Y.; Qin, H.; Alfred, M.; Ke, H.; Cai, Y.; Wang, Q.; Huang, F.; Liu, B.; Lv, P.; Wei, Q., Reaction modifier system enable double-network hydrogel electrolyte for flexible zinc-air batteries with tolerance to extreme cold conditions. *Energy Storage Materials* **2021,** *42*, 88-96.

153. Li, H.; Wang, H.; Zhang, D.; Xu, Z.; Liu, W., A highly tough and stiff supramolecular polymer double network hydrogel. *Polymer* **2018,** *153*, 193-200.

154. Wang, W.; Zhang, Y.; Liu, W., Bioinspired fabrication of high strength hydrogels from non-covalent interactions. *Progress in Polymer Science* **2017,** *71*, 1-25.

155. Yang, B.; Yuan, W., Highly Stretchable and Transparent Double-Network Hydrogel Ionic Conductors as Flexible Thermal–Mechanical Dual Sensors and Electroluminescent Devices. *ACS Applied Materials & Interfaces* **2019,** *11* (18), 16765-16775.

156. Zhu, R.; Zhu, D.; Zheng, Z.; Wang, X., Tough double network hydrogels with rapid self-reinforcement and low hysteresis based on highly entangled networks. *Nature Communications* **2024,** *15* (1), 1344.

157. Liu, Q.; Wang, C.; Guo, Y.; Peng, C.; Narayanan, A.; Kaur, S.; Xu, Y.; Weiss, R. A.; Joy, A., Opposing Effects of Side-Chain Flexibility and Hydrogen Bonding on the Thermal, Mechanical, and Rheological Properties of Supramolecularly Cross-Linked Polyesters. *Macromolecules* **2018,** *51* (22), 9294-9305.

158. Huang, X.; Nakagawa, S.; Houjou, H.; Yoshie, N., Insights into the Role of Hydrogen Bonds on the Mechanical Properties of Polymer Networks. *Macromolecules* **2021,** *54* (9), 4070-4080.

159. Wang, Y. J.; Zhang, X. N.; Song, Y.; Zhao, Y.; Chen, L.; Su, F.; Li, L.; Wu, Z. L.; Zheng, Q., Ultrastiff and Tough Supramolecular Hydrogels with a Dense and Robust Hydrogen Bond Network. *Chemistry of Materials* **2019,** *31* (4), 1430-1440.

160. Cohen, N.; Du, C.; Wu, Z. L., Understanding the Dissociation of Hydrogen Bond Based Cross-Links In Hydrogels Due to Hydration and Mechanical Forces. *Macromolecules* **2021,** *54* (24), 11316-11325.

161. Tamai, Y.; Tanaka, H.; Nakanishi, K., Molecular Dynamics Study of Polymer−Water Interaction in Hydrogels. 2. Hydrogen-Bond Dynamics. *Macromolecules* **1996,** *29* (21), 6761-6769.

162. Tamai, Y.; Tanaka, H.; Nakanishi, K., Molecular Dynamics Study of Polymer−Water Interaction in Hydrogels. 1. Hydrogen-Bond Structure. *Macromolecules* **1996,** *29* (21), 6750-6760.

163. Lin, F.; Wang, Z.; Chen, J.; Lu, B.; Tang, L.; Chen, X.; Lin, C.; Huang, B.; Zeng, H.; Chen, Y., A bioinspired hydrogen bond crosslink strategy toward toughening ultrastrong and

multifunctional nanocomposite hydrogels. *Journal of Materials Chemistry B* **2020,** *8* (18), 4002-4015.

164. Zhang, J.; Peng, P.; Chen, L.; Zhao, L.; Feng, J., Antifouling poly(N-(2-hydroxyethyl)acrylamide)/sodium alginate double network hydrogels with eminent mechanical properties. *Polymer Testing* **2021,** *95*, 107087.

165. Zhang, J.; Chen, L.; Shen, B.; Chen, L.; Feng, J., Ultra-high strength poly(N-(2-hydroxyethyl)acrylamide)/chitosan hydrogel with "repelling and killing" bacteria property. *Carbohydrate Polymers* **2019,** *225*, 115160.

166. Xu, J.; Guo, Z.; Chen, Y.; Luo, Y.; Xie, S.; Zhang, Y.; Tan, H.; Xu, L.; Zheng, J., Tough, adhesive, self-healing, fully physical crosslinked κ-CG-K+/pHEAA double-network ionic conductive hydrogels for wearable sensors. *Polymer* **2021,** *236*, 124321.

167. Tang, L.; Zhang, D.; Gong, L.; Zhang, Y.; Xie, S.; Ren, B.; Liu, Y.; Yang, F.; Zhou, G.; Chang, Y.; Tang, J.; Zheng, J., Double-Network Physical Cross-Linking Strategy To Promote Bulk Mechanical and Surface Adhesive Properties of Hydrogels. *Macromolecules* **2019,** *52* (24), 9512-9525.

168. Santhirasegaran, M. Doppelnetzwerk-Hydrogele auf Basis von Poly(2-methyl-2-oxazolin) und Acrylat-Copolymeren. Master Thesis, TU Dortmund, 2022.

169. Lee, M. J.; Shrotriya, D. R.; Espinosa-Marzal, R. M., Responsiveness of Charged Double Network Hydrogels to Ionic Environment. *Advanced Functional Materials* **2024,** *n/a* (n/a), 2402279.

170. Harjai, K.; Khandwaha, R. K.; Mittal, R.; Yadav, V.; Gupta, V.; Sharma, S., Effect of pH on production of virulence factors by biofilm cells ofPseudomonas aeruginosa. *Folia Microbiologica* **2005,** *50* (2), 99-102.

171. Sim, P.; Strudwick, X. L.; Song, Y.; Cowin, A. J.; Garg, S., Influence of Acidic pH on Wound Healing In Vivo: A Novel Perspective for Wound Treatment. *International journal of molecular sciences* **2022,** *23* (21).

172. Rosario, A. J.; Ma, B., Stimuli-Responsive Polymer Networks: Application, Design, and Computational Exploration. *ACS Applied Polymer Materials* **2024**.

173. Kim, B.; Shin, Y., pH-sensitive swelling and release behaviors of anionic hydrogels for intelligent drug delivery system. *Journal of Applied Polymer Science* **2007,** *105* (6), 3656-3661.

174. Gerlach, G.; Guenther, M.; Suchaneck, G.; Sorber, J.; Arndt, K.-F.; Richter, A., Application of sensitive hydrogels in chemical and pH sensors. *Macromolecular Symposia* **2004,** *210* (1), 403-410.

175. Li, X.; Peng, X.; Li, R.; Zhang, Y.; Liu, Z.; Huang, Y.; Long, S.; Li, H., Multiple Hydrogen Bonds–Reinforced Hydrogels with High Strength, Shape Memory, and Adsorption Anti-Inflammatory Molecules. *Macromolecular Rapid Communications* **2020,** *41* (14), 2000202.

176. Jing, Z.; Xu, A.; Liang, Y.-Q.; Zhang, Z.; Yu, C.; Hong, P.; Li, Y. Biodegradable Poly(acrylic acid-co-acrylamide)/Poly(vinyl alcohol) Double Network Hydrogels with Tunable Mechanics and High Self-healing Performance *Polymers* [Online], 2019.

177. Irfan, M.; Liu, J.-D.; Du, X.-Y.; Chen, S.; Xiao, J. J., Hydrogen bond-reinforced double-network hydrogels with enhanced mechanical strength: Preparation, characterization and swelling behavior. *Journal of Polymer Science* **2024,** *62* (15), 3426-3438.

178. Lee, S.-W.; Tettey, K. E.; Kim, I. L.; Burdick, J. A.; Lee, D., Controlling the Cell-Adhesion Properties of Poly(acrylic acid)/Polyacrylamide Hydrogen-Bonded Multilayers. *Macromolecules* **2012,** *45* (15), 6120-6126.

179. Hassan, S.; Kim, J.; suo, Z., Polyacrylamide hydrogels. IV. Near-perfect elasticity and rate-dependent toughness. *Journal of the Mechanics and Physics of Solids* **2022,** *158*, 104675.

180. Moharram, M.; Balloomal, L.; El-Gendy, H., Infrared study of the complexation of poly (acrylic acid) with poly (acrylamide). *Journal of applied polymer science* **1996,** *59* (6), 987-990.

181. Moharram, M. A.; Rabie, S. M.; El-Gendy, H. M., Infrared spectra of γ-irradiated poly(acrylic acid)–polyacrylamide complex. *Journal of Applied Polymer Science* **2002,** *85* (8), 1619-1623.

182. Dong, J.; Ozaki, Y.; Nakashima, K., Infrared, Raman, and Near-Infrared Spectroscopic Evidence for the Coexistence of Various Hydrogen-Bond Forms in Poly(acrylic acid). *Macromolecules* **1997,** *30* (4), 1111-1117.

183. Owens, D. E.; Jian, Y.; Fang, J. E.; Slaughter, B. V.; Chen, Y.-H.; Peppas, N. A., Thermally Responsive Swelling Properties of Polyacrylamide/Poly(acrylic acid) Interpenetrating Polymer Network Nanoparticles. *Macromolecules* **2007,** *40* (20), 7306-7310.

8. List of Abbreviations

Abbreviation	Definition
AA	Acrylic acid
AAm	Acrylamide
AMPS	2-Acrylamido-2-methyl-1-propanesulfonicacid
$CDCl_3$	Deuterated chloroform
$CHCl_3$	Chloroform
DBB	1,4-Dibrom-2-butene
DMA	N,N-Dimethylacrylamide
DMAP-MAA	N-[3-(Dimethylamino)propyl]methacrylamide
DNH	Double network hydrogel
DP	Degree of Polymerization
EtOx	2-Ethyl-2-Oxazolin
FTIR	Fourier-transform infrared spectroscopy
HEA	2-Hydroxyethyl acrylate
HEAm	N-(2-Hydroxyethyl)acrylamide
IG651	Irgacure 651 [2,2-Dimethoxy-2-phenylacetophenone]
IG2959	Irgacure 2959 [2-Hydroxy-4´-(2-hydroxyethoxy)-2-methylpropiophenone]
MBA	N,N`-Methylenbisacrylamide
MeOx	2-Methyl-2-oxazolin
M_W	Molecular weight
MWCO	Molecular weight cut-off
^1H NMR	Proton Nuclear Magnetic Resonance Spectroscopy
PAA	Poly(acrylic acid)
PAAm	Polyacryamide

Abbreviation	Definition
PAMPS	Poly(2-acrylamido-2-methyl-1-propanesulfonicacid)
PBS	Phosphate buffered saline
PDMA	Poly(N,N-dimethylacrylamide)
Đ	Polydispersity index
PEtOx	Poly(2-ethyl-2-Oxazolin)
PHEA	Poly(2-hydroxyethyl acrylate)
PHEAm	N-(2-hydroxyethyl)acrylamide
PMeOx	Poly(2-methyl-2-Oxazolin)
SEC	Size-exclusion chromatography
SN	Singel-network
TEGDMA	Tetraethylene glycol dimethacrylate
wt%	Weight percent